Master's thesis

NTNU
Norwegian University of Science and Technology
Faculty of Engineering
Department of Energy and Process Engineering

Henrik Andersen

Development of CO2 refrigeration systems and thermal energy storage for cruise ships

Master's thesis in Mechanical Engineering
Supervisor: Armin Hafner
Co-supervisor: Muhammad Zahid Saeed
June 2022

NTNU
Norwegian University of
Science and Technology

Henrik Andersen

Development of CO2 refrigeration systems and thermal energy storage for cruise ships

Master's thesis in Mechanical Engineering
Supervisor: Armin Hafner
Co-supervisor: Muhammad Zahid Saeed
June 2022

Norwegian University of Science and Technology
Faculty of Engineering
Department of Energy and Process Engineering

NTNU
Norwegian University of
Science and Technology

Preface

I am very grateful that I could apply the knowledge I have gained from the university on such an important and sustainable topic, and to hopefully contribute to research that can help the global society towards more green and efficient technology.

For their guidance and supervision, i would like to thank Muhammad Zahid Saeed, Armin Hafner and Cecilia Gabrielli. Further, I would also like to express my gratitude to my fellow students for the endless and inspiring hours of work at the university.

Abstract

Today typical refrigerants utilized on board cruise ships are associated with a significant impact on global warming. These refrigerants are becoming increasingly regulated, underlining the importance of applying sustainable refrigerants. As a result, CO_2 has resurrected as refrigerant for marine applications. Another measure towards zero emissions, will require ships to connect to on-shore power during port stays longer than two hours, to reduce the need for auxiliary engines.

A cruise ship have a great cooling demand from its hotel facilities. The comfort requirements related to the passengers, require large capacity chillers to generate chilled water for air conditioning (AC). Additionally, cruise ships often fully supply the provision at the port of origin, resulting in a large amount of provision that has to be preserved.

The aim of this work is to develop energy-efficient CO_2 refrigeration models in Dymola, and simulate to find the expected performances from such systems when applied to cruise ships. More specifically, an ejector supported two-staged evaporation AC system, and an ejector supported parallel compression provision system has been modeled and simulated. Performance is evaluated through the cooling COP, but also through heat recovery, as a high degree of integration is emphasised from modern systems. Furthermore, how cold thermal energy storage (CTES) can be utilized to supply the cooling demand related to a two hour port stay have been investigated. As for the refrigeration systems, the CTES is modelled and simulated in Dymola.

Three comprehensive reference cases containing three different cooling loads for each refrigeration system was defined. As the thesis only examine the systems during summer conditions, and the systems utilizes sea water cooling, the reference cases have sea water temperatures of 30°C, 23°C and 16°C, and are referred to as the warm-, medium- and cold case, respectively. The cooling load for the AC system is dynamic, while it is constant for the provision system.

The results shows that the AC system is able to operate with a cooling COP ($COP_{c,\ AC}$) about 2.89, 4.19 and 5.99 respectively for the warm-, medium- and cold case, while operating at the best obtainable high side pressure. Further, at the best operating point, the provision system is able to operate at a $COP_{c,\ prov}$ of 2.33, 2.98 and 3.54 respectively for the warm-, medium-, and cold case.

Further, the recovered heat from the AC system ranges from 400 kW at the lowest high side pressure during the cold case, to 5000 kW at the highest investigated pressure during the warm case. Furthermore, the recovered heat from the provision system ranges from 55 kW during the cold case, to 140 kW at the highest investigated high side pressure in the warm case.

Lastly, it has been found that a CTES, utilizing latent heat storage, needs to contain 21163 kg of water as phase change material, and a total volume of 38.0 m^3. As well as being discharged in 2 hours, it can charged by the AC system in 6 hours without influencing the overall peak load. However, the $COP_{c,\ AC}$ is decreased in the range of 6.13% - 9.73% during charging.

Sammendrag

Kjølemedier som er brukt om bord på cruiseskip i dag er assosiert med en betydelig innvirkning på global oppvarming. Disse kjølemediene blir stadig mer regulert, noe som understreker viktigheten av å bruke bærekraftige kjølemedier. Som et resultat har CO_2 gjenoppstått som kjølemedium for marine applikasjoner. Et annet tiltak for å redusere utslipp, vil kreve at skip kobler seg til landstrøm under lengre havneopphold enn to timer. Dette for å redusere utslippene som er assosiert med havneoppholdene.

Grunnet hotellfasilitetene har cruiseskip et stort kjølebehov. Passasjerenes komfortkrav krever store systemer som kan produsere kaldtvann til klimaanlegget. I tillegg bunkrer skipene ofte opp all den nødvendige provianten fra start, noe som resulterer i store mengder proviant som må bevares kjølig.

Målet med dette arbeidet er å utvikle energieffektive CO_2-kjølemodeller for cruiseskip i Dymola, samt simulere for å finne den forventede ytelsen fra systemene. Mer spesifikt, et ejektorstøttet to-trinns fordampning AC-system, og et ejektorstøttet parallell-kompresjon proviantsystem blitt modellert og simulert. Ytelsen ble evaluert gjennom systemenes kjøle-COP, men også gjennom varmegjenvinning, da høy grad av integrasjon vektlegges fra moderne systemer. Videre, er det undersøkt hvordan kald termisk energilagring kan utnyttes for å dekke kjølebehovet knyttet til to timers havneopphold. Dette er også undersøkt gjennom modellering og simulering i Dymola.

Tre omfattende referansesituasjoner som inneholder tre forskjellige kjølebehov for hvert kjølesystem ble definert. Da oppgaven kun undersøker systemene under sommerforhold, og systemene utnytter sjøvannskjøling, inneholder referansesituasjonene følgende tre forskjellige sjøvannstemperaturer: 30°C, 23°C og 16°C. Dette er henholdsvis referert til som varm-, medium- og kald situasjon. Kjølebelastningen for AC-systemet er dynamisk, mens den er konstant for proviantsystemet.

Resultatene viser at AC-systemet er i stand til å operere med en maksimal kjøle-COP på ca. 2.89, 4.19 og 5.99 for henholdsvis varm, medium og kald situasjonen. Videre, er proviantsystemet i stand til å operere med en kjøle-COP på 2.33, 2.98 og 3.54, for henholdsvis varm, middels og kald situasjon.

Den gjenvinnende varmen fra AC-systemet varierer fra 400 kW, ved det laveste gasskjølertrykket under den kalde situasjonen, til 5000 kW ved det høyeste undersøkte gasskjølertrykket under den varme situasjonen. Videre varierer den gjenvinnende varmen fra proviantsystemet fra 55 kW under den kalde situasjonen, til 140 kW ved det høyeste undersøkte gasskjølertrykket i den varme situasjonen.

Til slutt har det blitt funnet at et kaldt termisk energilagringssystem, som bruker latent varmelagring, må inneholde 21163 kg vann som faseendringsmateriale, og et samlet volum på 38.0 m^3. I tillegg til å bli utladet på 2 timer, kan den lades av AC-systemet på 6 timer uten å påvirke det maksimale kjølebehovet AC-systemet må kunne levere. Imidlertid reduseres AC-systemets kjøle-COP fra 6,13 % til 9,73 % under lading.

Contents

List of Figures

List of Tables

Nomenclature

Abbreviations

AC	=	Air Conditioning
AHU	=	Air Handling Unit
CFC	=	Chlorofluorocarbons
CO_2	=	Carbon Dioxide
COP	=	Coefficient Of Performance
DHW	=	Domestic Hot Water
FCU	=	Fan Coil Unit
FGBV	=	Flash Gas By-pass Valve
GHG	=	Green House Gas
GT	=	Gross Tonnage
GWP	=	Global Warming Potential
HCFC	=	Hydrochlorofluorocarbons
HFC	=	Hydrofluorocarbons
HVAC	=	Heating, Ventilation and Air Conditioning
IHX	=	Internal Heat Exchanger
LHS	=	Latent Heat Storage
LNG	=	Liquefied Natural Gas
LT	=	Low Temperature
MT	=	Medium Temperature
ODP	=	Ozone Depletion Potential
PCM	=	Phase Change Material
SHS	=	Sensible Heat Storage
TES	=	Thermal Energy Storage

Symbols

h	=	Specific enthalpy
$\dot{m}$	=	Mass flow rate
p	=	Pressure
$\dot{Q}$	=	Heat flow rate
T	=	Temperature
$\dot{W}$	=	Work rate
Δ	=	Difference
Φ	=	Entrainment ratio

Subscripts

AC	=	AC system
c	=	Cooling
comp	=	Compressor
CR	=	Cold Reservoir
evap	=	Evaporator
mf	=	Motive Flow
par	=	Parallel
prov	=	Provsion system
rec	=	Recovered
S	=	Suction
sf	=	Suction Flow
tot	=	Total

1 Introduction

The cruise industry is one of the fastest growing segments of the global tourism industry. From 2009 to 2019 the number of passengers increased from 18 million to 30 million [1]. At the same time has the size of ships experienced a spectacular increase the last decades. In the 1970s a typical cruise ship had a capacity of 800 passengers. Today there are several cruise ships with a capacity of over 6000 passengers [2].

There are great greenhouse emissions (GHG) related to the cruise industry. According to Western Norway research institute [3], 3% of the total GHG from Norway has its origin from the cruise industry, consuming about 170 million liters of fuel. However, burning fossil fuel is not the only source of GHG emissions. Today R134a, R404A and R407C are the dominating refrigerants on passenger ships [4], they have a global warming potential (GWP) of 1430 or greater [5]. Leakages of such synthetic refrigerants contributes significantly to the GHG emissions. Between 2008 and 2016 Swedish passenger and cargo ships reported an average of 16% leakage of total refrigerant charge. The total leakage of refrigerants from the global shipping industry constitutes about 2% of its total GHG emissions, including carbon dioxide (CO_2) emissions [4].

The cruise industry, like all other sectors, has to adapt in order reduce GHG emissions. Therefore, in 2014, EU introduced a new regulation on fluorinated greenhouse gases [6]. Here there is a ban for centralised refrigeration systems exceeding 40 kW capacity, relying on fluorinated greenhouse gases with a GWP of 150 or more.

Instead of looking into new synthetic refrigerants, it has been a rising interest into natural working fluids, such as water, ammonia, hydrocarbons, and carbon dioxide. Of these, CO_2 is the only non-toxic and non-flammable fluid which can operate in a vapor compression cycle below 0°C [7]. Thus, CO_2 is a great option in refrigeration systems that are both environmentally friendly and personal safe.

Carbon dioxide has been utilized as a refrigerant in the past, but the low critical point brought challenges during operation, especially in warm climates. Today we have overcome these challenges and can run systems transcritically [8]. Transcritical operation results in a great pressure difference between absorption and rejection side. As a consequence, great energy losses occurs in the expansion valve in a conventional vapor compression cycle. Hence, to make a CO_2 system competitive, there is a big interest in implementing alternative expansion devices, e.g. ejectors.

The cruise industry distinguishes significantly from other industries. A large cruise ship can in many ways compare to a small town, operating isolated at sea. The ship is not coupled to any external systems, so it must rely on the technology and equipment on board. This means that approximately all the demanded energy has to be covered by the only energy carrier on board, the fossil fuel. Hence, making each process as efficient as possible decreases the fuel consumption, and consequently the emissions. This very much applies to the heating, ventilation and air conditioning (HVAC) system on board, which relies on electricity generated by combustion engines. The HVAC system utilizes chilled water for AC purposes, requiring large capacity chillers. A lot of the electricity related to the HVAC system is required by the chiller, thus it is logical to focus on making this process as energy efficient as possible.

Furthermore, there are a lot of provision which has to be conserved by the provision cooling and freezing system on board a cruise ship. These system are of a capacity which are regulated by the new EU regulation introduced above. Hence it is a must to investigate provision system alternatives that utilizes

climate friendly refrigerants.

During port stays, ships either rely on auxiliary engines to generate electricity, or, for more contemporary ships, run their diesel-electric system on part load [9]. A process associated with a significant amount of GHG emissions and pollution of city centers. In fact, 20% of the consumed fuel by cruise ships in Norway is burned while the ships are in port [3]. Thus the EU has proposed, from January 2030, that all ships utilizing fossil fuel of more than 5000 GT staying in port for more than two hours have to connect to on-shore power supply [10]. A proposal which will eliminate much of the city center pollution and the GHG emissions associated with cruise ships port stays, as long as the electricity is generated from a sustainable energy source. As stated, this proposal will not regulate port stays less than two hours. Thus it is interesting to investigate if CTES can be utilized to cover the cooling demand for these port stays. A technology which is also interesting in relation to the zero emission requirements in the world heritage fjords in Norway from 2026 [11].

1.1 Objectives

In this subsection the objectives of this thesis are defined. All the investigation and work from here will be about answering and reaching these. To be considered are the following objectives:

- What are the expected performances from an energy efficient CO_2 air conditioning- and provision system for a cruise ship? And how does it change with different environmental conditions?
- How much heat can be recovered from these systems? And how does different high side pressures affect this capability?
- How can cold thermal energy storage be utilized to cover the cooling load of a 2 hours port stay? When should it be charged? What are the necessary dimensions?

1.2 Scope

The scope of this thesis is firstly limited to summer conditions, hence heat sink temperatures between 16°C and 30°C. The work is only considering refrigeration systems, and since CO_2 systems has its challenges related to hot heat sinks, it is logical to rule out colder conditions. Further, the HVAC system distribution strategy of the chilled water generated by the AC system is not investigated. The focus is on investigating the AC system itself, and the capability of supplying the demanded cooling load.

The heating demand of cruise ships is not studied. Hence, the utilization of recovered heat from the AC- and provision system is out of the scope. If this were to be included, heat recovery from other processes would have to be studied as well. This is done by fellow students, thus, regarding this aspect, this work can be seen in context with their work.

Most of the work is based on simulations, practical aspects as costs, mechanical assembly, the number of components, e.g. in the compressor racks, etc. is not thoroughly considered, only at a brief and simple level during design and configuration. Experimental validation was intend, however due to time limitations, it has not been conducted.

2 Literature review

To be able to reach the objectives, an important step is to understand the relevant theory and investigate literature within the field. A literature review gives insight on state of the technology, thus a good starting point. Thus, this section summarizes the relevant theory and information that was examined during the literature review.

2.1 CO_2 as a refrigerant

CO_2 or R744 has been utilized as a refrigerant for marine application before, but around 1950 it disappeared due to the introduction of synthetic working fluids. As time went on, one started to realize the impact the synthetic fluids had on climate change. This meant that CFC, HCFC and HFC refrigerants which once where accepted, now have been placed in a list of regulated substances. This has lead to a rising interest in environmentally friendly natural working fluids, like CO_2. Carbon dioxide is very interesting since it is extensively available, inexpensive, non-flammable, non-toxic and has no climate impact. The latter is due to CO_2 being a byproduct of industrial production, which implies it has a net global warming impact of zero, even though it has a GWP = 1. In addition has CO_2 a ozone depletion potential (ODP) = 0. This is characteristics and properties that are desirable for modern refrigerants.

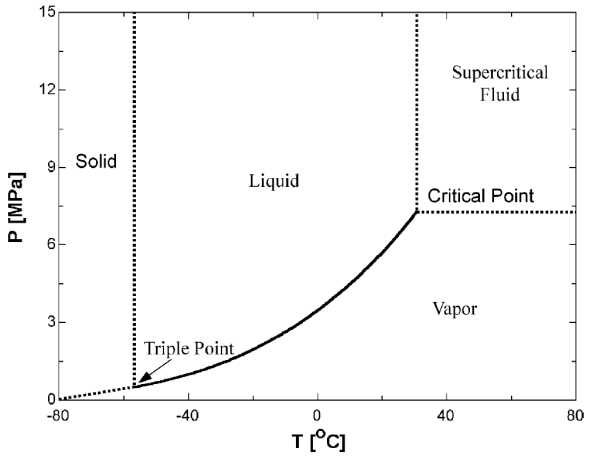

Figure 2.1: P-T diagram of CO_2 [7].

2.1.1 Characteristics and thermodynamic properties of CO_2

When designing a refrigeration system, the thermodynamic properties of the refrigerant are important. Table 2.1 compares the properties of CO_2 (R744) with other common refrigerants. Like previously stated is the ODP and GWP of CO_2 0 and 1 respectively. Approximately the same case are for the two other natural refrigerants R717 (ammonia) and R290 (propane). The synthetic refrigerants have a much higher GWP, and R12 and R22 also have a ODP > 0, due to being CFC and HCFC refrigerants, respectively. CO_2 is non-toxic and non-flammable, which is the case for the non-natural fluids as well.

Figure 2.1 shows the P-T diagram of CO_2. Carbon dioxide has a relative low critical temperature at 31.0 °C and 73.8 bar. Above the critical point, CO_2 is supercritical. A state where there is no distinct gas or liquid phase. Further, the triple point may also be seen in Figure 2.1. It occurs at -56.6°C and 5.2 bar

Table 2.1: Characteristics and thermodynamic properties for some refrigerants[a].

	R12	R22	R134a	R407C	R410A	R717	R290	R744
ODP/GWP	1/8500	0.05/1700	0/1300	0/1600	0/1900	0/0	0/3	0/1
Flammable/Toxic	N/N	N/N	N/N	N/N	N/N	Y/Y	Y/N	N/N
Molecular mass (kg/kmol)	120.9	86.5	102.0	86.2	72.6	17.0	44.1	44.0
Normal boiling point (°C)	-29.8	-40.8	-26.2	-43.8	-52.6	-33.3	-42.1	-78.4
Critical pressure (Bar)	41.1	49.7	40.7	46.4	47.9	114.2	42.5	73.8
Critical temperature (°C)	112.0	96.0	101.1	86.1	70.2	133.0	96.7	31.0
Reduced pressure[b]	0.07	0.10	0.07	0.11	0.16	0.04	0.11	0.47
Reduced temperature[c]	0.71	0.74	0.73	0.76	0.79	0.67	0.74	0.90
Refrigeration capacity[d] (kJ/m^3)	2734	4356	2868	4029	6763	4382	3907	22545

[a] Values are collected from Kim et al. [7].
[b] Saturation pressure at 0 °C to critical pressure ratio.
[c] 273.15 K to critical temperature in Kelvin ratio.
[d] Volumetric refrigeration capacity at 0°C.

[7]. This is where all three phases (solid, liquid and gas) occurs at the same time, in equilibrium. Below this pressure sublimation may occur, i.e., transition from solid to gaseous state.

Another important property listed in Table 2.1 is the volumetric refrigeration capacity. This is 3-8 times greater for CO_2 compared to HC, HFC, HCFC and CFC refrigerants [7]. This is due to high operating pressures in CO_2 systems, which results in high densities. The great volumetric refrigeration capacity results in CO_2 systems being more compact with smaller components. Other properties which contributes to compact designs are the transport properties of CO_2, e.i., thermal conductivity and viscosity. Kim et al. [7] concludes that CO_2 has very good thermal conductivity and low viscosity compared to other refrigerants, and that the low viscosity implies small pressure drops which again allows for compact designs.

When a supercritical fluid rejects heat, temperature and pressure are no longer coupled together. Thus, heat rejection happens at gliding temperature. This is in contrast to subcritical heat rejection which happens at constant temperature. Figure 2.2 illustrates the isobaric heat rejection for subcritical and transcritical fluids. For the subcritical case, heat rejection happens during a phase change, as the fluid condenses to a liquid. Thus heat rejection takes place at constant temperature. In contrast, when a fluid rejects heat in a transcritical state, the pressure and temperature are not coupled together, and heat rejection happens at a gliding temperature. Hence, the heat rejection takes place in a gas cooler and not in a condenser, which is the case for refrigeration systems during subcritical operation. As a result may the high side pressure be determined independently of the gas cooler outlet temperature, meaning that maximises the COP, e.i. the most common performance indicator, can operate at all times.

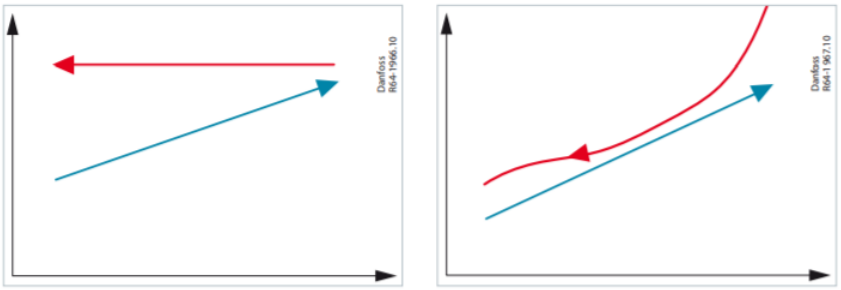

Figure 2.2: Sub-critical heat rejection (left) and supercritical heat rejection (right). [12]

Further, as seen in Figure 2.2, does the gradient of the supercritical heat rejection curve change. As a

consequence, will the pinch point, the point where the temperature difference between the two stream is the smallest, in the gas cooler not be at the inlet, but at the outlet or inside [13]. Kim et al. [7] shows that close to the critical point, the properties of supercritical CO_2 changes rapidly when undergoing an isobaric process. The specific heat capacity changes dramatically and reaches a maximum for distinct pressures. The maximum specific heat capacity for a given pressure is called a pseudo critical point. Figure 2.3 visualize how the specific heat changes for different pressures, and how it diverges towards infinity when the pressure and temperature approaches the critical point. This is an important characteristic since the gradient of the supercritical heat rejection curve, visualized in Figure 2.2, decreases with increasing specific heat. Consequently is it possible to control the location of the pinch point in the gas cooler.

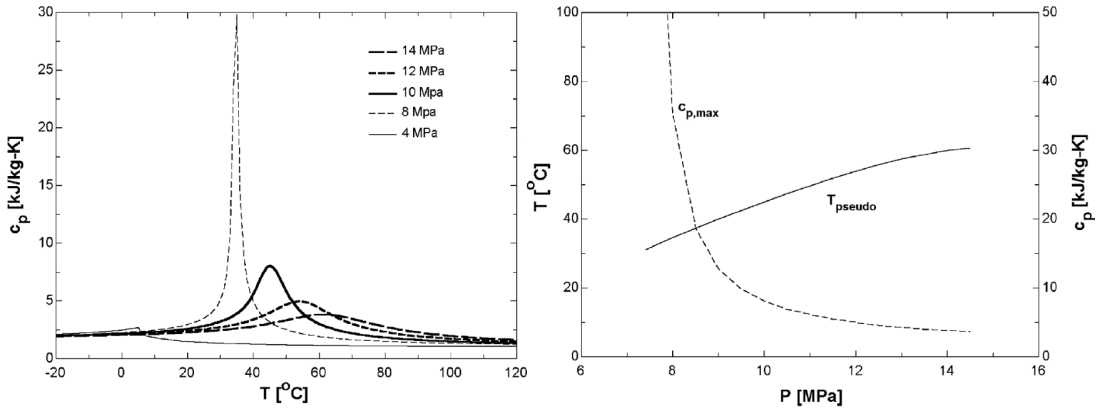

Figure 2.3: Pseudo critical points for varying pressure and temperature. [7]

As stated above, during transcritical operation there is a high side pressure which maximises the COP. Further may the high side pressure may be determined independently of the gas cooler outlet temperature. The COP maximising pressure can be found in numerous ways, and the method proposed by Kauf et al. [14] has proven to be a good approximation [13]. Kauf treats the outlet gas cooler temperature as the only independent variable, and states that the s-shape of the isotherms above the critical point in a p-h diagram means that there is a pressure maximising the COP. Consequently, a slight change in the high side pressure, can result in a relatively large change in specific enthalpy after the gas cooler. At the same time will the change in specific enthaply at the inlet be relatively small, due to the approximately linear isentropic process of the compressor. Kauf states that the maximising COP occurs when the partial derivative of the COP with respect to the high side pressure (p_H) is equal to zero;

$$\frac{\partial COP}{\partial p_{\mathrm{H}}} = \frac{-(\frac{\partial h_3}{\partial p_{\mathrm{H}}})_{\mathrm{T_3}}(h_2 - h_1) - (\frac{\partial h_2}{\partial p_{\mathrm{H}}})_{\mathrm{s}}(h_1 - h_3)}{(h_2 - h_1)^2} \stackrel{!}{=} 0 \ . \tag{1}$$

Here, state 1 refers to the compressor inlet, state 2 to exit compressor/inlet gas cooler and state 3 to outlet gas cooler.

2.1.2 Thermodynamic losses

As may be observed from Figure 2.2, the heat rejection curve for the supercritical case matches the heating-up curve of the heat sink better than for subcritical operation. This means that there are less thermodynamic losses associated with heat rejection of the supercritical fluid, represented as the area between the curves. The heating-up curve in Figure 2.2 is typical for heating of air or water. This makes

systems with supercritical heat rejection very suitable for heat pump purposes, or heating of domestic hot water (DHW) [7]. On the other hand, if the heat is rejected to an evaporating fluid, the area between the heat rejection curve and the heating-up curve will be larger, and consequently the losses.

The expansion process in a conventional refrigeration cycle is characterised by its isenthalpic operation, i.e. the specific enthalpy before and after the expansion are equal. The throttling involves frictional losses due to the kinetic energy caused by the pressure drop across the valve. These frictional losses relates to an increase in specific entropy. Figure 2.4 illustrates throttling losses related to expansion of R134a, R410A and CO_2 (R744). When CO_2 systems operates transcritically there is a large difference between the rejection and absorption pressure. As a result, the losses due to expansion are enormous relative to synthetic refrigerants (R134a and R410A) with the same operating conditions. In fact, as much as 40% of the energy losses in a CO_2 transcritical system can be caused by the expansion valve [15]. This massive exergy destruction rate gives the opportunity of utilizing work recovery expansion devices, to recover some of the energy and to better the system performance.

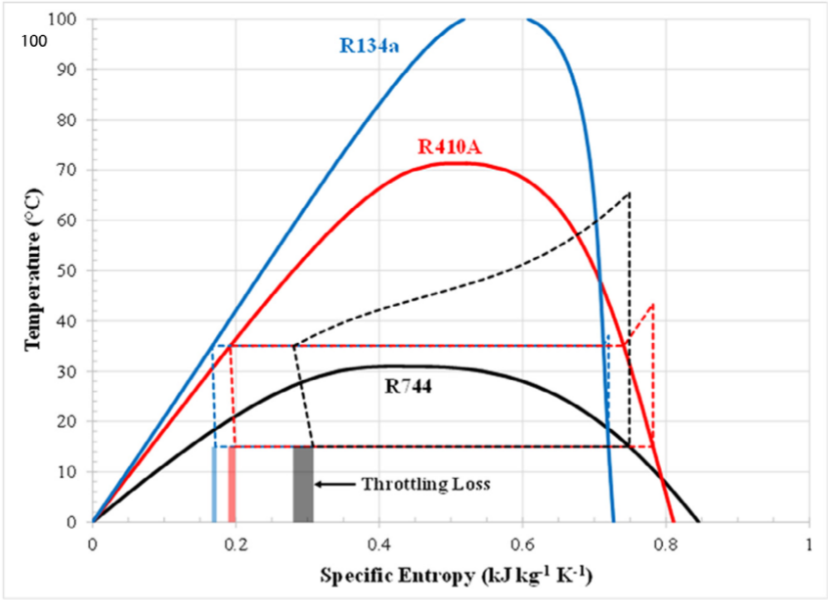

Figure 2.4: T-s diagram showing throttling losses in a vapor compression refrigeration cycle utilizing R744 (CO_2), R410A and R134A. [16]

2.2 CO_2 refrigeration systems

Figure 2.5 shows three schematic drawings of three different transcritical CO_2 cycles. They represent an evolution of CO_2 refrigeration system [17]. They are all designed for the same job, but have some important differences in configuration and components. Note that they are designed for supermarket application, but the principles applies to other applications as well. The first system, the "Booster" cycle, is similar to a conventional refrigeration system with two different evaporator pressures. After the gas cooler the CO_2 is throttled to an intermediate pressure and enters a liquid receiver. The liquid from the receiver is sent to the evaporators where it is throttled to the specified evaporator pressures. The pressure in the low temperature (LT) evaporators are lower than in the medium temperature (MT) evaporators, thus the CO_2 from the LT evaporators has to be compressed up to MT evaporator pressure. Here it meets the CO_2 from the MT evaporators, before being compressed up to high side pressure again

by the MT compressor. The vapor from the intermediate pressure liquid receiver is sent directly to the suction of the MT compressor through a by-pass valve.

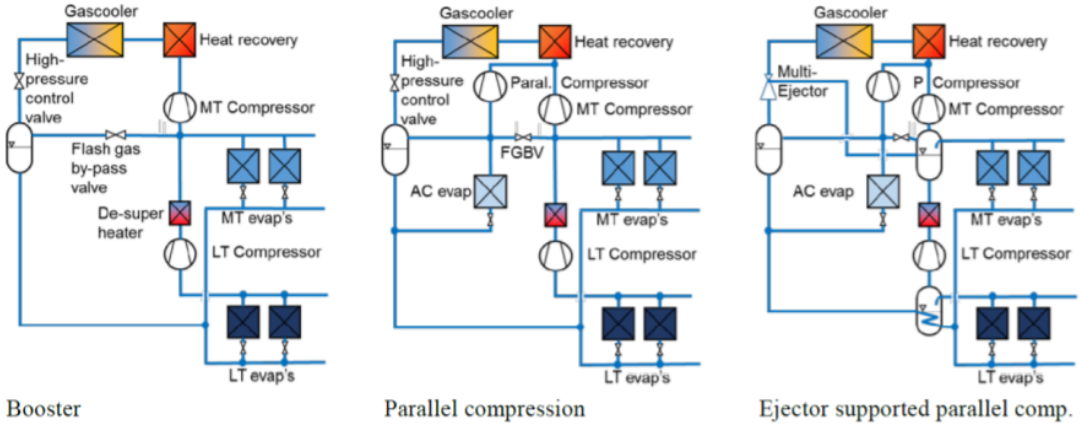

Figure 2.5: Three generations of transcritical CO_2 refrigeration systems for supermarket applications. [17]

The "Parallel compression" system is a way to moderately improve the efficiency of the "Booster" system [17]. It relies on a parallel compression rack, which directly compresses the vapor in the intermediate pressure liquid receiver to the high side pressure. This removes the unfavorable throttling of the vapor, only to compress it right away again. This configuration still has the by-pass valve, which is opened when there is not enough vapor in the tank for the parallel compressor to operate. How much this configuration improves the "Booster" design depends on the operating conditions, but the amount of flash gas in the receiver will increase with increasing heat sink temperature. This consequently favours a system with parallel compression.

The "Ejector supported parallel compression" system is the third generation. It introduces the multi ejector concept to recover some of the energy during expansion. As seen in Figure 2.5, a multi ejector replaces the expansion valve, and two receivers are introduced upstream of the MT compressor and the LT compressor. The working principle of a the multi ejector is described below, in Section 2.3, but the purpose is to pre-compress some of the refrigerant from the low pressure side. This means that the suction pressure of the parallel compressor can be much higher than that of the MT compressors, resulting in a more energy efficient system. As a consequence, the MT compressors will get more and more unloaded as the heat sink temperature rises. The multi ejector can both pre-compress vapor and liquid. The latter opens the possibility to operate the evaporators in flooded mode, meaning higher evaporator temperature and pressure, resulting in higher efficiency [17].

2.2.1 Internal heat exchanger

The impact of introducing an internal heat exchanger (IHX) into a refrigeration cycle has been done for many different refrigerants [18]. The cooling of refrigerant exiting the gas cooler and corresponding heating of refrigerant upstream of the compressor, gives two offsetting effects: Greater cooling capacity due to additional cooling after the gas cooler, and greater compressor work due to higher suction temperature. The combination of these gives a net positive thermodynamic benefit for some refrigerants, and negative for others [18]. This means that the influence of an IHX on the overall system performance depends on the refrigerant and its properties [7][18]. Furthermore, it also depends on the configuration and components in the system.

When employing an IHX in an ejector supported refrigeration system, there are several effects influencing the performance. In addition to the two fundamental offsetting effects, will an IHX increase the entrainment ratio, e.i. the suction- motive mass flow ratio, of the system, resulting in a reduced pressure lift and consequently an increase in compressor work. Combining these effects results in some situations where an IHX increases the system COP and others where it is decreased. A study by Zhang et al. [19] investigated the influence of intergation an IHX in an ejector supported system. It concluded that the system only had higher COP, relative to a similar system without an IHX, at low gas cooler pressures. This can be seen in Figure 2.6. Here, the blue and red curve represents a IHX ejector system with 0.8 and 0.6 IHX efficiency, respectively. The black curve represents a similar system without IHX. From the figure it may be seen that when the outlet temperature from the gas cooler is 40°C, the system COP is higher with an IHX for a gas cooler pressure up to approximately 90 bar. Furthermore, the point where the COP gets less shifts to higher pressures with increasing gas cooler outlet temperature. It is also worth noticing that the IHX efficiency does not seem to influence the COP much. A final note, there is a jointly agreement in the literature that the optimum high side pressure is decreased when employing an IHX.

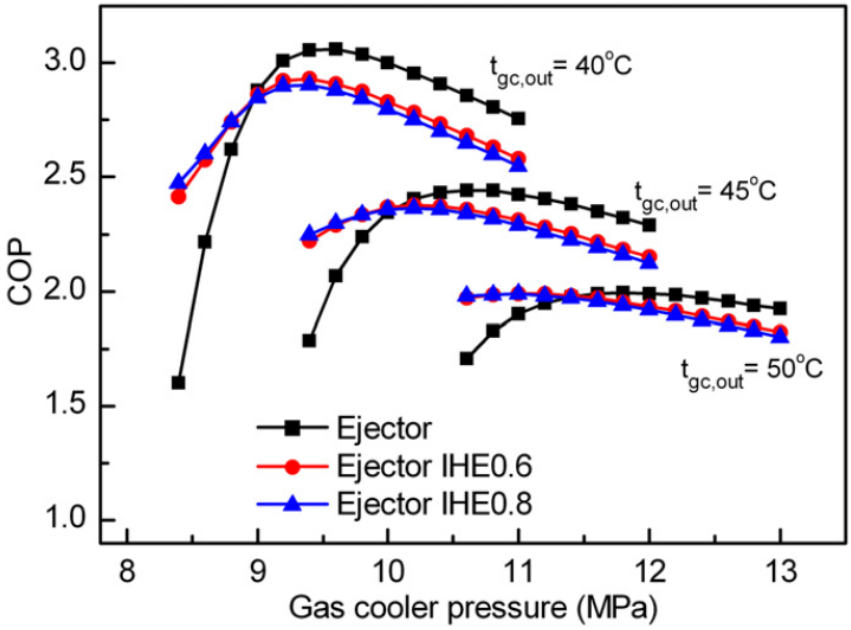

Figure 2.6: How COP is influenced by gas cooler pressure. Blue and red curve is ejector supported systems with IHXs having 0.8 and 0.6 IHX efficiency, respectively. The black curve is a similar system without an IHX. [19]

2.3 Ejector

As stated above, there are great expansion losses associated with CO_2 systems. For this reason, expansion devices, like ejectors, which can recover some of this lost energy is of particular interest. In section 2.2 the purpose of the ejector was briefly described. In this section it will be described deeper. To better explain the ejector, its design and working principle is illustrated in Figure 2.7.

The ejector has two inlets and one outlet. One high pressure stream (P_H) enters at the back, this is often termed "motive flow". And one low pressure stream (P_L) enters at the side, often termed "suction flow". The high potential pressure energy in the P_H stream is converted into high velocity kinetic energy through a nozzle. The high velocity after the nozzle causes a drop in static pressure (P_S), resulting in

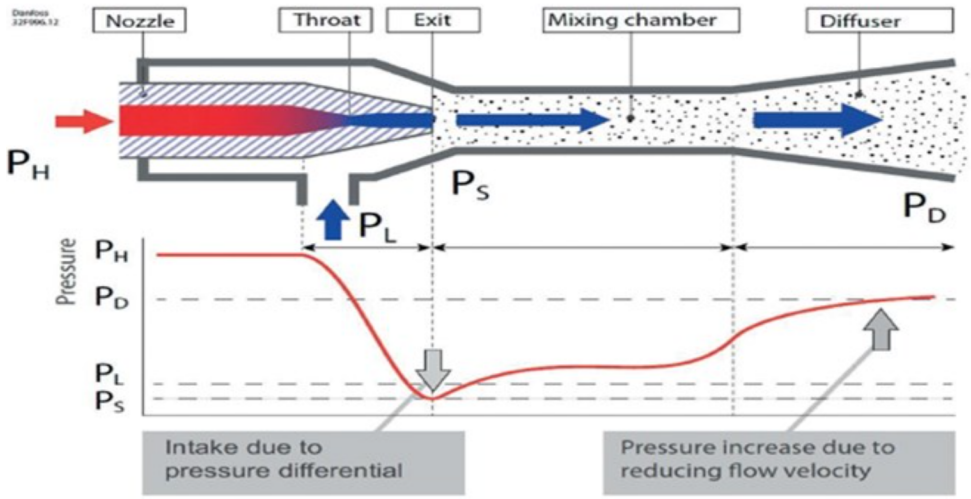

Figure 2.7: A section view and the working principle of an ejector. [20]

suction of the low pressure flow. The two flows enters the mixing section, where they are mixed before entering the diffuser. The conical design of the diffuser decelerates the mixed flow and thereby increase the static pressure. The flow then leaves the ejector through the outlet. The corresponding pressure levels to the different processes inside the ejector, is illustrated at the bottom of Figure 2.7. Here it may be seen that the motive flow (P_H) lifts the suction flow pressure from P_L to P_D, and therefor has recovered some of the energy from the expansion. A conventional expansion valve is characterised by its isenthalpic process, meaning that the internal energy is constant. This is not the case for an ejector where its converted into kinetic energy, and are therefor comparable with an isentropic process [13] [21].

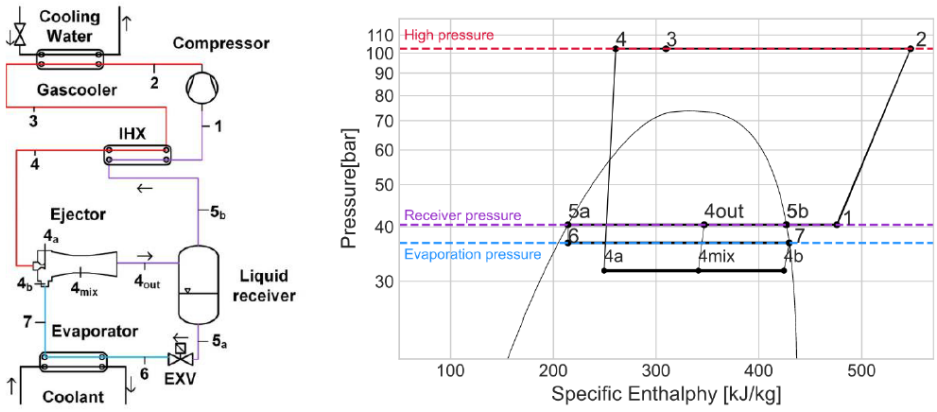

Figure 2.8: A basic configuration for a transcritical CO_2 ejector cycle, with corresponding log(p)-h diagram. [13]

Figure 2.8 shows a basic transcritical CO_2 ejector cycle. From this it can seen that the motive flow comes from the gas cooler and that the suction flow comes from the evaporator. They get mixed in the ejector and are discharged to a receiver. From the receiver the vapor is directed to the high side and the liquid to the low side of the cycle. Figure 2.8 also shows the process in a log(p)-h diagram. Here it can be easily seen that the cycle operates at three different pressure levels, and that the high side pressure is above the critical point, i.e. the cycle is transcritical. Another interesting observation is how the refrigerant is lifted from the evaporator pressure in point 7, to the receiver pressure in point 4out. This is caused by the ejector, and is the same process described above in this section. By using an ejector and

not a conventional expansion valve one will experience two fundamental positive effects on the system. Firstly, the ejector contributes to the compression of the refrigerant. This means that compression from absorption pressure to rejection pressure is not solely done by the compressor. Hence, less compression work is needed. And secondly, since the ejector process is more comparable with an isotropic process, there will be an reduction in flash gas at the outlet. Hence, a greater specific cooling capacity is available for the evaporator [13].

Ejectors are not a new technology, in fact Henry Giffard invented the condensing type back in 1858. And already back inn 1931 it was proven that a two-phase ejector could improve the performance in refrigeration systems [21]. Ever since the reinvention of trancritical CO_2 systems the last decades, the performance is considered to be improved by ejectors [21]. Another great thing about the ejector is the fact that there are no moving parts. This results in a simple component with relatively low investment costs and maintenance [22].

2.3.1 Multi ejector

Since a single ejector has no moving parts, it is not able to control its geometry and therefore not the high side pressure [21]. In order to do so, either an adjustable needle based ejector or a multi ejector can be adopted. The former works by having a needle which extends into the throat of the nozzle. The high side pressure can then be controlled by changing the throat area. The lowest high side pressure is obtained by fully retracting the needle. A drawback with the adjustable needle based ejector, is the increasing losses as the needle reduces the area. This compromises the ejector efficiency, thus also the system performance [21]. The other alternative is to introduce a multi ejector. To better explain the function and concept of the multi ejector a section view is shown in Figure 2.9.

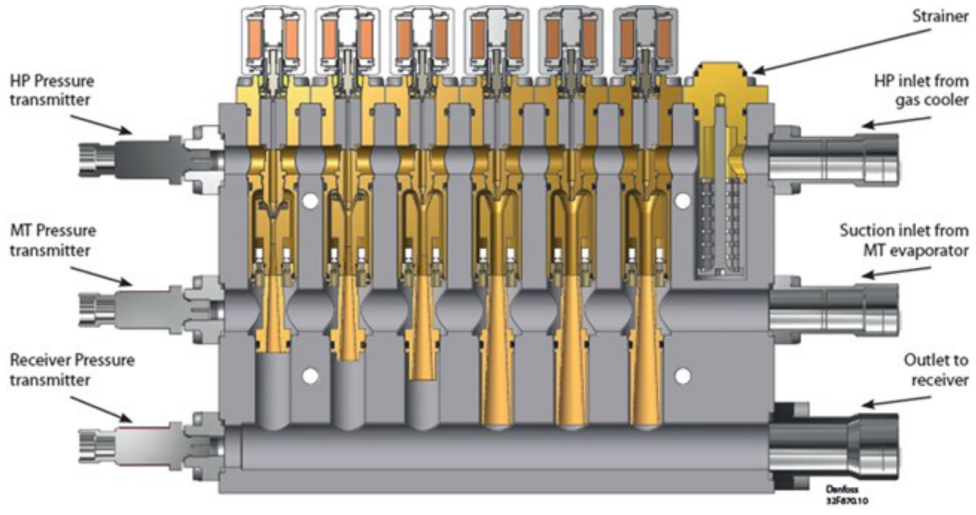

Figure 2.9: A multi ejector and its components. [20]

The multi ejector shown in Figure 2.9 consists of six ejectors in parallel. On the right side there are two inlets and one outlet. The inlet at the top is for the high pressure motive flow, the inlet in the middle is for the low pressure suction flow, the outlet at the bottom is the intermediate pressure discharge flow. At the top there are six solenoid valves, one for each ejector, and a strainer, which the high pressure motive flow passes through, eliminating the need for external filters [20]. On the left side there are three pressure transmitters, one for each flow. The pressure transmitters are, together with other sensors in the

refrigeration system, coupled to a controller which decides which ejectors to open to meet the demanded capacity. As the controller activates a solenoid valve, the motive flow enters the corresponding ejector and is accelerated through the nozzle. The low static pressure generated from the high velocity fluid opens a check valve, and pulls in the low pressure suction flow. The two flows then get mixed prior deceleration in the diffuser, it is then discharged through the outlet port. A benefit of a multi ejector is its compact design and the elimination of additional valves to prohibit backflow, which is necessary when installing single ejectors.

As may be seen from Figure 2.9 are the parallel ejectors of different sizes. This is to have capacity control. The ejectors are binary coupled of varying capacities. For the specific multi ejector shown in Figure 2.9, the first four ejectors (from left to right) have a capacity of 6 kW, 12 kW, 25 kW and 50 kW, respectively. The remaining two ejectors have 50 kW capacity too. This provides a total of 193 kW of refrigeration capacity, which means that systems with greater demands have to couple more multi ejectors in parallel. The binary coupling for this multi ejector allows for 32 different capacity modes, from 0 kW to 193 kW, each separated by 6 kW capacity steps. This means that the demand dictates which ejectors that opens. The different steps are shown in Figure 2.10, here ejector 1 is the smallest ejector in Figure 2.9.

The ejectors inside the multi ejector in Figure 2.9 are vapor ejectors. The motive flow is a supercritical fluid, and the suction flow is vapor. But it exists other types of ejectors as well; two-phase ejector, condensing ejector and liquid ejector [21]. The latter is a promising concept which can increase the refrigeration system performance even further. Normally the evaporators has to superheat the refrigerant some degrees to protect the compressor. This means that the final part of the evaporator has to be dedicated to superheat the refrigerant. By adding a liquid ejector the evaporators may be flooded, in other words, increase the massflow into the evaporators. The liquid exiting the evaporators will than be pumped back to the intermediate pressure receiver by the liquid ejector [23]. The overfeeding allows for higher evaporator temperatures, about 4-6 K compared to systems with superheat control [23]. This results in reduction of expansion, compression and heat exchange losses. With overfed evaporators the energy savings in the system may be as high as 15%, because the performance of the evaporators have been maximized [23].

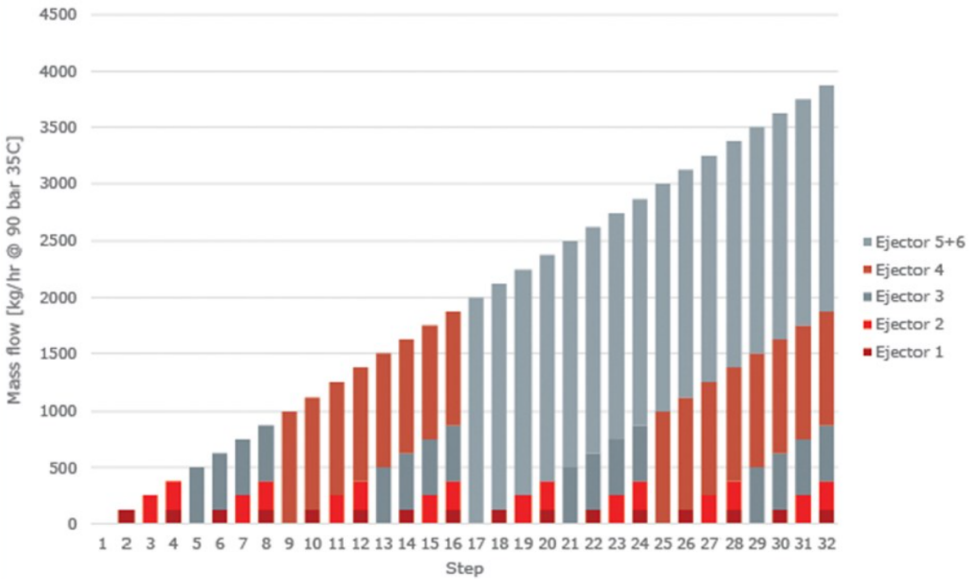

Figure 2.10: Multi ejector capacity control. [20]

The introduction of the ejector is especially relevant for situations where the heat sink temperature is high, i.e. in warm climates. This is due to the high pressures related to CO_2 systems in these situations. Li and Groll et al. [24] reported a COP improvement of up to 16%, for a CO_2 air condition system with an ejector compared to a conventional expansion valve refrigeration cycle. Their study where conduct with a heat rejection pressure of 100 bar and a gas cooler outlet temperature of 40°C. Ozaki et al. [25] reported COP improvements of 20% when employing an ejector, with ambient temperature of 35°C. Deng et al. [26] performed an energy and exergy analysis on an ejector supported CO_2 refrigeration system, and compared with a conventional throttling system. It was found that the ejector system increased the COP by 22%. It was also found that the ejector reduced the exergy destruction due to expansion by 34.29%. All in all are the literature jointly agreed upon that ejectors better the COP of CO_2 refrigeration systems.

2.4 Heat recovery from CO_2 refrigeration systems

Today, a higher degree of system integration is pursued to get the most energy effective and environmentally friendly systems, as well as reducing the operational costs, maintenance and investment. Hence heat recovery from a refrigeration system should be employed if there is a heating demand present. This section briefly describes the control strategy that should be applied when recovering heat from a CO_2 refrigeration system. The control strategy is adopted from Danfoss et al. [27].

Heat recovery is normally employed by having a heat exchanger dedicated for this purpose after the compressor as the first gas cooler, like shown in Figure 2.5. Here, normally water is utilized as cooling medium which again can for instance be used for space heating or as DHW. The priority of refrigeration system is always to supply enough cold. With that in mind, the following measures can be applied in the following prioritised order.

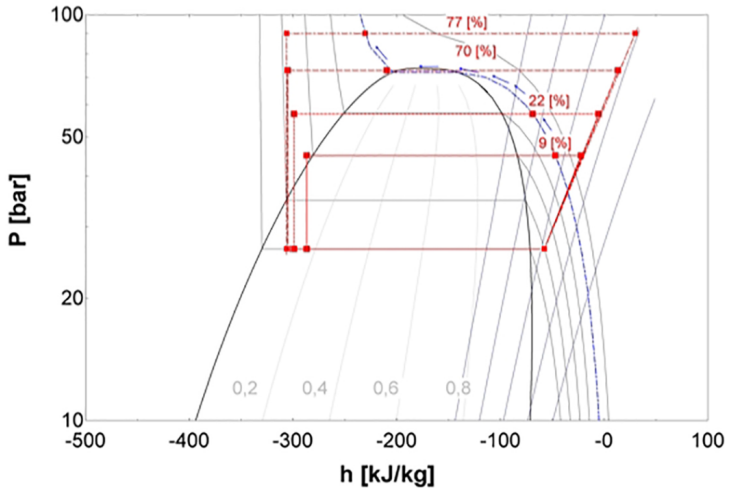

Figure 2.11: Heat recovery from a co_2 refrigeration system. [27]

With the refrigeration system operating at the highest COP without any heat recovery as the point of origin, the first measure will be to engage the heat exchanger for heat recovery. This is done by turning a three-way-valve, so refrigerant enters the heat exchanger, and switching on the water pump. The speed of the pump is controlled by the water exit temperature to satisfy the set point temperature. As shown in Figure 2.11 the share of recovered heat is small, thus if this not satisfy the heat demand, the next measured is engaged.

The next step would be to increase the condenser/gas cooler pressure. By doing so, more heat is possible to reclaim as illustrated in Figure 2.11. At the same time the compressor work is increasing, thus there is a trade off between increasing heat recovery and increasing compressors work. Due to the gradient of the isotherms increasing drastically above the critical pressure, there is a point where even higher pressure wont pay off [27]. The increasing pressure also allows the water exit temperature to increase if needed, due to higher compressor exit temperature.

To recover even more heat the system specific cooling capacity has to be decreased. In this measure the fan- or pump speed for the cooling medium inside the gas cooler after heat recovery would be decreased. The result is an increase in gas cooler exit temperature, hence a reduction in specific cooling capacity. Now, more of the heat may be reclaimed and the decrease in cooling capacity has to be compensated with an increase in refrigerant mass flow. The maximum amount of heat recovered occurs when the gas cooler is bypassed [28].

If the heat demand is still not met, more drastic measures like a false MT evaporator may be employed [28]. But this is not relevant for this work, and is therefore not considered.

2.5 Thermal energy storage

Thermal energy storage (TES) is the process where thermal energy is added to a medium and discharged later when needed. It can be used to both store cold or hot thermal energy. There can be many different reasons for applying TES, but it is often due to a mismatch between available energy and energy demand, or because of great energy peaks. There are three common types of TES; latent heat storage, sensible heat storage, and thermochemical energy storage [29]. The two former will be briefly explained below.

2.5.1 Sensible heat storage

Sensible heat storage (SHS) is the simplest method of storing thermal energy. The principle is to heat or cool a liquid or solid medium. Examples are molten salts, sand, rocks or water, with water being the most popular medium. Among other things, this is due to water being inexpensive, having high specific heat, being non-toxic and can be pumped [30]. The total amount of stored thermal energy in a medium depends on temperature difference, specific heat capacity (c_p) and the mass (m), and is given by the following equation;

$$Q = m \int_{T_1}^{T_2} c_p \, dT \tag{2}$$

Where T_1 and T_2 are the initial and final temperature, respectively.

As water is the most common medium utilized, are water tank storage a well-known technology. It is a very cost effective option and may have a very good efficiency when ensuring good isolation and stratification [30]. Stratification is important since a typically system will contain multiple tanks in series like shown in Figure 2.12. Here, all tanks, expect from the first and last, are coupled from the top to the bottom of the next one. When tank 1 is discharged, cold water is charged at the bottom of tank 4. If the stratification is poor, the discharged water from tank 1 will not be as hot as required, resulting in a poor efficiency. Thus, its important to have good diffusers at the inlet of all tanks to prevent mixing

which will compromise the stratification.

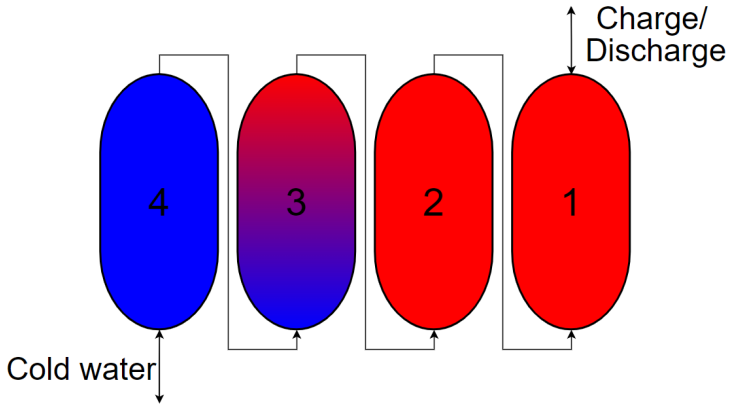

Figure 2.12: Water tank sensible heat storage.

2.5.2 Latent heat storage

Latent heat storage (LHS) has gained more attraction then SHS recently. This is due to its high energy storage density, which can be up to 14 times greater than SHS [29], and it enables approximately constant temperature thermal energy storage [30]. LHS utilizes a so called phase change material (PCM) to store energy. The PCM undergoes a phase change when the thermal energy is charged or retrieved. The amount of energy stored is based on the material latent heat of fusion [30], hence thereby the name. The latent heat of fusion is how much energy that is need to be added/retrieved for the material to undergo the phase change. The amount of energy stored in a system (Q) is given by the following equation;

$$Q = m \int_{T_1}^{T_{\mathrm{pc}}} c_{\mathrm{p,s}}\, dT + mL + m \int_{T_{\mathrm{pc}}}^{T_2} c_{\mathrm{p,l}}\, dT \ . \tag{3}$$

Here, m is the mass of the PCM, L is the latent heat of the phase transition, $c_{p,s}$ and $c_{p,l}$ are the specific heat capacities for solid and liquid phase, respectively. T_1, T_{pc} and T_2 represents the temperature initially, during phase change and finally, respectively. So, the first and the last part of the equation represents any sub-cooling and superheating of the material. And the middle part represents the phase change.

LHS can use a PCM either changing phase between solid and liquid or liquid and vapor. The latter often involves a greater latent heat of fusion than the former, but the huge density difference between liquid and vapor makes it more challenging [30], thus the former is more convenient. There are many different properties to consider when choosing a PCM, Veerakumar et al. [29] summarised some of them. First of all should the melting/evaporation temperature be around the operating conditions. Further, it should have a high density, heat of fusion and thermal conductivity. This is to have large capacity and enable easy charging/discharging. The PCM should have low volume change during phase change, be less corrosive to system materials and have low degree of supercooling. The latter is the temperature difference between maximum heat flow during melting and freezing as illustrated in Figure 2.13. Moreover is it important that it is chemical stable and has low degradation, so the PCM properties doesn't change and compromises its performance. And finally, its a benefit if it is easily available and inexpensive.

It exists many types of solid-liquid PCMs and they are usually divided into three groups; organic, inorganic

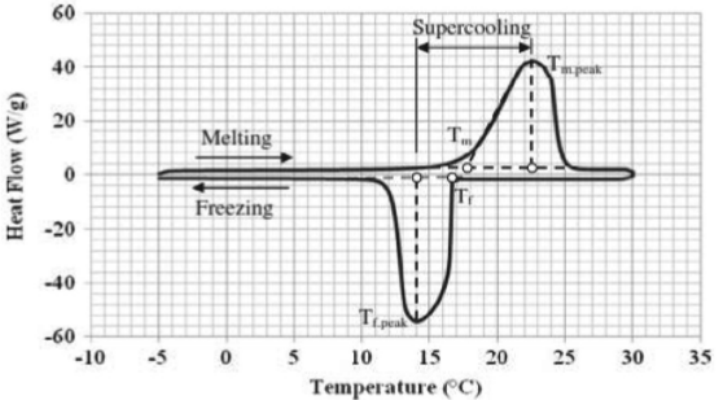

Figure 2.13: Freezing and cooling curves of av PCM illustrating supercooling. [29]

and eutectic. Organic PCMs are compounds which are carbon based, and they are further divided into paraffin and non-paraffin. They are recognized by being chemical stable, non-corrosive and with little or no supercooling [29] [30]. The inorganic PCMs are generally hydrate salts and metals. They are recognized by their good thermal properties and low degradation, but they can be corrosive to the system materials and need more maintenance [29] [30]. The eutectic PCMs are mixtures of the two other groups, both within the groups, but also across them. A crucial PCM property is the melting point and by having a mix it can be influenced and tailored to the application [29]. For high temperature applications metal alloys, molten salts and paraffin is used, for medium temperature organic and hydrated salts and for low temperature storage ice and water gels are applied [30].

3 Cruise ships as application area

This section summarize the factors making cruise ships different from other application areas. Further, a typical cruise ship energy distribution is examined, and finally a typical HVAC system, which is the origin of the AC cooling demand.

3.1 Important factors to consider

Applying technology to a cruise ship is interesting in many ways because it differs very much from other industries. First of all, because of its hotel facilities. These facilities utilize a significant amount of the total energy on board. This is in contrast to other ships, where propulsion is the only dominant system. The hotel facilities generates a great demand for electrical and thermal energy, in parallel with the mechanical energy demand from the propulsion system. A second aspect making ships quite unique, is the isolated operation. Obviously, during sailing, the ship is not connected to any external energy source. This means that it has to relay on the technology on board to generate the required energy forms. This has to be done from the energy carriers on board, which often is the fossil fuel only. A third aspect is its mobility. Cruise ships are designed to sail long journeys, exposing it to very different climates. This means that the technology on board, like the refrigeration systems, has to operate with very different conditions and loads. Obviously, a cruise far north generates less cooling demand in the colder conditions, and a cruise at the equator has a great cooling demand in the warm climate.

Mechanical energy is demanded from the propulsion system. Either it is directly from the propellers, or from generating electricity. The former is typical for conventional cruise ships utilising marine diesel. The latter is related to gas-electric ships, which are expected to be more common with the introduction of liquefied natural gas (LNG), as the limitations on nitrogen and sulphur oxides and restrictions on CO_2 emissions are expected to get stricter [13]. Today, the heat generated by the propulsion system is normally used to cover the heat demand from the hotel facilities [31]. This is done by using economizers to generate steam. Future ships may not use fuels that generates heat to the same extent, which means that it is important to recover heat from other processes on board as well [13]. The ship hotel facilities also require mechanical energy to generate the demanded electricity, independently on the propulsion system. One of the main electrical utilizers are the AC system. Thus, it is important to design the AC system as efficient as possible, because it influences the fuel consumption, and thus the ship emissions [13].

Furthermore, a typical cruise involve very contrasting days. Some are in ports, others are at sea at near maximum propulsion. All of which often resulting in a mismatch between energy availability and demand. The generated heat from the propulsion system is not available when the mechanical energy is low. When sailing in tropical climates at high speeds, heat is readily available, but the heat demand is very low. As a consequence, to make the cruise ship as efficient as possible, at all times, the processes on board needs to be flexible and agile to respond to the varying availability and demand of energy. Historically many ships has relied on boilers and auxiliary engines coupled to generators to generate the thermal and electrical energy. Today a higher degree of integration between energy systems are emphasised [31].

A final note is that the cruise industry earn their profit on customers. This means that it is important to have a compact design to maximises the number of cabins. On the other hand, may efficiency be the driving argument when designing processes to a ship, as it reduces the operational costs.

To be able to reach the climate goals, the cruise industry also needs to contribute by reducing its emissions. This is especially important for the propulsion system as it is the greatest contributor. A promising alternative to conventional combustion engines is to implement fuel cells. Compared to conventional combustion engines, fuel cells have some limiting factors. It is associated with longer start up times and a lower response ability, making it less agile to energy demand fluctuations [32]. Additionally the fuel and systems requires a significant increase in investment costs. Therefore, a thorough and comprehensive analysis of the ship's energy demand is vital, to prevent mismatches between supplied and demanded energy and to keep the system size and costs as low as possible.

To summarize, there are many factors which has to be considered when applying technology to cruise ships. Hence a thorough investigation is important when designing one. However, this work is not designing systems for a specific ship, but is revealing the potential from the investigated systems, which again can be used when applying this technology on specific ships.

3.2 Energy distribution

Typically, when a ship is designed, the energy demand is estimated through a load balance approach [32]. This is done by estimating the energy demand for all energy consumers, and then all systems is designed for the energy peak load. The load balance approach estimates the energy demand by examine different modes, e.g. at sea running at maximum speed, at sea running at design speed, in harbor etc. For every mode the energy consumption of each component is estimated, and further added together to find total energy demand for each mode.

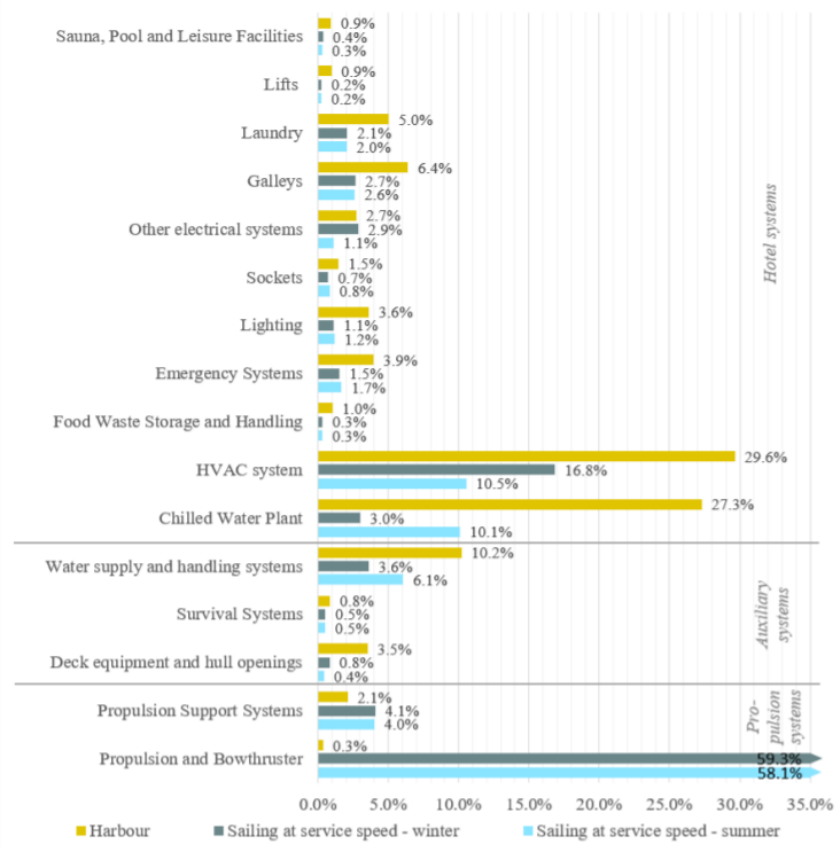

Figure 3.1: The energy proportion of different systems on board a fuel cell driven cruise ship. [32]

Through a load balance approach, Boertz et al. [33] calculates the power demand for a fuel cell driven cruise ship. The results are illustrated in Figure 3.1. As may be seen, during sailing, the propulsion system has the greatest power demand, followed by the HVAC system and chilled water plant (AC system). When in harbour, the HVAC system and chilled water plant are the only dominant power utilizers, demanding almost 57% of the total ship power. Underling the importance of designing these systems as efficient as possible.

When applying the load balance approach the energy demand for each mode is given as a steady state operation, it does not reflect anything about the dynamic energy demands occurring during different cruise ship operations. This has been sufficient for a conventional combustion engine cruise ships, not for ships with new technology like fuel cells [32]. Thus a comprehensive energy analysis that includes dynamic loads is required when designing modern ships.

3.3 HVAC system

As the AC system supplies chilled water to the HVAC system. One first needs to understand the HVAC system, to understand the origin of the AC cooling demand.

The HVAC system is responsible for processing the air in all rooms on board a cruise ship. It has to be able to meet the comfort requirements at all times, including temperature, humidification and little noise. Additionally, it should be as small and compact as possible, due to the space limitation. Together with the outdoor temperature and weather, the HVAC system design and configuration generates the ship‘s cooling demand. Thus, common HVAC designs will follow.

Independent on the supplied room, the air treatment normally works in two stations, separated from each other. Firstly, the air is passed through an air handling unit (AHU). The purpose of the AHU is to supply fresh air for air exchange [13]. It is decentralized and supplies several areas/rooms at the same time. Therefore, there is a second station for each area, located directly in each area or in the duct system [13], enabling the possibility to individually tune the supplied air.

A simplified schematic of an AHU is shown in Figure 3.2. Fresh air firstly enters a recovery device. This is a rotatory heat exchanger which recovers enthaply from the exhaust air in the form of temperature and humidity [13], normally with an efficiency in the range of 70-90% [34]. Further, the air is heated or cooled in fin and tube heat exchangers, prior being supplied to the second station. If the air needs to be humidified, there is a humidifier downstream of the heater. The heat exchanger which cools the air, also acts like an dehumidifier, and in extreme climates, another cold heat exchanger may be installed, dedicated to dehumidification only [13]. The hot water supplied to the AHU is mainly generated by the exhaust gas from the engine or by auxiliary boilers. Chilled water is generated by a AC system, often referred to as the chilled water plant.

The second system unit, which is supplied by the AHU, is dependent on the comfort requirement of the supplied area. In terms of air quality, passenger cabins are considered the areas with the highest standards [13]. The cabin climate needs to be able to be changed in a simple and quick way, and since several cabins are supplied by the same AHU, each of the cabin climates shall not be influenced by their neighbour cabins. Thus, a fan coil unit (FCU) is employed. Figure 3.3 shows a simplified schematic of a FCU, and how it can be integrated. The supplied air from the AHU is mixed with air from the FCU, before it is discharged into the cabin. The amount of circulated air is dependent on the desired room climate and the state of the supplied air. It is only circulated enough air to thermally influence the

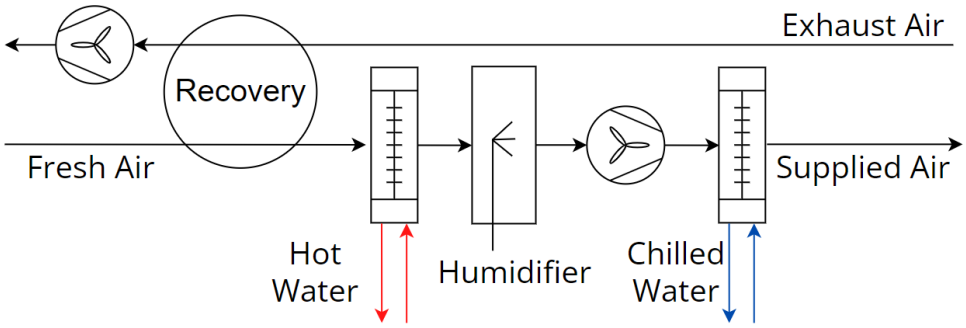

Figure 3.2: A simplified schematic of an air handling unit (AHU).

supplied air when mixed. The cooling within the FCU is done by chilled water, and the heating by an electrical heater. A major advantage of this solutions is a quick response to changes in desired climate conditions, and the temperature range that can be covered [13]. Additionally it reduces the number of AHUs, and the size of ducts and chillers [35]. On the other hand, the FCUs needs connections to chilled water, adding to the pipes already required by the AHUs [13].

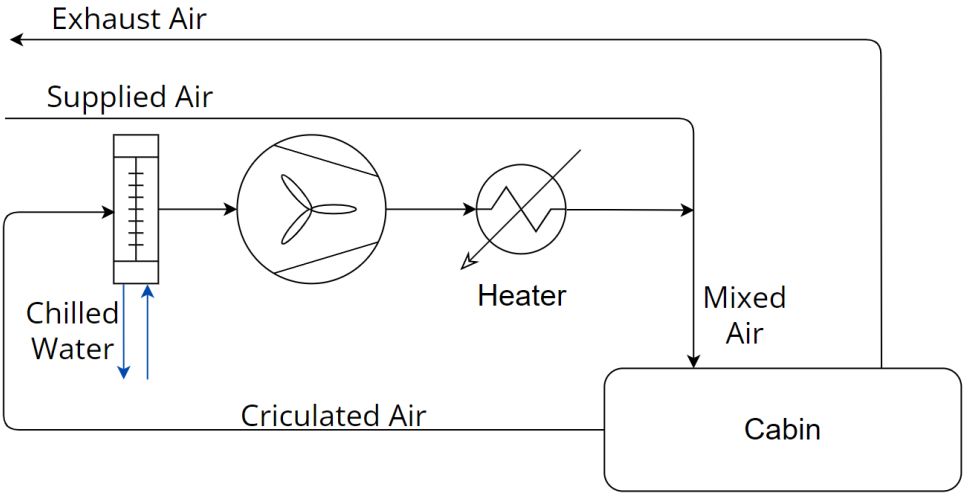

Figure 3.3: A simplified schematic of a fan coil unit (FCU).

In areas where the comfort requirements are less, FCUs are not necessary. Instead more simple cabin units can be installed [13]. Cabin unites are a very compact, and usually only able to heat the supplied air with an electrical heater. This means that most of the conditioning has to be done by the AHU, resulting in a longer response time to changes in desired climate conditions. Additionally, since the cabin unit only is able to heat, the supply air temperature from the AHU has to be equal or less than the area with the lowest desired temperature. This can result in area temperature being influenced by each other. Additionally this solution generates greater air flow from the AHU, resulting in higher noise emission, which has to be compensated by silencing equipment [13]. Areas where cabin units are applicable are typically in crew cabins, staircases, toilets, corridors etc [13]. Furthermore, for large areas FCUs and cabin units may be combined to supply the desired climate conditions. This is typical for areas like restaurants, galleys, lounges etc. [13].

4 Reference case

To be able to conclude on the system applicability and performance, it should be applied on specific scenarios. Furthermore, the scenarios should be representative of real applications. Thus, reference cases are defined in this section. It is very time consuming to design and calculate comprehensive and representative reference cases for a cruise ship. Thus, they are based on collect data from literature. The cases for the AC system, provision system and the CTES are defined separately. However, they have many similarities, especially when it comes to environmental conditions.

4.1 Air conditioning

To the author's knowledge, it exists very few studies on passenger ships AC cooling demand. Thus, the reference cases are based on two studies, Ancona et al. [36] and Boertz et al. [33].

The study conducted by Ancona et al. [36] is of a 177 m long and 28 m wide passenger ship traveling between Stockholm and Mariehavn in Sweden. The purpose of the study was to optimize to load allocation on the energy systems on the ship, maximise the energy efficiency and minimize the heat dissipation and fuel consumption. As a part of the work, energy demand was gathered through measurement and calculation. This was done for winter, spring/fall and summer. Since this work is focusing on summer conditions, data from here are the one of interest. The mechanical, electrical, heat and cooling demand are shown in Figure 4.1. The process of gathering this data was elaborated in greater detail in [31].

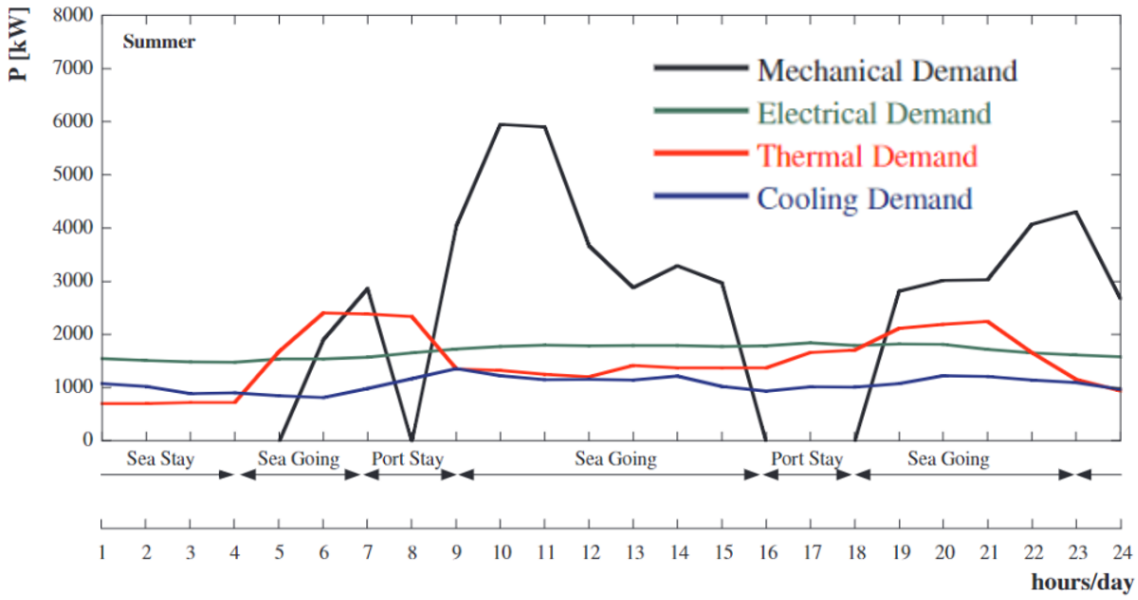

Figure 4.1: Typical load curves for a cruise ship in Sweden during summer [36]

The ship makes the same route every day. As indicated by the timeline in Figure 4.1, the operational mode can be divided into port stay, sea going and sea stay. The ship leaves Stockholm around 06:00 PM, after reaching open sea, it stops for some hours prior reaching Mariehavn early in the morning. It leaves again one hour later and arrives back in Stockholm 04:00 PM. The different operational modes is obviously influencing the mechanical demand the most, while the cooling load is more constant, with an average value of approximately 1000 kW, and a peak load of almost 1400 kW occurring at 09:00 AM. This reference case is referred to as the cold reference case, and in this situation the system has to be

able to operate with an ambient temperature rang of 21-14 °C, and a sea water temperature of 16 °C, which corresponds to typical temperatures in Stockholm during summer [37].

Further its necessary to define cases in hotter climates. As already briefly addressed in section 3.2, Boertz et al. [33] calculated the energy demand of a 139 m long and 22 m wide fuel cell driven expedition cruise ship. This was done for different types of operational days, in different climates. However, the cooling demand is only explicitly listed for a day with constant sailing at design speed. The hottest investigated climate was with weather data collected from Singapore, the resulting cooling demand curve is shown in Figure 4.2. As may be seen, the load is relatively constant with an average demand of 3617 kW and a maximum of 4090 kW. The load profile is discussed later in this section. This reference case is referred to as the warm reference case, in this situation the system has to operate with an ambient temperature range of 31-26 °C, and a sea water temperature of 30 °C, which are typical temperatures in Singapore [37].

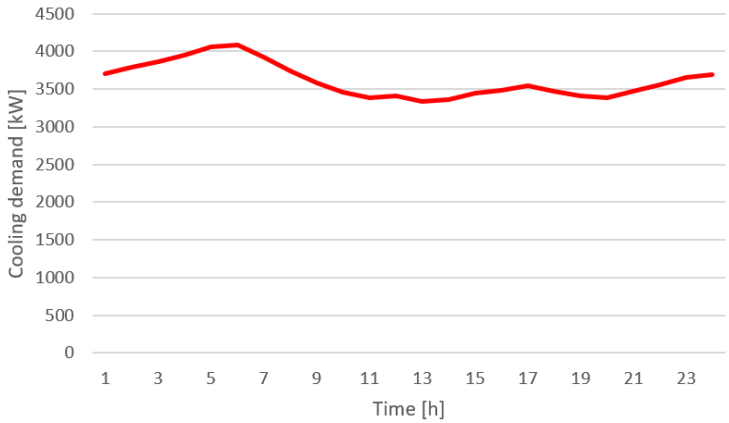

Figure 4.2: Typical cooling demand for a cruise ship in Singapore during summer. Cooling load collected from [33].

Furthermore, Boertz has calculated the cooling demand with weather data from Amsterdam during summer. However, these conditions are similar to the conditions for the cold reference case. Although the cooling demand was calculated for Amsterdam climate, the profile is fairly similar to the Singapore case. Therefore, to get a case in between, the demand was linearly interpolated on the basis of weather data collected from Barcelona during summer. The resulting cooling demand curve is shown in Figure 4.3. As expected, this demand is fluctuating less then the warm case with an average load of 2721 kW, and a maximum load of 2935 kW occurring at the same time as the warm case. This case is referred to as the medium case. During this case the system has to operate in ambient temperatures in the range of 27-20 °C, and a sea water temperature of 23 °C [37].

Figure 4.4 shows the three different cooling demands in the same plot. Firstly, the load profile for the warm and medium case is quite similar. However, for the cold case, the cooling demand is fluctuating more, although it has the coldest environmental conditions. This is due to the cold case being from a ship operating with different operational modes during the day, i.e. in port, sea going and sea stay. The cooling demand of a ship is mostly influenced by the environmental conditions, crew- and passenger behaviour [33], thus the unloading of people in port makes the cooling demand for the cold case fluctuate more. Whereas, for the two hotter cases, the ship is sailing at constant speed, i.e. the passengers are on board the ship all the time.

Furthermore the position of peak load is interesting. For the two hottest cases it appears early in the

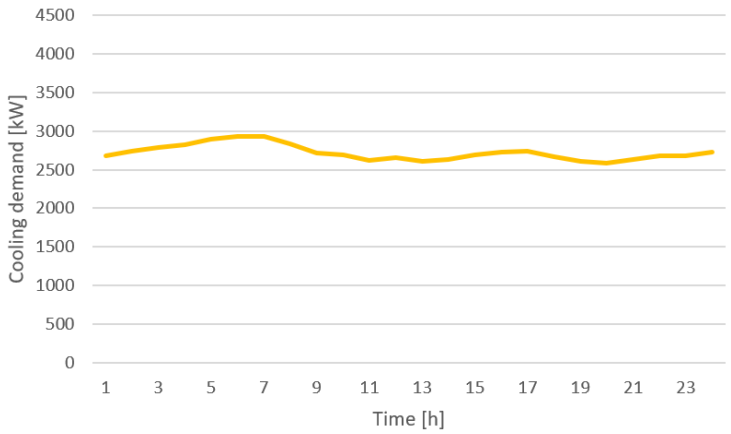

Figure 4.3: Typical cooling demand for a cruise ship in Barcelona during summer. Cooling load based on values collected from [33].

morning. This is due to several factors. Firstly, the passenger cabins are only supplied with 100 % fresh air when occupied [33], which is the case during night and early morning. Secondly, the ventilation in public spaces are switches off night mode, preparing the indoor climate for the day. And thirdly, crew and passenger activity starts. When everything is considered together the peak load emerge in the morning hours [33]. In contrast to the two hottest cases, the cold case does not have the same cooling demand during the night. The relatively cold environmental conditions reduce the need of cooling the air before it is supplied. Instead, the peak emerges after leaving port, when passengers have boarded the ship. The key values for each reference case is listed in Table 4.1.

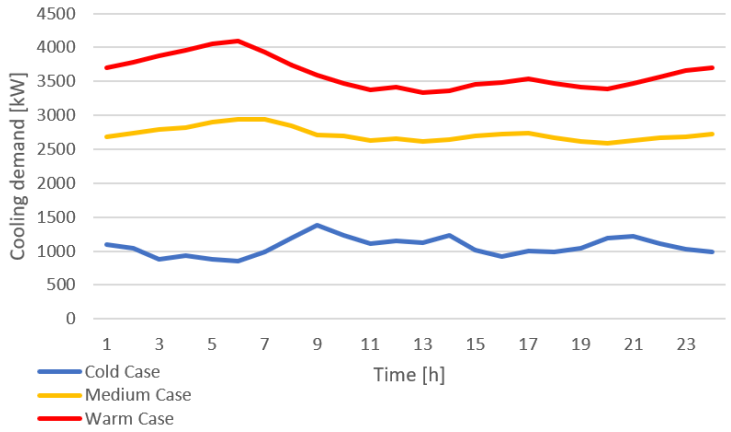

Figure 4.4: The cooling demand for the three different cases. The cooling load of the two hottest cases are collected and calculated from [33]. The cooling load for the cold cases is collected from [36].

Table 4.1: A summary of key values from the air condition reference cases. Values collected and calculated from [33].

Reference case		Cold	Medium	Warm
Ambient temperature range	°C	21-14	27-20	31-26
Sea water temperature	°C	16	23	30
Average cooling demand	kW	1065	2721	3617
Maximum cooling demand	kW	1375	2935	4090
Minimum cooling demand	kW	851	2590	3340

4.2 Provision cooling and freezing

The total amount of provision on board a cruise ship is very dependent on the route the ship is sailing. Some ships visit very small harbours and even sail to remote places to lie on anchor, while others sail the same weekly route every time. Obviously the former cruise would need more provision storage capacity then the latter. Further, ships can either fully supply at the start of the cruise or resupply along their route. However, since the logistics associated with loading a cruise ship with provision are immense, and high standards of food quality and reliability has to met. The food is usually ordered several months in advance. Therefore most ships fully supply prior cruise start, at its port of origin [38].

It exists very little information, at least to the author's knowledge, about the amount of provision needed on board a cruise ship. Therefore, it is assumed that the ship would need a food capacity equivalent to a medium sized supermarket. Additionally, it is assumed that the activity is low, and that the provision is already chilled/frozen when it is stored, i.e. loading and unloading does not influence the cooling and freezing demand. It is also assumed that the construction and placement of cabinets and rooms result in a constant heat leakage, i.e. the cooling and freezing demand is constant. The cooling and freezing demand are collected from Tosato et al. [39], where a medium sized supermarket of approximately 1750m^2 was studied, hence 90 kW of cooling and 22 kW of freezing is demanded. The system will operate under the same environmental conditions as the AC system. As a result, are three different cases with the same load, but different environmental conditions created. The key values for each case are listed in Table 4.2.

Table 4.2: Key values for the three different cases for provision cooling and freezing. Cooling- and freezing load collected from [39].

Reference case		Cold	Medium	Warm
Ambient temperature	°C	21-14	27-20	31-26
Sea water temperature	°C	16	23	30
Cooling load	kW	90	90	90
Freezing load	kW	22	22	22

4.3 Cold thermal energy storage

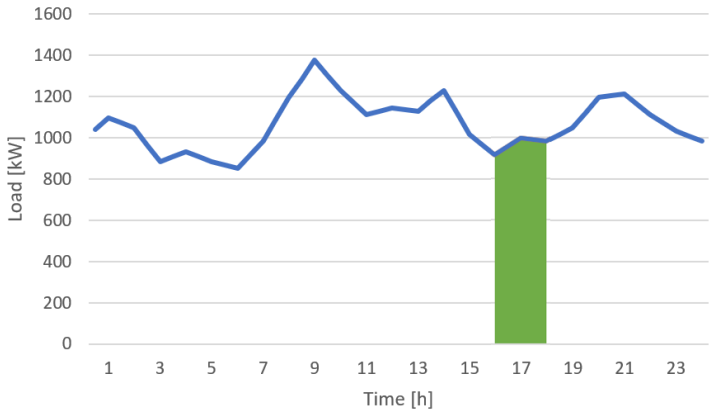

Figure 4.5: The cooling demand of the coldest AC reference case, and the cooling demand that is to be covered by the CTES (green shaded area).

Since the ship in the coldest reference case in Figure 4.4 includes port stays, it is convenient to collect data for the CTES from here. In the study [36], where the cooling demand for the coldest AC reference

case is collected, the demanded cooling during the port stays can be found. The ship has two port stays, one hour in the morning and two hours in the afternoon. From the cooling demand of the second port stay it can be found that the CTES will have to supply 1914 kWh of cold, with a peak load of 998 kW during a two hour port call.

Figure 4.5 shows the cooling demand of the coldest AC reference case, represented by the blue fluctuating curve, and the cooling demand that must be supplied by the CTES, indicated by the green shaded area.

5 System design and configuration

The following subsections will discuss important aspects to consider, different configurations and possible features of the final designs. Performance is investigated through literature, and by modeling and simulating systems in the dynamic simulation software Dymola, with components from libraries supplied by TLK Thermo. Finally, the schematics of the final designs are presented.

5.1 Important aspects to consider

When developing a refrigeration system, different aspects has to be considered. They are very dependent on what situation the system is to be applied. Thus, all cases has to be considered individually. However, performance and costs will always be key aspects. They are normally very dependent on each other, e.g. an increase in performance may mean more components, resulting in greater investment costs, and poor performance often equates greater operational costs. Performance and price has to be balanced in a way that satisfies its user and investor. Many different configurations may be able to get the job done, but the goal is always to find the one which performs best, to a reasonable price.

System performance is most commonly measured through its coefficient of performance (COP). This indicates the useful cooling or heating provided in relation to the required work input. The COP is more discussed and later defined in section 6.3. Consequently, higher COPs equates better performance. Furthermore, another performance factor is the ability to work with different boundary conditions, i.e. different heat sink temperatures and different cooling demands. As discussed above, the mobility of a cruise ship exposes it to very different climates, which the system has to be able to perform in. The COP may be impressively high in one situation, but if it is not able to satisfy the demands in others, it is not a well performing system. Additionally, the system has to be agile in responding to the fluctuating demand, generated by changing environmental conditions and the daily activity on board the ship.

Costs is something which is inevitable to consider when developing a system. The system configuration influences the investment costs and its performance, and further, the performance influences the operational costs. Thus, there can be a trade off between greater investment costs and less operational costs, and vice versa. Consequently, it is important that this is thoroughly investigated to avoid a situation where a great investment do not pay of in the long run. However, due to time limitations and investigations done through simulation, cost analysis is out of the scope of this thesis and only taken into consideration on a brief and simple level.

Another important aspect to consider for a cruise ship application is the system size. Since shipping companies earn their revenue on passengers, the on board systems has to be small and compact in order to make space for passenger facilities. Thus, compact solutions should be prioritized. Like discussed in Section 2.1.1, the thermodynamic properties of CO_2 result in CO_2 systems being smaller. So, in this relation, CO_2 is a great option. Further, the compactness of the system is dependent on the number of components and their mechanical assembly. Thus, as compact assembly as possible would be beneficial, but due to maintenance purposes, this is impractical. Therefore the mechanical assembly has to be investigated carefully when designing a system. However, it is out of the scope of this thesis. As a consequence, like for costs, the size aspect is only taken into consideration on a brief and simple level.

5.2 AC- and provision system

Prior designing the systems, the framework which they have to be capable to operate within has to be set. The work intend to show that a CO_2 refrigeration system is suitable as an AC chiller and for provision cooling and freezing on board cruise ships, as an environmentally friendly and safe alternative. The following list of requirements has to be met by the designed AC- and provision system.

- Cover the cooling demand related to air conditioning through generation of 6°C chilled water to the HVAC system.
- Operate with a heat sink temperature of up to 30°C. Rejecting heat for heat recovery purposes and to sea water.
- Recover heat through low temperature heating water generation, generating water at 45°C.
- Be as energy-efficient as possible, e.g. utilizing work recovery, heat recovery, optimum high side pressure etc.
- Cover the provision cooling and freezing demand.

Since both cooling demand related to air conditioning and provision is to be covered, it is convenient to establish two separate systems. Firstly, this is beneficial because the thermal energy demand associated with the provision is located in a more confined space, compared to the AC system which needs to supply cold water to the whole ship. Thus it can also be practical to divide the AC system further, into several systems operating in parallel. Furthermore, the AC cooling demand fluctuates, whereas for provision cooling and freezing demand it is constant. Thus, the AC system will need more components than the provision system to be capable to respond to the fluctuating load.

The ejector and especially the multi ejector concept is a technology which is getting more mature, and as discussed in section 2.3, since it recovers some of the compressor work it improves the COP of a CO_2 system. The multi ejector is compact, small and relatively simple, hence making it very attractive for this type of application.

A simple ejector supported system is shown at the left side in Figure 5.1. From the liquid receiver the vapor is compressed up to high side pressure and rejects heat in the gas cooler. The liquid in the receiver is extracted from the bottom, and expanded through an expansion valve before it evaporates in the evaporator. The high side refrigerant enters at the back of the ejector and the refrigerant from the evaporator enters at the side. The ejector discharge flow enters the liquid receiver, completing the cycle.

The diagram in Figure 5.1 shows a typical log(p)-h diagram for the same system. The main factor of this system is that the high pressure flow lifts the low pressure flow from point 7 to point 4. Thus, the evaporator pressure is lower than the compressor suction pressure. This diagram does not illustrate the process inside the ejector, this is illustrated and discussed in Section 2.3. Since the discharge flow from the ejector is a two phase flow, the refrigerant takes one of two ways from the liquid receiver, depending on the phase. This means that there is extremely unlikely that the high side- and low side mass flow is the same. As a consequence may the COP never be calculated from this log(p)-h diagram. To do the calculation the ejector entrainment ratio has to be known, this is the ratio between the low side mass flow and the high side mass flow. The entrainment flow is further discussed and defined below in Section 6.3. The entrainment ratio is also important for the pressure lift of the low side refrigerant, that is the

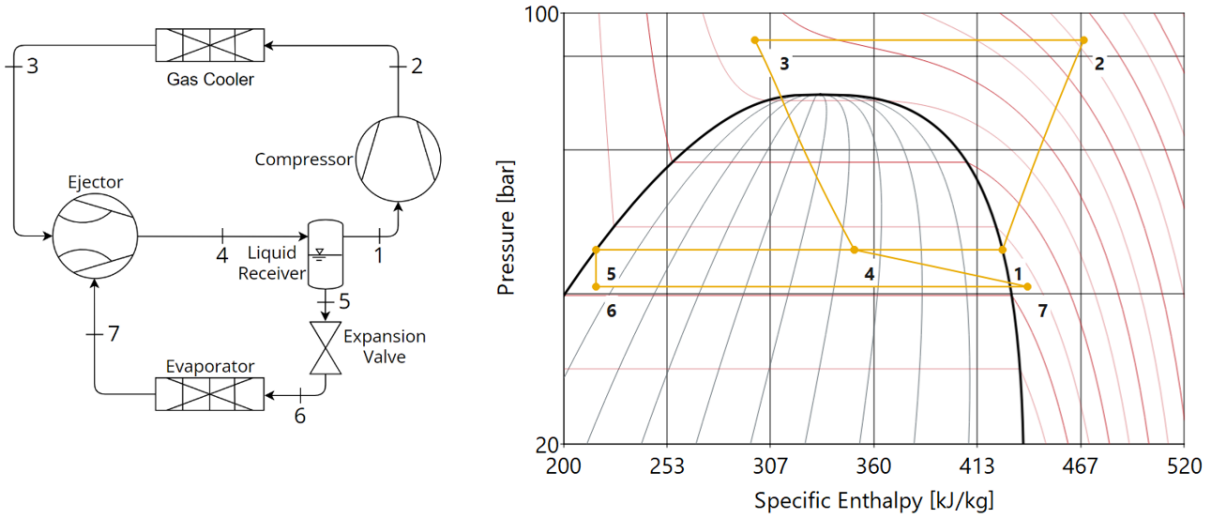

Figure 5.1: A simple transcritical CO_2 ejector supported system. (Left) system schematic; (Right) log(p)-h diagram.

pressure difference between point 7 and point 4. If the entrainment ratio is decreasing, consequently will the pressure difference increase. As point 1 indicates, is the compressor suction flow saturated vapor. In theory, this is not a problem, but it makes the compressor vulnerable to liquid droplets. This is a problem since it may damage and possible ruin the compressor. Hence, some degrees of superheat are beneficial. How the system can secure superheat is discussed below in Section 5.2.1.

It is well known that parallel compression increases the COP of a refrigeration system. A study conducted by Sarkar and Agrawal et al. [40], calculated the COP improvement when employing parallel compression. It was performed with evaporator temperatures 5°C and -45°C, and gas cooler exit temperatures of 30°C and 60°C. It was found that the COP improvement is greatest when operating at lower evaporator temperatures. At evaporator temperature of -45°C and gas cooler exit temperature equal to 30°C, the COP improvement was calculated to 37%. When the evaporator temperature was increased to 5°C the corresponding COP improvement was found to 18%. Hence, it is interesting to investigate what impact parallel compression has on the simple ejector supported system in Figure 5.1.

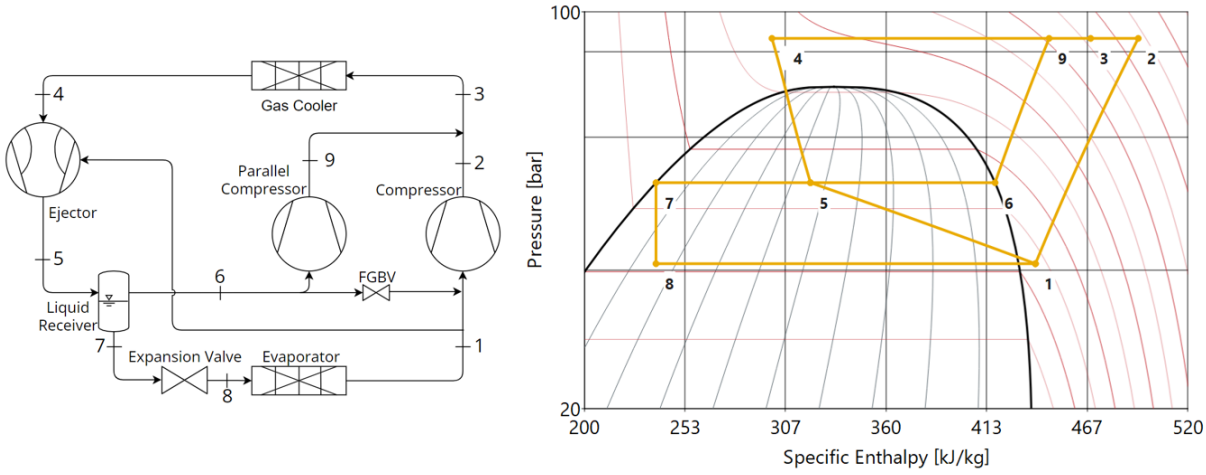

Figure 5.2: A transcritical CO_2 ejector supported system utilizing parallel compression. (Left) system schematic; (Right) log(p)-h diagram.

Figure 5.2 shows an ejector supported system utilizing parallel compression. The gas in the liquid receiver is compressed to high side pressure through the parallel compressor, and the liquid is expanded through an expansion valve prior entering the evaporator. Some of the refrigerant leaving the evaporator is lifted by the ejector, the rest is compressed by the main compressor. The flash gas by-pass valve (FGBV) is opened if the amount of gas in the liquid receiver is to small to run the parallel compressor. The amount of refrigerant lifted by the ejector is dependent on the pressure difference across the ejector. If the gas cooler pressure increases, consequently will the ejector suction mass flow too. If the parallel compressor suction pressure is reduced, the ejector suction mass flow will increase. Thus, the system in Figure 5.2 will become the system in Figure 5.1 under some circumstances, e.g. in warm climates.

To investigate the performance impact parallel compression has on an the simple ejector supported system, both systems were modeled in Dymola as schematically shown on Figure 5.1 and Figure 5.2. Further, both systems were simulated with the same cooling demand and boundary conditions, gas cooler exit temperature was set to 35°C and the evaporator pressure was set to 36 bar. For the systems with parallel compression, the parallel compression suction pressure was specified to 45 bar. The results revealed a reduction of 4% in compressor power. This reduction is relatively small, and when the need for more components in taken into consideration, e.g. one more compressor, FGBV, piping etc., the system in Figure 5.1 is considered a better option.

5.2.1 Internal heat exchange

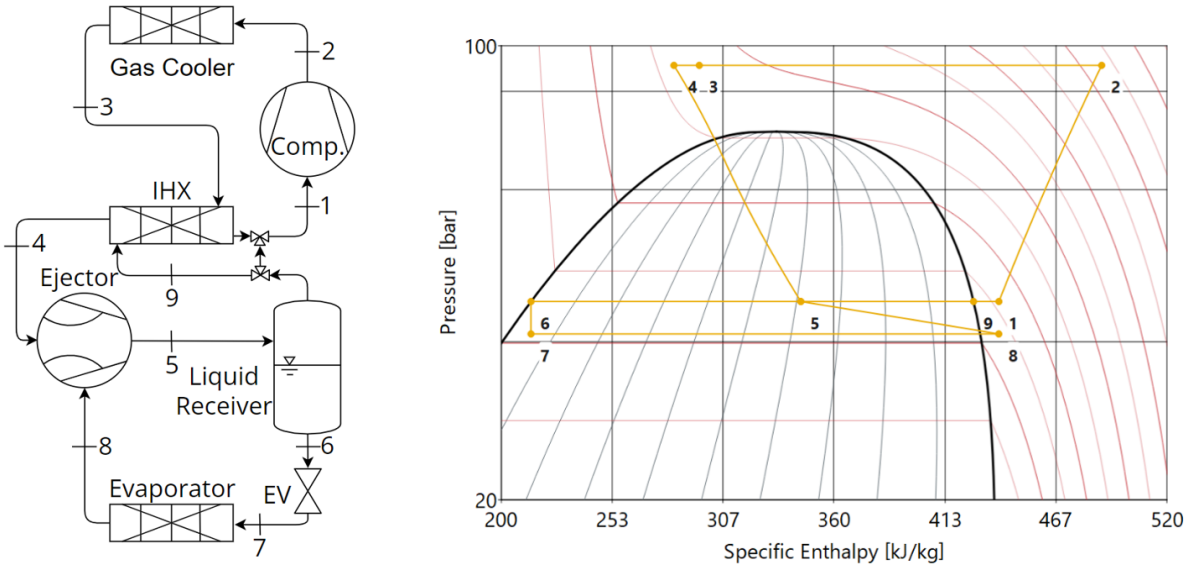

Figure 5.3: Ejector supported system utilizing internal heat exchange.

To protect the compressor against liquid droplets, the refrigerant has to be superheated directly upstream of the compressor. Liquid droplets can damage the compressor, therefore, compressor suppliers require some degrees of superheat, or else the requirements for the compressor warranty will not be met. To superheat the compressor suction refrigerant, an IHX may be employed. In the IHX, refrigerant exiting the gas cooler rejects heat to the compressor suction refrigerant. As discussed above in Section 2.2.1, IHX in an ejector supported system will increase the COP in some situations and decrease it in others. Anyhow, the IHX is necessary to protect the compressor, thus if none other measures have been engaged, an IHX will always have to be utilized when saturated vapour is discharged from the liquid receiver.

A three-way valve is provided upstream of the IHX. Consequently, the IHX may be partially or fully bypassed to control the compressor suction superheat. Figure 5.3 shows an ejector supported system utilizing an IHX. The log(p)-h diagram clearly illustrates the internal heat exchange, i.e. the process from point 3 to point 4 and from point 9 to point 1.

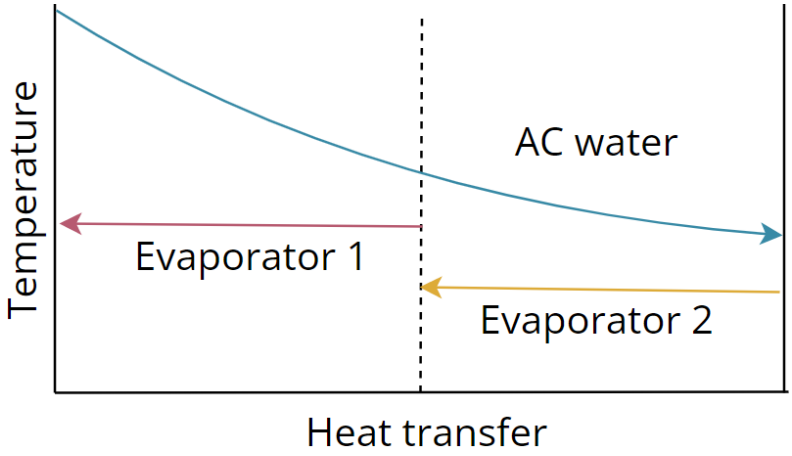

Figure 5.4: Two staged evaporation.

To minimize the exergy losses associated with evaporation, two staged evaporation may be utilized. This is done by having two evaporator temperatures. As shown in Figure 5.4, two staged evaporation decreases the area between the curves in the heat exchangers, thus also the exergy losses. Furthermore, compressor work is reduced due to a higher pressure in one evaporator. Both of these effects influence the system performance in a positive way. On the other hand, both of the pressures needs to fixed. So, if the system utilizes an ejector, the potential pressure lift may not be fully enhanced.

5.2.2 Final AC-system design

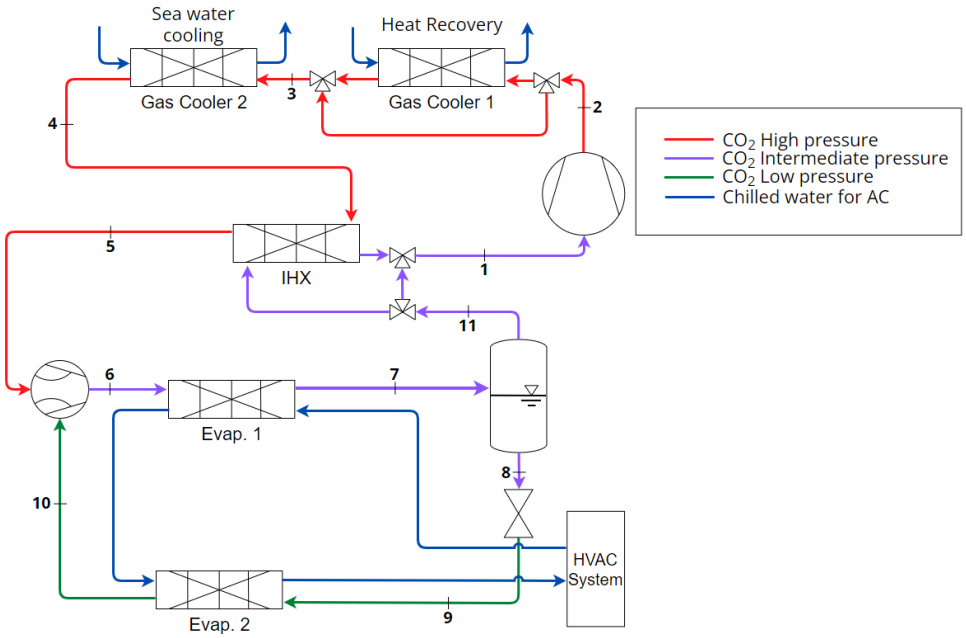

Figure 5.5: A simplified schematic of the final design.

The final design of the AC system is based on the investigations above, and is shown in Figure 5.5. Compared to an actual system, that would have been implemented on a ship, this system is simplified. Due to this work investigating the performance of a CO_2 refrigeration systems through simulation, several simplifications have been made. However, these will not compromise the results. The simplifications are further discussed below in Section 6.1.1. In the schematic, the bold numbers refers to the state points in Figure 5.6.

From the compressor the refrigerant enters the first of two gas coolers, dedicated to heat recovery. Depending on the heat recovery demand, the gas cooler may be fully or partially bypassed through a three-way-valve. The rest of the heat is rejected in the last gas cooler to sea water. The cooled down refrigerant enters an IHX. Here, it is subcooled by the refrigerant upstream from the compressor. For work recovery purposes the expansion device is an ejector. The expansion of the high pressure fluid conveys the refrigerant from the secondary side (suction flow). The discharged flow then enters the first evaporator before it is discharged into the liquid receiver. From here, the liquid is throttled by and expansion valve, which corresponds to the ejector pressure lift. Further, the fluid enters the second evaporator before it is conveyed by the ejector. Due to the ejector being a vapor ejector, the refrigerant needs to be fully evaporated in the second evaporator prior suction. The discharge flow from the first evaporator is a two phase fluid. The vapor from the liquid receiver enters the IHX where it is superheated before it is compressed by the compressor. A three-way-valve is installed to be able to control the superheat of the compressor suction flow.

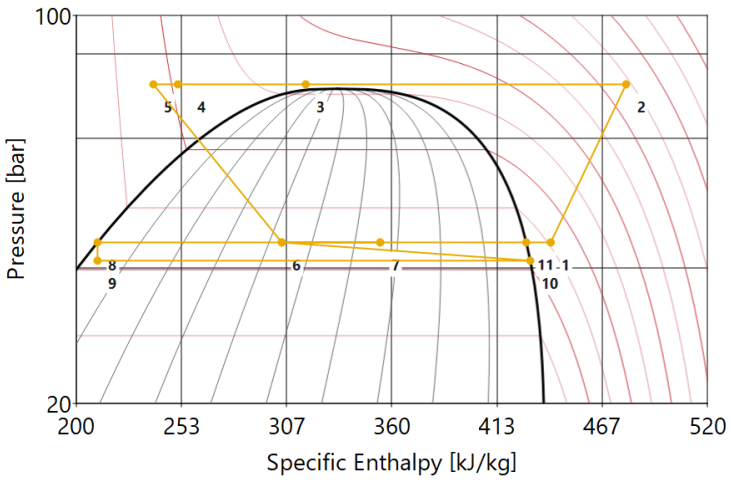

Figure 5.6: A typical log(p)-h diagram for the final AC-system design.

Next, Figure 5.6 shows a typical log(p)-h diagram for the final AC-system design during transcritical operation. It is not very different from the log(p)-h diagrams discussed above, but the implementation of two staged evaporation adds the process from point 5 to 6 in the diagram.

5.2.3 Final provision cooling and freezing system design

The provision cooling and freezing system is shown in Figure 5.7. As for the AC-system the bold numbers refers to the different state point in Figure 5.8. The configuration is an ejector supported parallel compression system. From the MT compressor the refrigerant enters gas cooler 1 for heat recovery. Heat is recovered by cooling water. The rest of the heat rejection happens in gas cooler 2 which utilizes sea water. Further, the refrigerant passes through the IHX where it is cooled further before entering the

ejector. The ejector conveys refrigerant from the suction line of the MT compressor and the mixed fluid is discharged into a liquid receiver. Since the system supplies cold to both cooling and freezing of provision, it has two evaporators which are fed with liquid from the receiver. The pressure in the LT evaporator is lower than in the MT evaporator, hence this refrigerant enters the LT compressor before it is mixed with the refrigerant from the MT evaporator. The vapor in the liquid receiver is drawn by the parallel compressor through the IHX before it is compressed to high side pressure. Due to the ejector, increasing gas cooler pressure shifts compressor work from the MT compressor to the parallel compressor, therefore the MT compressor is not needed in warm climates as long as the receiver pressure is sufficiently low enough.

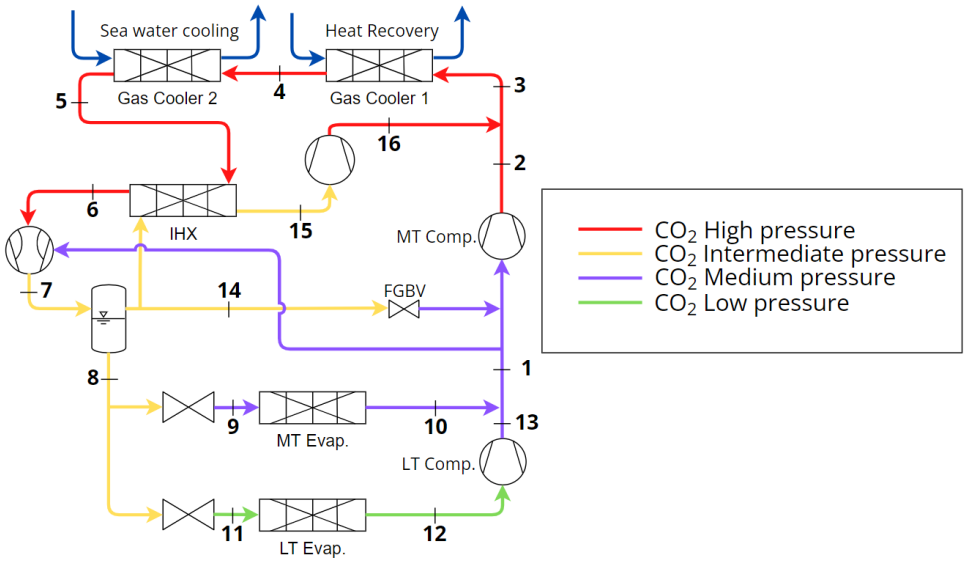

Figure 5.7: A simplified schematic of the final provision cooling and freezing demand.

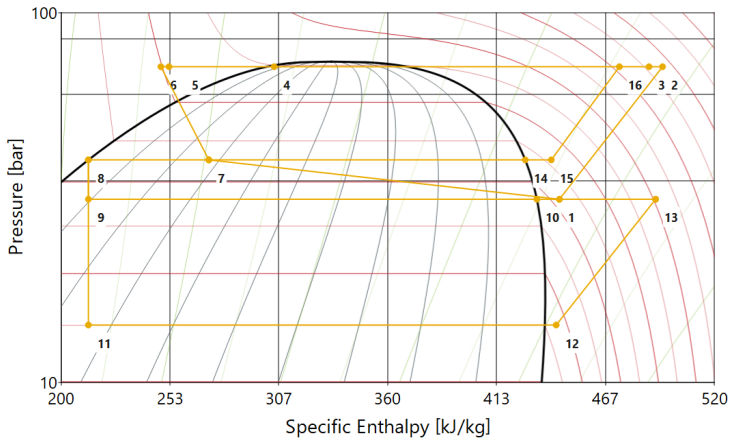

Figure 5.8: A typical log(p)-h diagram for the final provision cooling and freezind system.

Figure 5.8 shows a typical log(p)-h diagram for the provision system. As may be seen, is the system operating at four different pressure levels. The small subcooling after the second gas cooler can also be noted, this is because of the IHX and the relatively small mass flow through the parallel compressor. As the gas cooler outlet temperature increases, consequently will the mass flow through the parallel compressor too and thus increase this subcooling.

5.3 Cold thermal energy storage

There are mainly two types of TES applicable for this situation, i.e. sensible heat storage (SHS) and latent heat storage (LHS). As discussed in Section 2.5 the latter has a greater energy density than the former. In many ways space on board a cruise ship can be seen as a scarce resource, thus the energy density of LHS makes it the obvious choice. LHS utilizes a PCM to store the thermal energy. The criteria which has to be considered when choosing a PCM was discussed in section 2.5.2. For the CTES in this work, water is chosen as the PCM. That is because, firstly water has a melting point around the operating conditions. The HVAC system has to be supplied with 6 °C chilled water. Secondly its relatively high density and very high heat of fusion reduces the size of the system. And thirdly, Water is easily available and inexpensive.

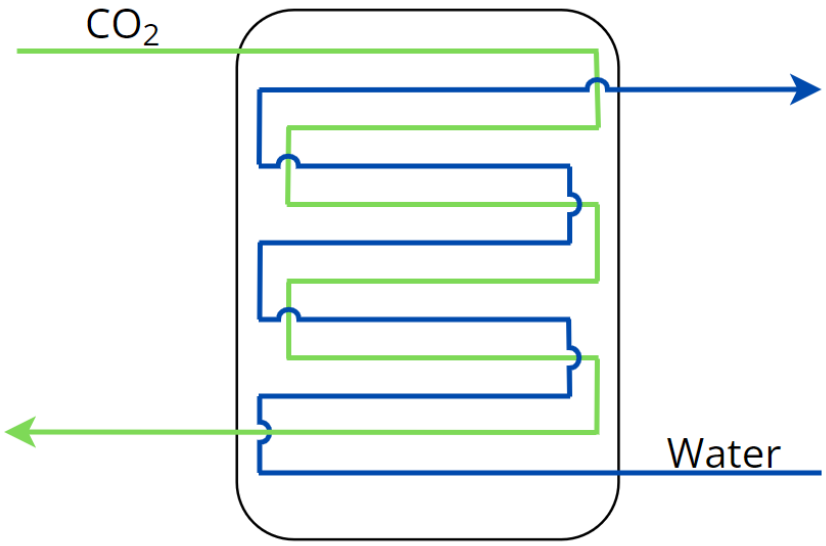

Figure 5.9: Double bundle TES.

The CTES system have to be able to be charged during sailing and discharged in port. The charging will be done by the CO_2 in the AC-system, and the discharging is done by circulating water connected to the HVAC system. As space on board a cruise ship is limited, will the final system contain several CTES systems in parallel. Since the PCM is stored in containers the designed systems will utilize double bundle containers, as shown in Figure 5.9. By having double bundle TES, they can be charged when the AC system is running during sailing, and discharged by a simple water pump during port calls. Thus, the electricity demand related to AC during port stays will be greatly reduced, compared to running the entire AC system.

To investigate what impact CTES charging has on the AC system performance, the AC system is further developed. Figure 5.10 shows a schematic where the AC system configuration is equipped with CTES. When charging is initiated, liquid from the receiver is throttled by a valve before entering the LHS. Downstream the refrigerant is compressed to intermediate pressure, before it is mixed with the refrigerant from the IHX. This figure only shows how one LHS is integrated. With multiple, they would have been connected in parallel. Figure 5.10 also illustrates how the CTES can be discharged. Water from the HVAC system is chilled in the LHS and returns.

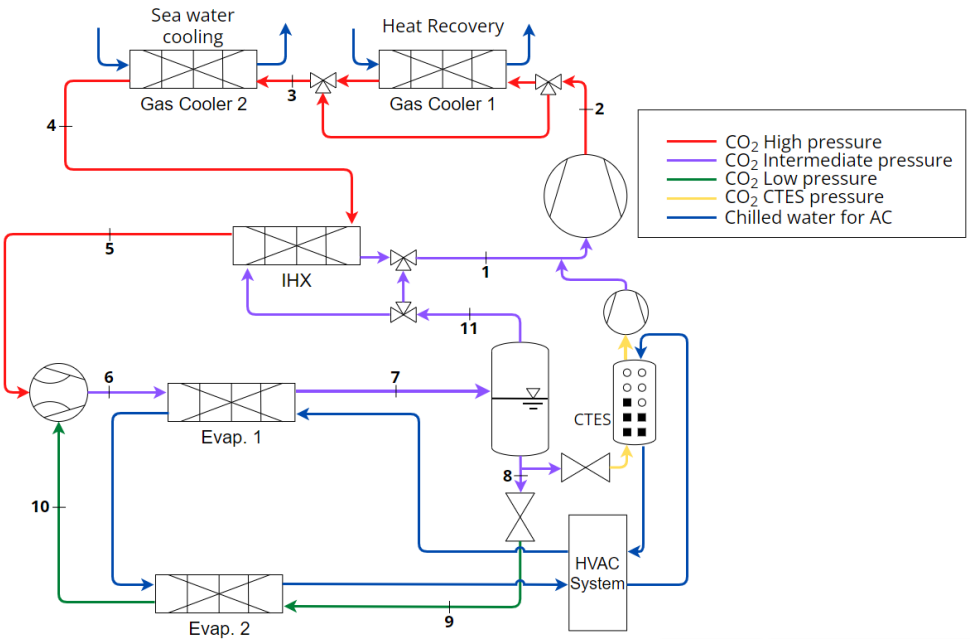

Figure 5.10: A simplified schematic of the AC system equipped with CTES.

When discharging, constant cold supply is pursued together with the capability of absorbing a large amount of heat at a short period of time. Further, during charging, the system should be able to charge over a longer period, so it can be charged without increasing the peak of the overall cooling load for the AC system.

6 Calculation work and modeling

To investigate the performance, all systems have been modeled and simulated in the dynamic simulation software Dymola with components from libraries supplied by TLK Thermo. In the software, the user can specify all boundary conditions and component properties. The thermodynamic equations for each component and refrigerant properties are already specified in the provided library. It is possible to access the equations and properties to change them, however, it has not been done in this work. Dymola generates a Matlab file which can be opened in the visualisation software DaVE, also supplied by TLK Thermo. DaVE can either be used to calculate the desired values or it can generate an Excel file. From here, the desired manual calculations can be performed. In this section, the modeling of each system will be presented and discussed. At the end, the most important equations regarding the results are presented.

6.1 Modeling of the AC- and provision system

6.1.1 Simplifications

To simplify the simulation effort the models have been simplified. The systems are simulated as one large system, but in reality it would have been divided into several systems operating in parallel. This also applies for the different components within the systems, e.g. the compressor would in reality have been a compressor rack consisting of several compressors in parallel. This is something which has to be considered when a physical system is designed, which is out of the scope of this work. Further the models are not considering oil circulation back to the compressor, this is also something which as to be considered for a physical system. Further simplifications, regarding each system, are presented in their respective subsection below.

6.1.2 Assumptions

The system are simulated dynamically, but some values are assumed constant for both systems at every load and condition. The following list summarise the overall assumptions. Other, more specific assumptions are presented in the following subsections.

- The refrigerant outlet temperature from the gas cooler is assumed to be 5°C hotter than the sea water inlet temperature.
- The isentropic efficiencies are assumed to be constant for the compressors, specified to 0.7. The ejector efficiency is set to 0.3. When having only one of each component this is not a good approximation, as they would change under different conditions. But by since each component represent several coupled in parallel, it is a better approximation.
- All processes, except the heat exchangers, are assumed adiabatic.
- There are no pressure losses in heat exchangers or pipes.
- The gas coolers are counter flow plate heat exchangers, with heat transfer coefficient, alpha, assumed to 2000 W/m^2K.

– The power driving the water and sea water pumps are assumed small, and are neglected in all results.

– The vapor and liquid exiting the liquid receiver are assumed saturated.

6.1.3 Modeling of the AC-system

The modeled AC system in Dymola is shown in Figure 6.1. It is modelled according to the schematic in Figure 5.5 in Section 5.2.2. The evaporators are modelled and simulated as heat sources instead of heat exchange with water. This is to better control the system, however, it disables the possibility to investigate the CO_2 stream adsorption curve inside the evaporators. 40% and 60% of the cooling load are supplied by the first and second evaporator, respectively. Since the second evaporator pressure is determined by the ejector pressure lift, basic hand calculations has proven that this allocation is best with regards to the temperature differences in the evaporators, which are set to 6 K. The first evaporator pressure is set to 39 bar, the ejector suction flow is saturated vapor and the IHX ensures 5 K superheat into the compressor.

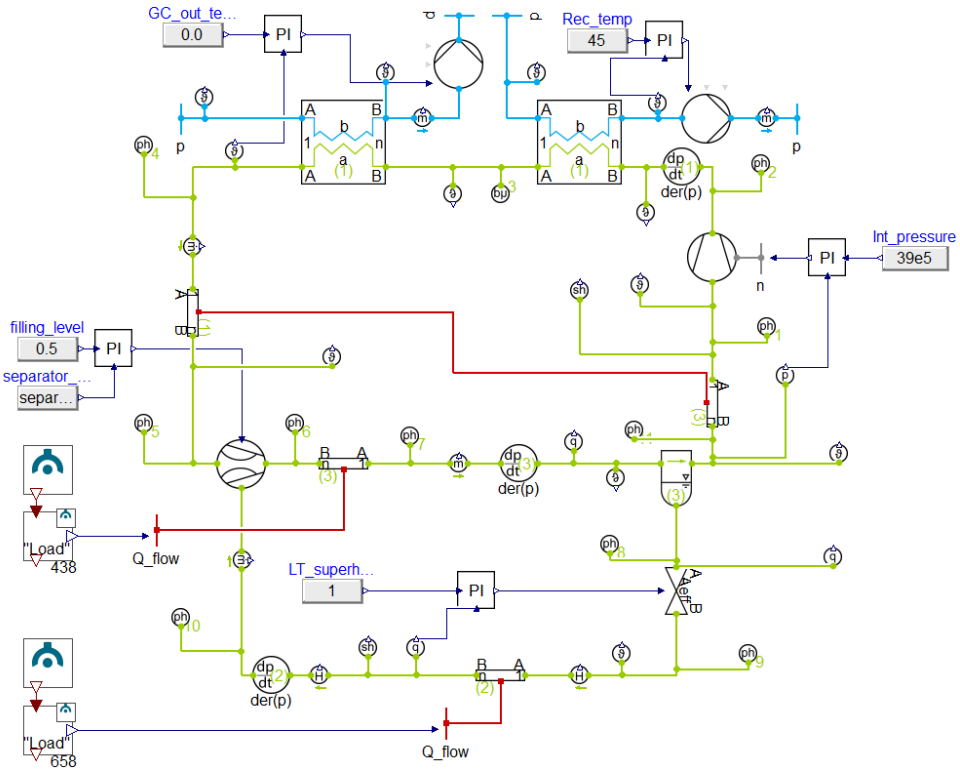

Figure 6.1: The simulated AC system model.

As stated above the first gas cooler is dedicated to heat recovery through generation of 45°C low temperature heating water. It is a plate heat exchanger, and the size and other key parameters are shown in Table 6.1. The inlet temperature of the water in this gas cooler is constantly 10°C warmer than the sea water temperature in every case. This temperature is of course very dependent on many factors, however, the utilization of recovered heat is out of the scope in this work, thus the temperature is assumed to this value. The second gas cooler is also a plate heat exchanger utilizing sea water as heat sink. The purpose of the gas cooler is to get the desired gas cooler outlet temperature. To be able to control high side pressure, the heat transfer area of this gas cooler is varied throughout simulation. This is explained more

in Section 6.1.5.

Table 6.1: Key properties of the AC system gas cooler 1, utilized for heat recovery

Gas cooler 1	Unit	Size
Number of plates	-	350
Plate length	m	2
Plate width	m	0.5
phi	°	60
Material	-	Steel
U-value	W/(m^{2}K)	2000

6.1.4 Modeling of the provision system

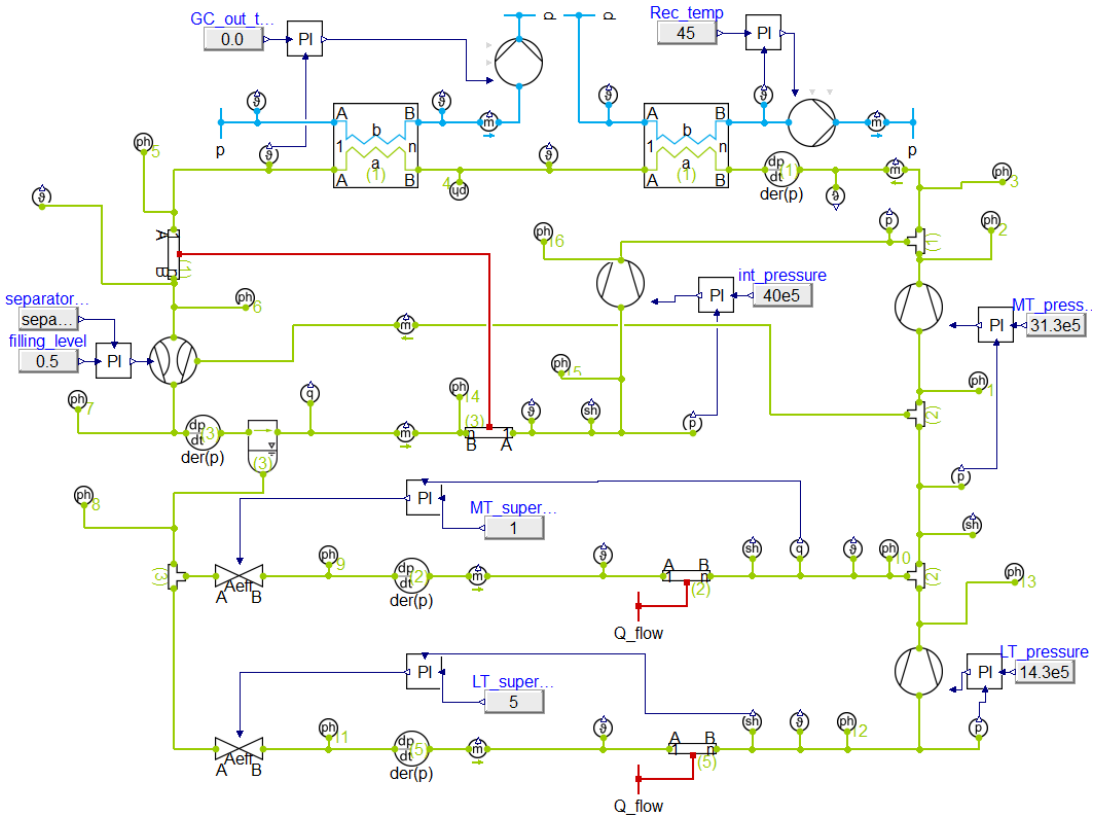

Figure 6.2: The simulated provision cooling and freezing system model.

The modeled provision cooling and freezing system in Dymola is shown in Figure 6.2. It is modelled according to the schematic in Figure 5.7 in Section 5.2.3. As for the AC system, the evaporators are modeled as heat sources. In a real system, these evaporators would be placed inside the rooms and cabinets where the cold is to be supplied, thus the heat sources typically replace air to VLE fluid heat exchangers. The evaporator pressures are specified to 31.3 bar and 14.3 bar for the MT- and LT evaporator, respectively. This corresponds to CO_2 evaporation temperatures of -4°C and -30°C. The discharged refrigerant from the LT evaporator is superheated 5°C before entering the LT compressor. The discharged refrigerant from the MT evaporator is saturated vapor and mixed with the discharged refrigerant from the LT compressor. This ensures superheat into the MT compressor, thus also the suction flow of the ejector is superheated. The parallel compressor maintain a pressure of 40 bar after the ejector, and the

IHX ensures 5°C superheat of the suction flow. Finally, as for the AC system, the cooling water inlet temperature in the first gas cooler is set 10°C hotter than the sea water temperature.

Table 6.2: Key properties of the provision cooling and freezing system gas cooler 1, utilized for heat recovery

Gas cooler 1	Unit	Size
Number of plates	-	140
Plate length	m	0.35
Plate width	m	0.12
phi	°	60
Material	-	Steel
U-value	$W/(m^2K)$	2000

As for the AC system, the first gas cooler is dedicated to heat recovery. The provision system is significantly smaller, thus this gas cooler is smaller. Furthermore, the second gas cooler area is varied to controlled the high side pressure. As stated above, this is explained more thoroughly in Section 6.1.5. Both gas coolers are modelled as plate heat exchangers.

6.1.5 AC- and provision system control system

Different control systems have not been investigated in this work. However, to be able to simulate and provide results, some controllers have to be implemented. This is done by employing PI controllers, as can be seen in Figure 6.1 and 6.2. They work by getting an input value from a sensor and tune its component to obtain its set point value. The PI controller has two parameters, a proportional gain constant (k) and an integral time constant (T_i). They can be tuned to influence the responsiveness of the controller, which can be a fine balance. Controllers that quickly responds to fluctuations are desired with regards to an agile system, but it can also make the system vulnerable to instability.

As may be seen from Figure 6.1 and 6.2, a PI controller is connected to every compressor, expansion valve, ejector and pump. The compressors are equipped with variable speed drives, i.e. they have fixed displacement and the speed is controlled by the PI controller. Every compressor are tuned according to its suction flow pressure. The expansion valves controls the superheat after their following evaporator. So, the PI-controllers are tuning their throat area to reach the superheat set point. The liquid receiver filling levels is controlled by the ejectors and are set to 0.5. Their PI-controllers are controlling the motive flow throat area. The set point value of the filling level gives the system flexibility to adapt to the fluctuating load. Water are pumped through the gas coolers. In the first gas cooler, the pump speed is tuned according to the water exit temperature, which is set to 45°C. In the second gas cooler the pump speed is tuned according the CO_2 exit temperature. This temperature is always set 5°C hotter than the sea water inlet temperature.

The provision system is equipped with three different compressors, as may be seen from its model. In Section 5.2 it was concluded that even when this configuration decreases the compressor work, the change is relatively small. And due to more components, this configuration is not considered the best option, thus the MT compressor can be removed and the ejector can lift all the refrigerant instead. However, the employment of the MT compressor in the provision system, gives better control of the MT evaporator pressure during simulation in Dymola, this will again lead to more reliable and better results. On that basis, the MT compressor is included in the configuration.

As stated above, the second gas cooler heat transfer area in both systems are varied to be able to control the high side pressures. As the high side pressure is not controlled by any PI controller, its value is a result of the converging solution in the simulation. The high side pressure is very dependent on gas cooler heat transfer area, therefore it can be changed to influence the pressure. A great heat transfer area results in a lower high side pressure and vice versa. The area cannot be changed during simulation, thus the number of plates and their width and height had to be changed manually. To get the desired high side pressure, the corresponding heat transfer area had to be found through trial and error. To better see the impact on recovered heat with increasing high side pressure, the areas of the first gas coolers was not changed, but fixed to the values shown in the tables above. Hence, only the heat transfer area of the second gas cooler was varied.

6.1.6 Validation

An important part of investigating system performance, is to validate the results. This can be done in several ways, e.g. experimental validation. Experimental validation was intended to be conducted in this work, however, due to time limitations it has not. Thus, validation is done through literature.

To be able to compare with results in literature, simple expansion valve systems was modeled, and simulated under the same conditions as the AC- and provision system above, in every case. The models can be found in the appendix. The expansion valve systems were simulated with static loads, therefore, for the AC validation, the static load was specified to the maximum load of the AC cooling loads, listed in Table 4.1. From the results, the COP improvement can be found and further be compared with literature for validation.

As the second evaporator pressure in the AC system is determined by the ejector pressure lift, and thus fluctuates. This does not influence the COP calculations for the AC system, thus the evaporator pressure of the expansion valve AC system is still set to 35 bar.

6.2 Modeling of cold thermal energy storage

In the library supplied by TLK Thermo there is no component for double bundle TES. Thus the CTES is modelled as two models, e.i. one for charging and one for discharging.

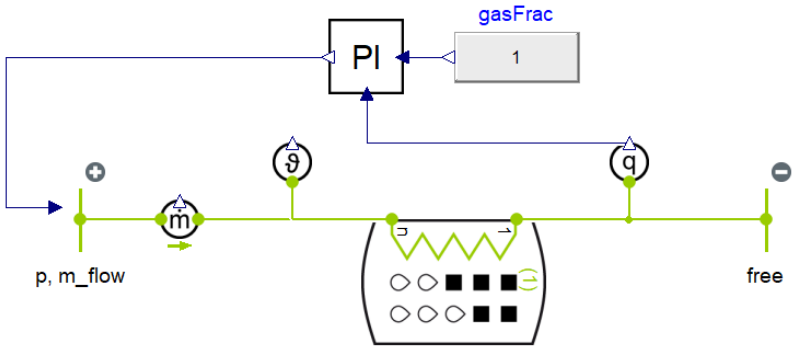

Figure 6.3: The simulated CTES charging model.

Figure 6.3 shows the CTES charging model. The LHS is modelled according to the values in Table 6.3. CO_2 at 31 bar and a specific enthalpy of 210 kj/kg enters the LHS and saturated vapor exits from the

outlet. The massflow is controlled by the PI controller to obtain saturated vapor after the LHS. The LHS is initialized as fully discharged at 0.1°C.

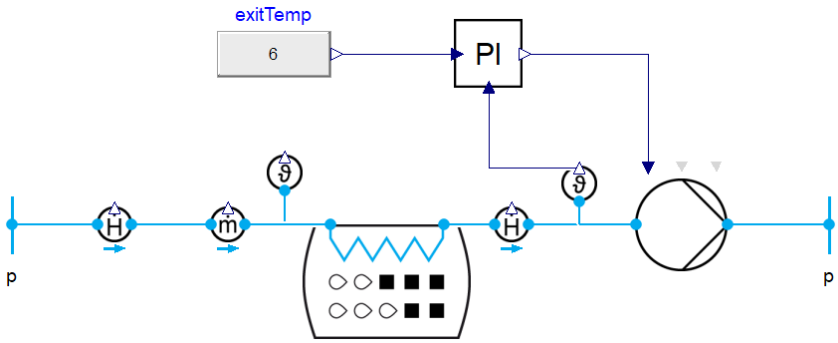

Figure 6.4: The simulated CTES discharging model.

Further, the simulated CTES discharging model is shown in Figure 6.4. As for the charging model is the LHS modelled according to Table 6.3. Water returns from the HVAC system at 12°C prior entering the LHS, and chilled water at 6°C is discharged from the outlet. A PI controller is employed to control the pump speed to achieve the desired water discharge temperature. The LHS is initialized as fully charged at 0°C.

Table 6.3 summarizes the key values for the CTES. This TES is not large enough to supply the total cooling demand. The dimensions in the table are specified to get the desired charging and discharging time according to the reference case. A short time period is required during discharging, hence more discharging pipes than charging pipes. Based on the results, the final size is determined according to the density of ice, since water expands when it freezes.

Table 6.3: Key values CTES

CTES	Unit	Size
Height	m	1,9
Width	m	1,9
length	m	1,9
Number of serial charging tubes	-	100
Number of parallel charging tubes	-	100
Number of parallel charging tube side flows	-	100
Number of serial discharging tubes	-	42
Number of parallel discharging tubes	-	42
Number of parallel discharging tube side flows	-	42
Total mass of water	kg	4633
Material	-	Copper
U-value	$W/(m^2K)$	2000

To investigate the impact CTES charging has on the AC system, the AC system model is further developed by implementing CTES. This is done by simulating the CTES as an heat source with the total CTES cooling load found from the initial simulations described above. The AC model with CTES can be found in the appendix. As may be seen in the model, saturated liquid refrigerant from the liquid receiver is throttled to 31 bar. It then enters a tube containing the CTES heat source, where it is evaporated and superheat 5°C. The refrigerant is then compressed back up again to 39 bar and mixed with the rest of the refrigerant in the suction line of the main compressor.

6.3 Equations

Coefficient of performance (COP) is a measure of, as the name states, the performance of a system. It is the ratio between useful heating or cooling, depending on what the desire of the system is, and the compressor work. As a result, one have both $\text{COP}_{\text{heating}}$ and $\text{COP}_{\text{cooling}}$. The systems have different components and configurations, for this reason they have different ways of calculating COP. All of the states in the equations refers the corresponding states in the typical log(p)-h diagrams in Section 5.

In order to calculate the COP of an ejector supported system, the entrainment ratio (Φ) has to be calculated first. This is the ratio between the ejector suction flow ($\dot{m}_{\text{sf}}$) and motive flow ($\dot{m}_{\text{mf}}$), thus it is given as;

$$\Phi = \frac{\dot{m}_{\text{sf}}}{\dot{m}_{\text{mf}}} \ . \tag{4}$$

With the entrainment ratio, the cooling COP for the AC system ($\text{COP}_{\text{c, AC}}$) can be calculated with the following equation;

$$COP_{\text{c, AC}} = \frac{\dot{Q}_{\text{CR}}}{\dot{W}} = \Phi \ \frac{\dot{m}_{\text{mf}} \ \dot{Q}_{\text{evap 1}} + \dot{Q}_{\text{evap 2}}}{\dot{W}_{\text{comp}}} = \Phi \ \frac{\dot{m}_{\text{mf}} \ (h_7 - h_6) + h_{10} - h_9}{h_2 - h_1} \ . \tag{5}$$

Further may the pressure lift ($\Delta p_{\text{lift, AC}}$) contributed by the ejector in the AC system be calculated by;

$$\Delta p_{\text{lift, AC}} = p_6 - p_{10} \ . \tag{6}$$

As the provision cooling and freezing system has two evaporators after the liquid receiver and has three different compressors the cooling COP of the system ($\text{COP}_{\text{c, prov}}$) is given by;

$$COP_{\text{c, prov}} = \frac{\dot{Q}_{\text{CR}}}{\dot{W}_{\text{tot}}} = \frac{\dot{Q}_{\text{MT evap}} + \dot{Q}_{\text{LT evap}}}{\dot{W}_{\text{par. comp}} + \dot{W}_{\text{MT comp}} + \dot{W}_{\text{LT comp}}}$$

$$= \frac{\dot{m}_{\text{MT evap}} \ (h_{10} - h_9) + \dot{m}_{\text{LT evap}} \ (h_{12} - h_{11})}{\dot{m}_{\text{par. comp}} \ (h_{16} - h_{15}) + \dot{m}_{\text{MT comp}} \ (h_2 - h_1) + \dot{m}_{\text{LT comp}} \ (h_{13} - h_{12})} \ . \tag{7}$$

And the ejector pressure lift ($\Delta p_{\text{lift, prov}}$) in the provision system is defined as;

$$\Delta p_{\text{lift, prov}} = p_7 - p_1 \ . \tag{8}$$

If heat recovery is included in the evaluation of the system performance, it is convenient to have a COP reflecting the recovered heat and compressor work ratio (COP_{rec}). For the AC system, the $\text{COP}_{\text{rec, AC}}$ is given by;

$$COP_{\text{rec, AC}} = \frac{\dot{Q}_{\text{rec}}}{\dot{W}} = \frac{\dot{Q}_{\text{gc 1}}}{\dot{W}_{\text{comp}}} = \frac{h_2 - h_3}{h_2 - h_1} \ . \tag{9}$$

Furthermore, the COP_{rec} for the provision system $\text{COP}_{\text{rec, prov}}$ is given by;

$$COP_{\text{rec, prov}} = \frac{\dot{Q}_{\text{rec}}}{\dot{W}_{\text{tot}}} = \frac{\dot{Q}_{\text{gc 1}}}{\dot{W}_{\text{par. comp}} + \dot{W}_{\text{MT comp}} + \dot{W}_{\text{LT comp}}}$$

$$= \frac{\dot{m}_{\text{par. comp}}\dot{m}_{\text{MT comp}}\ (h_3 - h_4)}{\dot{m}_{\text{par. comp}}\ (h_{16} - h_{15}) + \dot{m}_{\text{MT comp}}\ (h_2 - h_1) + \dot{m}_{\text{LT comp}}\ (h_{13} - h_{12})}\ . \tag{10}$$

Further, when heat recovery is included, the total system COP for the AC system ($\text{COP}_{\text{t, AC}}$) and provision cooling and freezing system ($\text{COP}_{\text{t, prov}}$) are respectively defined as followed;

$$COP_{\text{t, AC}} = COP_{\text{c, AC}} + COP_{\text{rec, AC}} \tag{11}$$

$$COP_{\text{t, prov}} = COP_{\text{c, prov}} + COP_{\text{rec, prov}}\ . \tag{12}$$

7 Results

In this section, the obtained results are presented, to answer the objectives in Section 1.1. All the results are presented objectively, with some discussion for explanation purposes. However, further discussions are conducted in the next section.

7.1 AC system performance

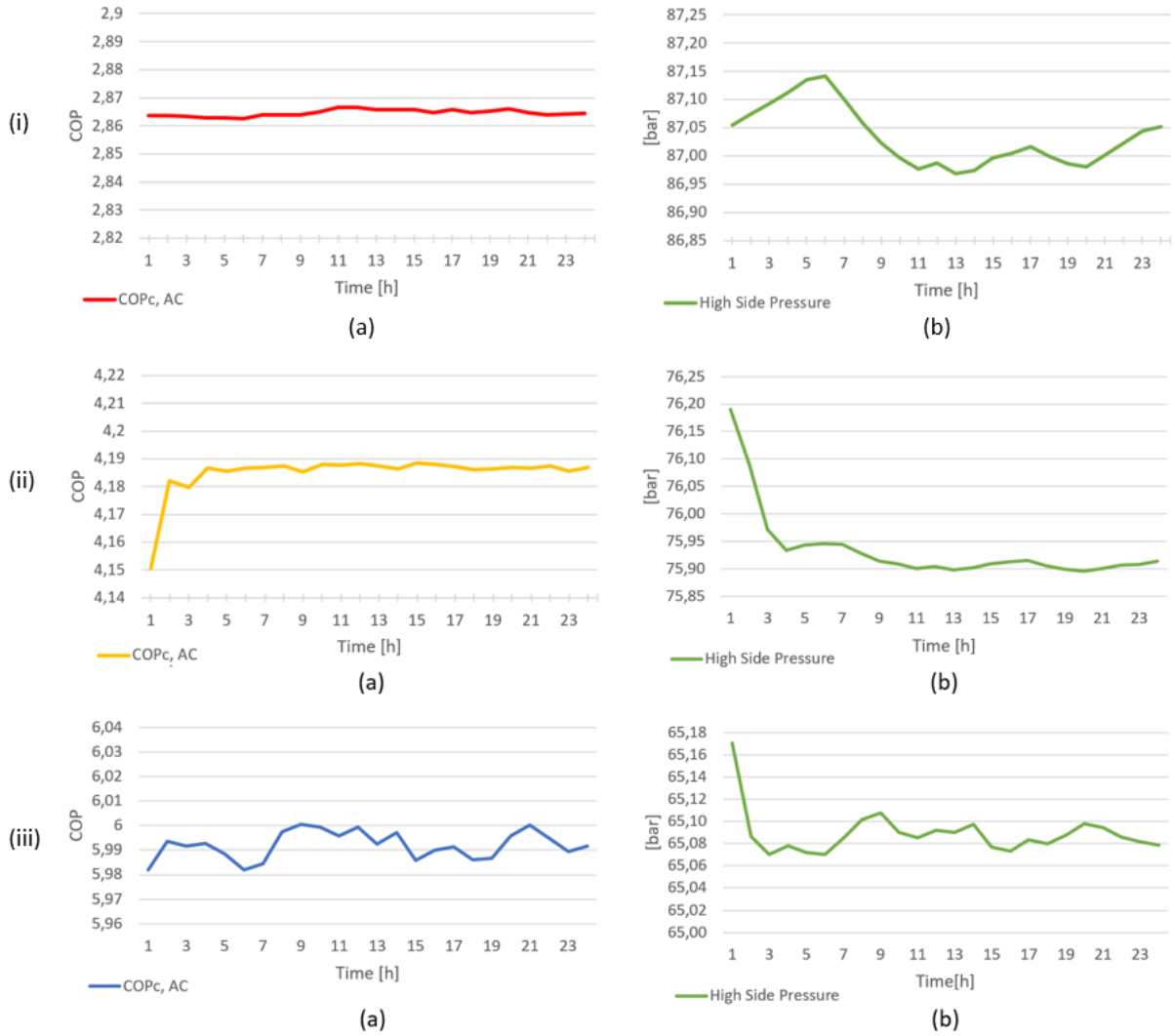

Figure 7.1: AC system dynamic performance for each case. (i), (ii) and (iii) represents to the warm, medium and cold case, respectively. (a) illustrates the $COP_{c,\ AC}$ and (b) the corresponding high side pressure.

The graphs in Figure 7.1 shows the dynamic performance of the modelled AC system. The dynamic $COP_{c,\ AC}$ for each case is shown on the left side, and are calculated with Equation 5. The corresponding high side pressure is shown on the right. The $COP_{c,\ AC}$ curves represent the best obtainable performance from the simulated system during each case. Since it is very dependent on the high side pressure, and the high side pressure is controlled by the heat transfer area in the second gas cooler, the curves are obtained by implementing the greatest area which results in a convergent solution. During the warm case, the

system operates with a $COP_{c,\ AC}$ in the range of 2.863-2.867. Further, in the medium case, it is able to operate in the range of 4.185-4.188. And finally, in the coldest case, the $COP_{c,\ AC}$ is in the range of 5.982-6.000. Note that during the first hours, the medium and cold case have not yet converged, thus values from here are unreliable.

As expected, the high side pressures increases with increasing cooling load. Further, it was expected that the lowest $COP_{c,\ AC}$ would occur with the highest pressures, and vice versa. This trend can only be seen in the warm case. At 6 am, the maximum pressure occurs together with the minimum $COP_{c,\ AC}$, and later, the maximum $COP_{c,\ AC}$ occurs at the lowest pressures. Unexpectedly, this is not the situation for the two other cases. As a matter of fact, in the coldest case, the highest $COP_{c,\ AC}$ occurs with the highest pressures. However, the fluctuations in $COP_{c,\ AC}$ are very small, so it is most likely due to instabilities in the control system and small state changes in other parts of the system. This is further discussed in Section 8.1.

7.2 Provision cooling and freezing system performance

Table 7.1: Provision system performance and key numbers.

Reference case	Unit	Warm	Medium	Cold
$COP_{c,\ prov}$	-	2.334	2.977	3.538
High Side Pressure	bar	86	76	70
Gas cooler outlet temperature	°C	35	28	21
Parallel compressor work	kW	28.45	12.98	6.18
MT compressor work	kW	14.86	20.02	20.80
LT compressor work	kW	4.67	4.67	4.67
Entrainment ratio	-	0.31	0.20	0.13

From Table 7.1 the provision system performance can be seen. The $COP_{c,\ prov}$ is calculated with Equation 7. As for the AC system, the listed $COP_{c,\ prov}$ is the highest obtainable system performance for each case. As expected are the $COP_{c,\ prov}$ greatest for the coldest case and least for the warm case. This is of course due to the heat sink temperature being greatest for the warm case and least for the cold state. This is also reflected by the high side pressure. The difference in heat sink temperature is also influencing the allocation of work between the compressors. The LT compressor work is the same for all cases, but one can see that work is shifted from the MT compressor to the parallel compressor with increasing heat sink temperature. Due to the increase in gas cooler exit temperature and the increase in ejector entertainment ratio, more work has to be done by the parallel compressor and less is required by the MT compressor.

7.3 Heat recovery and optimum high side pressure for the AC- and provision system

In this section the possibility of heat recovery will be presented. Since the first gas cooler in both systems are dedicated to heat recovery, an increase in high side pressure will shift heat rejection from the second to the first gas cooler. At the same time can the optimum high side pressure for each system be investigated. Hence, it is presented together. The COP_{rec} is calculated with Equation 9 and Equation 10 for the AC- and provision system, respectively. Further is the COP_t for the AC system and provision system respectively calculated with Equation 11 and Equation 12.

7.3.1 Heat recovery and optimum high side pressure for the AC system

Since the AC system is simulated with a dynamic cooling load, the $COP_{c,\ AC}$ fluctuate, as shown above. Therefore, the values in this section are collected from the point where the system is supplying maximum cooling load.

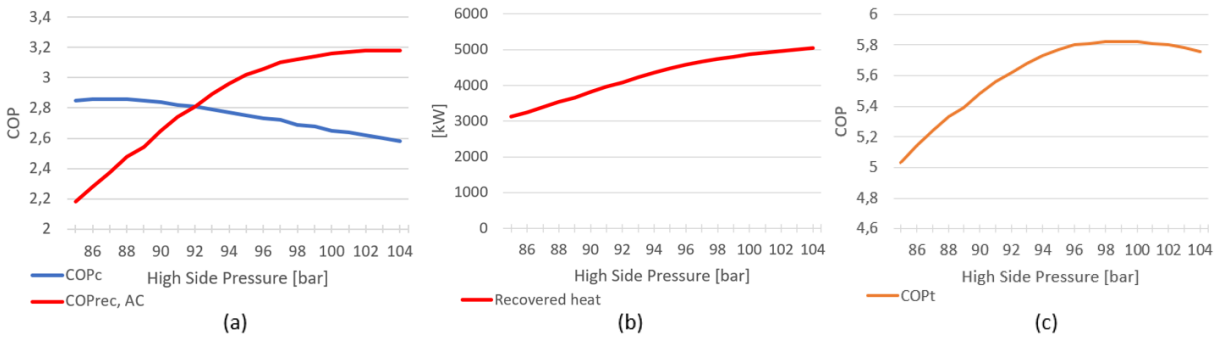

Figure 7.2: Heat recovery and optimum high side pressure for the AC system during the warm case. With increasing high side pressure: (a) the change in COP_c and $COP_{rec,\ AC}$; (b) the change in total amount of heat recovered; (c) the change in COP_t. Gas cooler outlet temperature = 35°C.

In Figure 7.2 (a) it can be seen that the $COP_{c,\ AC}$ has its greatest value at a high side pressure of 87 bar during the warm case. Thus, if the system is to be operated at best performance with regards to cooling, this is the optimum high side pressure. Further, the reduction in $COP_{c,\ AC}$ with increasing pressure is relatively small. As expected, does the $COP_{rec,\ AC}$ increase with increasing high side pressure before it reaches a maximum of approximately 3.2. From Figure 7.2 (b) the total recovered heat is shown. The investigated high side pressures allows the system to recover between 3000 kW and 5000 kW of heat. The gradient is approximately constant before it decreases after reaching 96 bar. In Figure 7.2 (c) the $COP_{t,\ AC}$ is shown. It reaches a maximum at approximately 99 bar. From here, increasing high side pressure will result in decreasing $COP_{t,\ AC}$. In other words, if the pressure is increased more, the payback of cold and heat is less than the electricity required to drive the compressor.

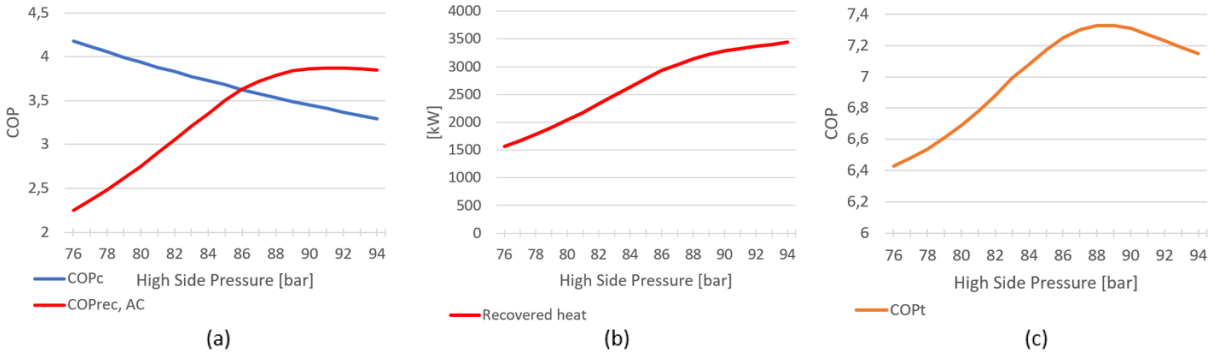

Figure 7.3: Heat recovery and optimum high side pressure for the AC system during the medium case. With increasing high side pressure: (a) the change in COP_c and $COP_{rec,\ AC}$; (b) the change in total amount of heat recovered; (c) the change in COP_t. Gas cooler outlet temperature = 28°C.

As shown in Figure 7.3 (a), the $COP_{c,\ AC}$ always decrease with increasing high side pressure for the medium AC case. This is in contrast to the warm case where the system can reach an optimum high side pressure with regards to $COP_{c,\ AC}$. It can also be noted that it decreases faster than in the warm case as the pressure is increased. On the other hand is the $COP_{rec,\ AC}$ increasing fast before reaching a maximum of approximately 3.9. Further, in Figure 7.3 (b), the gradient of the recovered heat curve is

greatest in the beginning prior decreasing from 86 bar. With transcritical operation, this was expected, but the increase in gradient was expected to be more considerable. This is discussed more below, in Section 8.3. From the last curve, in (c), it can be seen that the $COP_{t,\ AC}$ reaches a maximum at 88 bar.

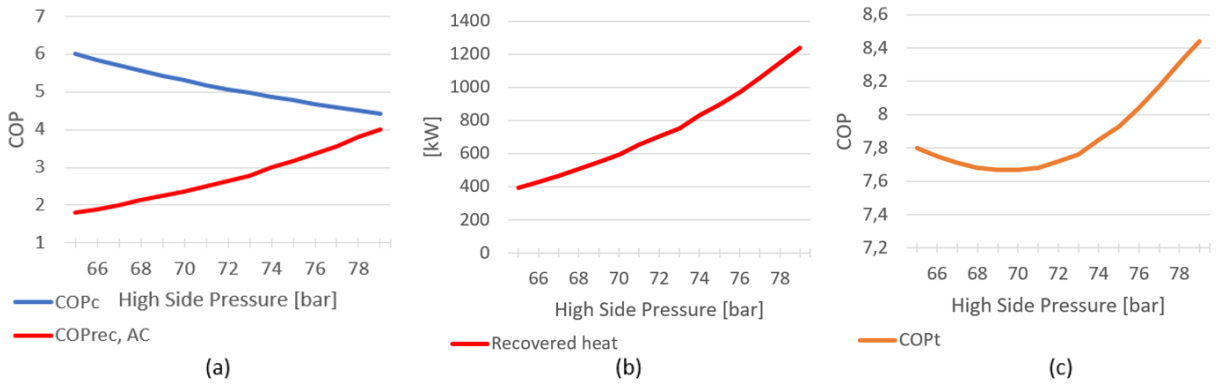

Figure 7.4: Heat recovery and optimum high side pressure for the AC system during the cold case. With increasing high side pressure: (a) the change in COP_c and $COP_{rec,\ AC}$; (b) the change in total amount of heat recovered; (c) the change in COP_t. Gas cooler outlet temperature = 21°C.

Figure 7.4 illustrates the results from investigating heat recovery and optimum high side pressure for the cold AC case. From (a) it can be seen that the $COP_{c,\ AC}$ is strictly decreasing and that the $COP_{rec,\ AC}$ is strictly increasing with increasing high side pressure. The slope of the $COP_{c,\ AC}$ curve is approximately constant, while the slope of the $COP_{rec,\ AC}$ increases with transcritical operation. This can also be seen from the recovered heat curve in (b). Again, as stated above, this is as expected, but it was expected to be more considerable. As seen in (b), the AC system is capable of recovering between 400 kW and 1200 kW of heat, for the investigated high side pressures. As seen in (c), before the $COP_{t,\ AC}$ reaches a minimum at approximately 70 bar, is it descending. This is due to $COP_{c,\ AC}$ decreasing more than the $COP_{rec,\ AC}$ increases. This changes at the minimum point, thus the curve starts to increase, and more rapidly as the system enters transcritical operation. This is due to slope of the isotherms above the critical point in a P-h diagram, and are further discussed below in Section 8.3.

7.3.2 Heat recovery from the provision system and optimum high side pressure

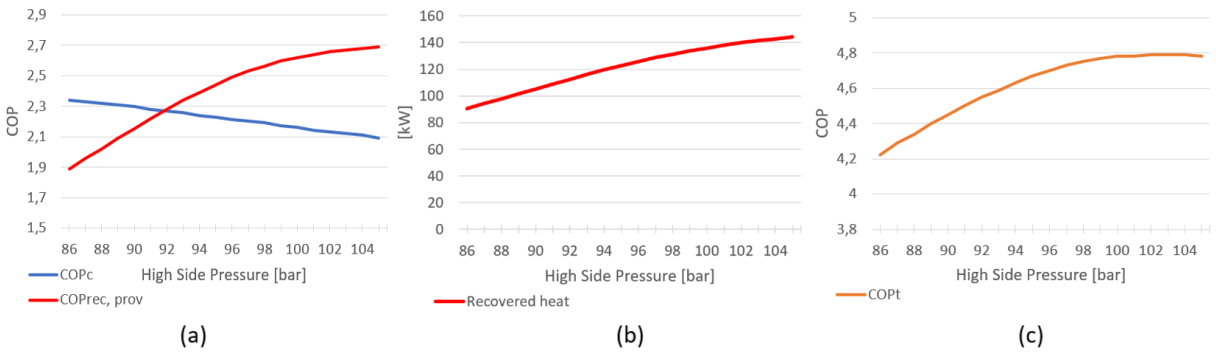

Figure 7.5: Heat recovery and optimum high side pressure for the provision system during the warm case. With increasing high side pressure: (a) the change in COP_c and $COP_{rec,\ prov}$; (b) the change in total amount of heat recovered; (c) the change in COP_t. Gas cooler outlet temperature = 35°C.

Figure 7.5 illustrates the results from investigating heat recovery and optimum high side pressure for the provision system during the warm case. The $COP_{c,\ prov}$ is depicted in (a). In contrast to the AC

system, the provision system is not able to reach a maximum COP. In parallel is the $COP_{rec,\ prov}$ strictly increasing. It does not reach a maximum either, but starts to flatten out at the highest pressures. The heat recovery gas cooler in the provision system is relatively small compared to the one in the AC system, therefore will the relatively small heat transfer area cause the curve to flatten out slower and later. Further is the total heat recovered depicted in (b). The system is able to recover between 90 kW and 140 kW of heat, depending on the high side pressure. Obviously it can recover more heat by increasing the pressure further, but as shown in (c) is the maximum $COP_{t,\ prov}$ located at approximately 103 bar. So from an energy efficiency point of view, should the high side pressure not be increased further.

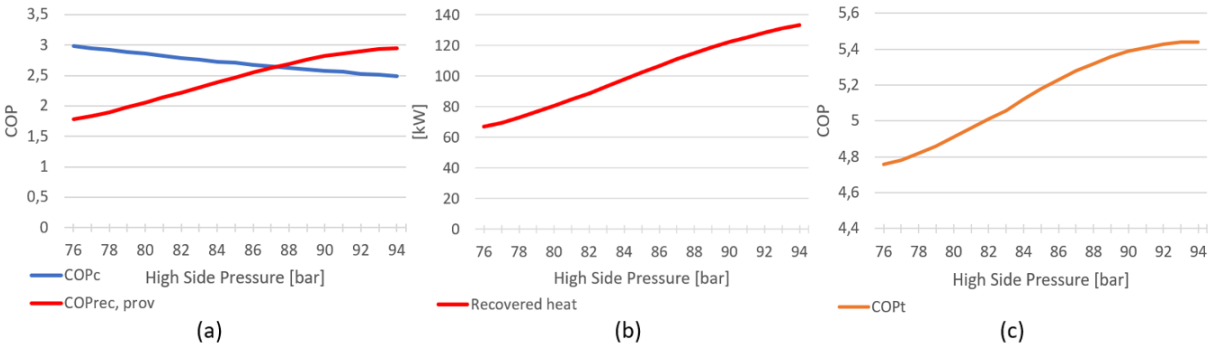

Figure 7.6: Heat recovery and optimum high side pressure for the provision system during the medium case. With increasing high side pressure: (a) the change in COP_c and $COP_{rec,\ prov}$; (b) the change in total amount of heat recovered; (c) the change in COP_t. Gas cooler outlet temperature = 28°C.

As shown in Figure 7.6 (a), the $COP_{c,\ prov}$ for the medium case decrease approximately linearly with increasing high side pressure. At the same time is the $COP_{rec,\ prov}$ increasing. As for the warm case, does the $COP_{rec,\ prov}$ start to flatten out when operating at the highest pressures, but not reaching a maximum. From (b) it can be seen that system can recover between approximately 70 kW and 135 kW of heat, for the investigated high side pressures. Lastly, from (c), the optimum high side pressure with regards to $COP_{t,\ prov}$ is 94 bar.

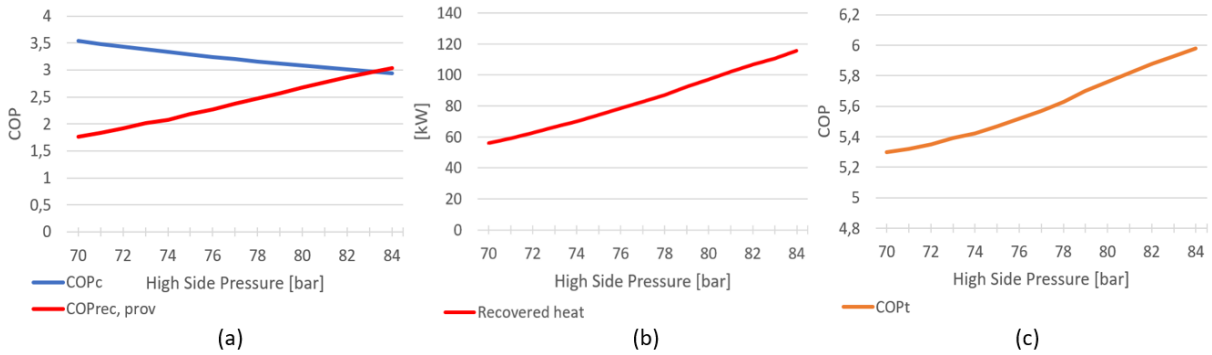

Figure 7.7: Heat recovery and optimum high side pressure for the provision system during the cold case. With increasing high side pressure: (a) the change in COP_c and $COP_{rec,\ prov}$; (b) the change in total amount of heat recovered; (c) the change in COP_t. Gas cooler outlet temperature = 21°C.

Finally, Figure 7.7 shows the results from the investigations of heat recovery and changes in performance from the provision system during the cold case. The model can barely operate subcritical, as the lowest obtainable pressure is 70 bar. For the investigated pressures, the $COP_{c,\ prov}$ ranges between 3.5 and 3, and the $COP_{rec,\ prov}$ between 1.8 and 3. From (b) it can be seen that the system can supply between 55 kW and 115 kW of heat. Finally, since the $COP_{c,\ prov}$ and $COP_{rec,\ prov}$ is decreasing and increasing

approximately linearly, the $COP_{t,\ prov}$ is also approximately linear.

7.4 Cold thermal energy storage

To meet the total cooling demand, several CTES modules will have to operate in parallel. From the simulated results the total system will have to include 21163 kg of water as PCM and a total volume of 38.0 m^3. This translates to 4.56 parallel modules of the one specified in Table 6.3. The total CTES volume includes 23.07m^3 for PCM, 13.48 m^3 for discharging and charging tubes and the rest for wall material.

7.4.1 CTES discharging

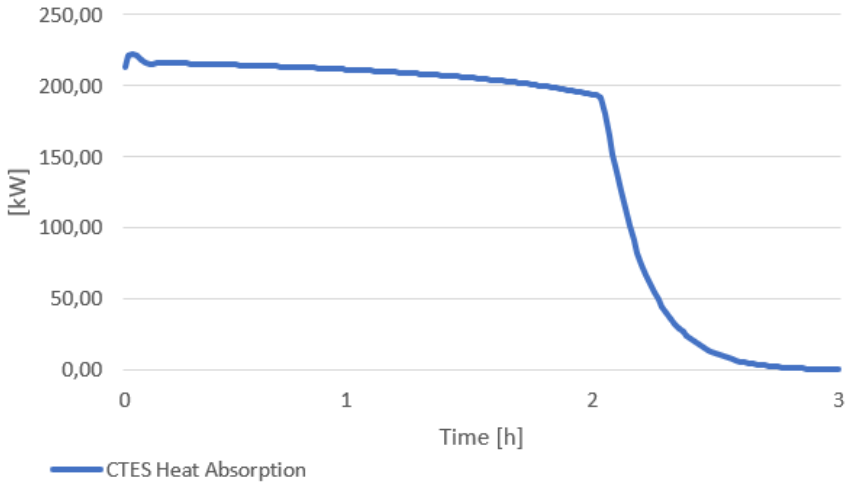

Figure 7.8: The dynamic Q flow during CTES discharging.

Figure 7.8 shows the CTES discharging curve. It is discharged in two hours, hence the sudden drop in heat absorption, and supply a total of 419 kWh of cold with an average load of 210 kW. The PCM and HVAC supply water reaches the same temperature after approximately 3 hours. As the thermal conductivity of ice is greater than liquid water, is the heat absorption decreasing. As liquid is formed, it will increase the thermal resistance. This implies that the mass flow rate of chilled water is reduced. The decline in supplied cold can be limited by increasing the number of tubes. On the other hand will it increase the system size. So, there is a trade of between size and performance.

7.4.2 CTES charging

Figure 7.9 shows the CTES charging curve. The charging operation is finished after approximately 6 hours. As ice is formed, the greater thermal conductivity of ice causes the incline during charging. This is also affected by the relatively low amount of charging pipes, more pipes would have flatten the curve a bit as well as shortening the charging period. The charging time can also be shortened by decreasing the CO_2 pressure, this is further discussed below in Section 8.5. The following sensible heat rejection is completed after approximately 40 minutes. Due to the lower specific heat capacity of ice compared to liquid water, the sensible heat rejection process is quicker than during discharging.

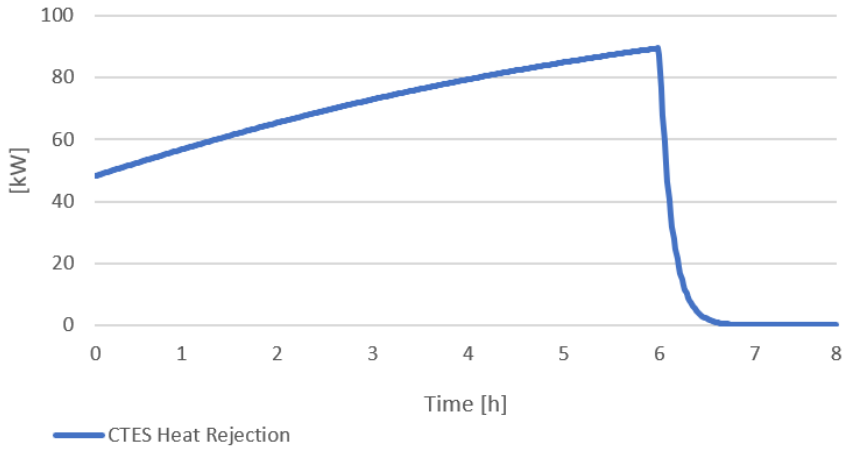

Figure 7.9: The dynamic Q flow during CTES charging.

7.4.3 CTES charging strategy

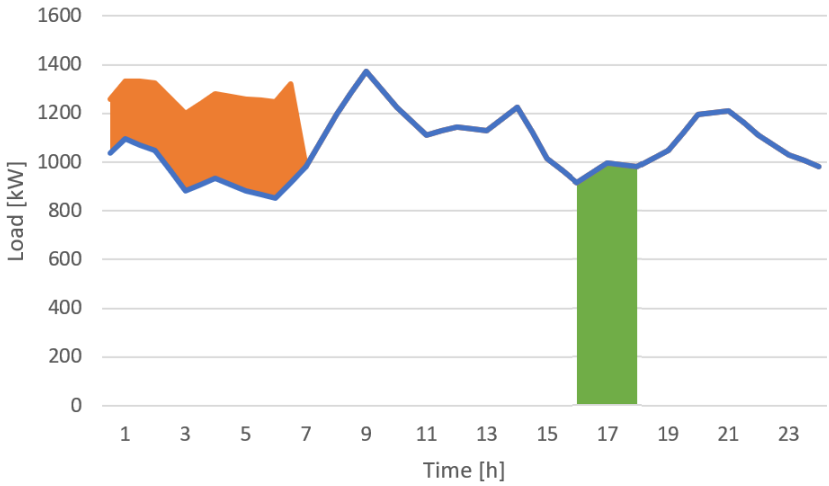

Figure 7.10: CTES charging strategy, CTES discharging and overall cooling load. Charging is shown as the orange shaded area and discharging as green.

If all of the parallel storage modules are charged at the same time, Figure 7.10 illustrates a possible charging strategy. As seen in the figure, is the CTES fully discharged from 4 PM to 6 PM. After leaving port and reaching open sea, charging is initiated from 00:30 Am to 06:30 AM. As seen in the figure, does the relatively long charging time enable the CTES to be charged without increasing the AC-system peak load, which still occurs at 9 AM. This strategy increases the overall cooling load with 219 kW at minimum and 407 kW at maximum.

7.4.4 CTES influence on AC system performance

The charging is done by the AC system, hence it is interesting to investigate what impact it has on the overall AC system performance. Figure 7.11 shows the first 6.5 hours when the AC system operates with and without CTES. The $COP_{c,\ AC}$ without CTES, is collected from the AC system while it operates at 68 bar high side pressure during the coldest AC case, and the $COP_{c,\ AC}$ with CTES is exactly the same

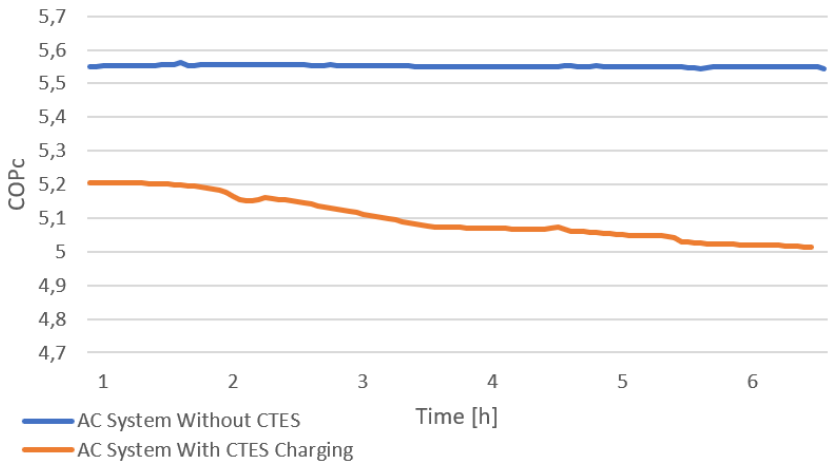

Figure 7.11: The difference in AC system COP with and without CTES charging.

system, but with CTES charging as well. In the figure, the first minutes of the simulation are omitted, as the system had not yet converged. After 6.5 hours the CTES is fully charged. As expected, the $COP_{c,\ AC}$ is least influenced at the beginning and decreases further with increasing CTES cooling load. During charging the $COP_{c,\ AC}$ is decreased in the range of 6.13% - 9.73%, as the system operates in the $COP_{c,\ AC}$ range of 5.206 - 5.012.

8 Discussion

8.1 AC system performance

As briefly discussed in Section 7.1, is the behavior of the $COP_{c,\ AC}$ during the cold case not as expected. It increases with increasing high side pressure. There are some uncertainties related to why, however, as already pin pointed in the Section 7.1, is it most likely due to instabilities during simulation when operating at lower high side pressures. In Figure 8.1, the AC system operates at a higher high side pressure, as may be seen in (b). At this operating pressure the system is behaving as expected. As shown in (a), the $COP_{c,\ AC}$ decreases with increasing pressure, and vice versa. The system reaches its minimum at 9 AM, when the system supplies maximum cooling load. This substantiates that the issue is mostly related to the agility when meeting fluctuating demand, and not the overall system performance.

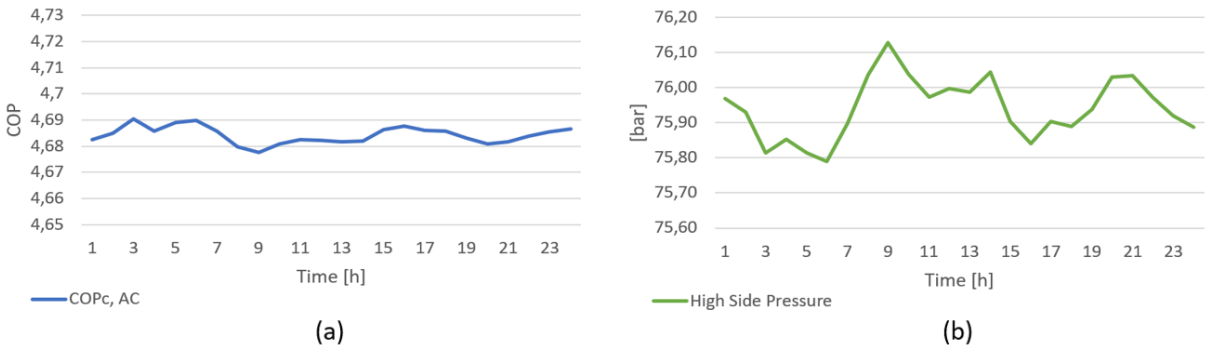

Figure 8.1: AC system operating around 76 bar high side pressure during the cold case. (a) the dynamic COP, (b) the dynamic high side pressure.

Another interesting observation from Figure 8.1, is the increasing fluctuation of the high side pressure. Since the high side pressure is controlled by the heat transfer area in the second gas cooler, the fluctuation will increase with greater operating pressures. As a consequence, will the steepness of the $COP_{c,\ AC}$ curves in Figure 7.2, 7.3 and 7.4 be greater than they actually are, since the values are collected at maximum load. Thus, it would have been better to look at the average COP instead. However, due to constant heat sink temperatures, the high side pressure fluctuations are still relatively small, thus also the COP fluctuations. So, the curves are still a good representation of the AC system performance.

8.2 AC model

In reality, such a system would have had an expansion valve in parallel with the ejector. Because of the two-staged evaporation, both the low side pressure and the receiver pressure has to be fixed. By routing a proportion of the refrigerant through the valve, the system is able to control the pressure lift generated by the ejector, thus the pressure levels in the heat exchangers. However, this has not been done in the AC model. As a consequence, since the receiver pressure is fixed, the low side pressure will fluctuate due the dynamic load. This could have been an issue if the evaporators were modeled as heat exchangers, as the fluctuating pressure would influence the pinch point. However, since the evaporators are modeled as heat sources, this is not an issue and makes the model a good approximation with regards to overall performance. Additionally it does not influence the conducted COP calculations, as this is not dependent on the second evaporator pressure.

Due to the addressed issue, it would have been interesting to compare the AC system with an ejector supported one-staged evaporator system. When only having one evaporator pressure, the receiver pressure may fluctuate, thus all of the pre-compression capacity of the ejector can be utilized. On the other hand, as discussed in Section 5.2.1, the employment of one-staged evaporation would increase the exergy destruction rate.

8.3 Heat recovery

Figure 8.2 shows the log(p)-h diagram of the AC system, when running subcritical at 65 bar high side pressure, during the cold case. The temperature after the heat recovery gas cooler is 29.64°C, as shown in the diagram, and the specific recovered heat, is the enthaply change from point 2 to point 3. As a result, most of the heat rejection happens in the second gas cooler, and is thus not recovered. However, as discussed in Section 2.4, in the literature review, transcritical running modes will enable more to be recovered. The change in gradient of the isotherms above the critical point, can shift most of the enthaply exchange over to the heat recovery gas cooler.

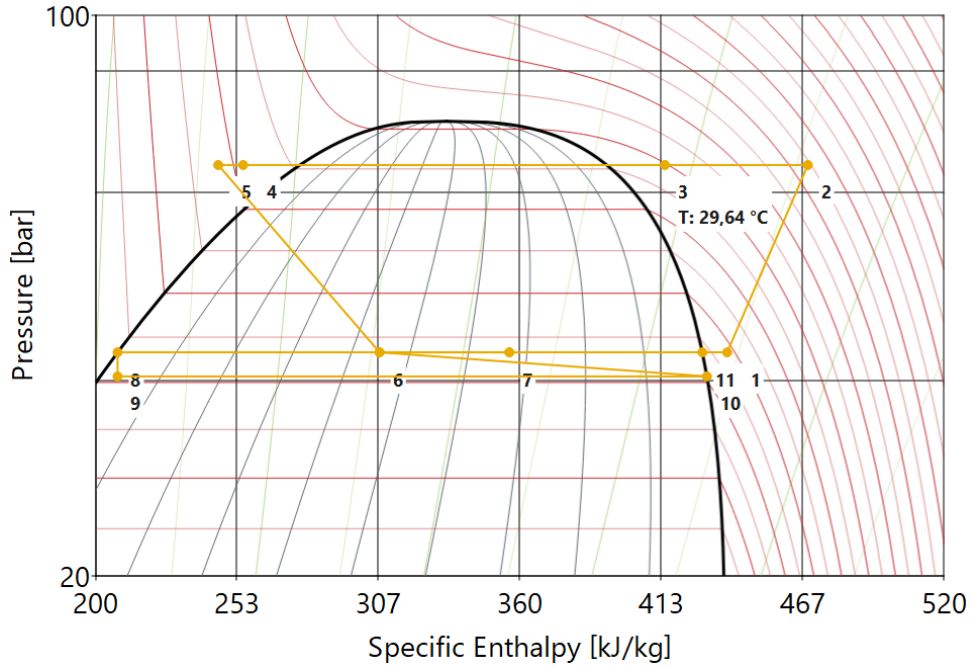

Figure 8.2: The log(p)-h diagram of the AC system during subcritical operation.

Figure 8.3 depict the log(p)-h diagram of the AC system during the same case as the diagram above in this section. Now the high side pressure have been increased to 76 bar, resulting in transcritical operation. As claimed above, point 3 has now shifted towards the left side, thus the specific heat recovered has greatly increased, and therefore also the total amount of recovered heat. However, the exit temperature from the heat recovery gas cooler has also increased, to 32.36°C. Due to the models not being able to control the exit temperatures from the heat recovery gas coolers, will it increase with increasing high side pressure. As a consequence, can not the system achieve the full potential of heat recovery. Hence, does not the COP_{rec} increase as rapidly as expected when the system enters transcritical operation, as briefly discussed and presented in Section 7.3. This applies for both the AC- and provision system, in all cases, but especially the provision system as the heat recovery gas cooler is relatively small compared to the

one in the AC system.

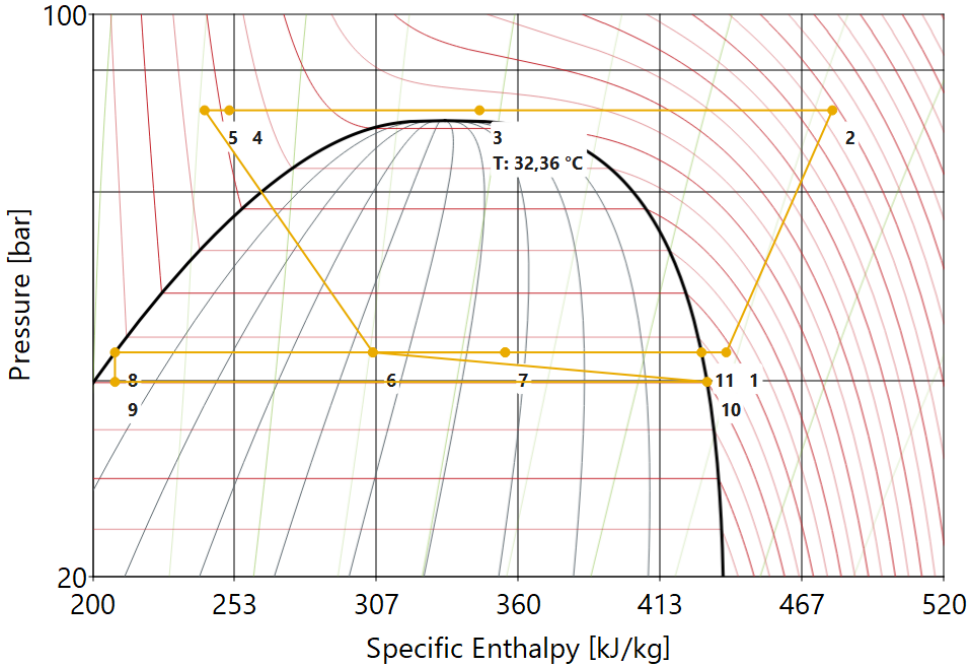

Figure 8.3: The log(p)-h diagram of the AC system during transcritical operation.

Finally, it is important to underline that there is no point in increasing the high side pressure to recover more heat if the heat is not utilized. The increase in high side pressure implies an increase in compressor work. So if the heat is not utilized and goes to waste, the system is basically just operating at a worse COP_C than needed. A cruise ship generates a heating demand from several processes on board, but also recovers heats from others, e.g. the engine. Thus it is important to analyse the heating on board a cruise ship, which have to include all processes that generates heat or a heating demand, to find out when and how much heat to be recovered from the refrigeration system. As stated in the introduction, has the utilization of recovered heat been out of the scope in this work, but heat recovery and -demand has been studied in the master thesis (integrated thermal system for hydrogen and ammonia driven cruise ship) by Magnus Egerdahl, a fellow student.

8.4 Optimum high side pressure

The system performances as a function of high side pressure was presented in Section 7.3. With regards to COP_c, the AC system is the only system which are able to achieve an optimum high side pressure, but only during the warm case. This was unexpected. When operating subcritical, i.e. in the coldest cases, there is no optimum high side pressure with regards to COP_c. So, the best performance occurs while operating at the lowest possible high side pressure. However, it was expected that there would be an optimum high side pressure for the provision system during the warm case, and for both systems during the medium cases too, due to their transcritical running modes. In the medium case, the gas cooler exit temperature of 28°C is relatively low. Thus, an increase in high side pressure does not influence the gas cooler exit specific enthalpy as greatly as if it would be higher. Hence there will not be an optimum high side pressure when the systems operates in the medium case, even though it is running transcritically.

An optimum high side pressure does neither occur for the provision system during the warm case, even though the gas cooler exit temperature is relatively high (35°C). Figure 8.4 shows the log(p)-h diagram of the provision system when operating during the warm case at the best obtainable $COP_{c,\ prov}$. In the figure, point 5 represents the gas cooler outlet state. As the pressure is changed, this point will follow the red isotherm it is placed upon. Thus, if the model was capable of reducing the pressure further, the specific enthalpy of point 5 would shortly increase quite drastically, resulting in a higher gas fraction at point 7. Consequently would the $COP_{c,\ prov}$ decrease. Therefore, it is reasonable to believe that the provision system is operating closely to its optimum high side pressure at 86 bar, when operating during the warm case.

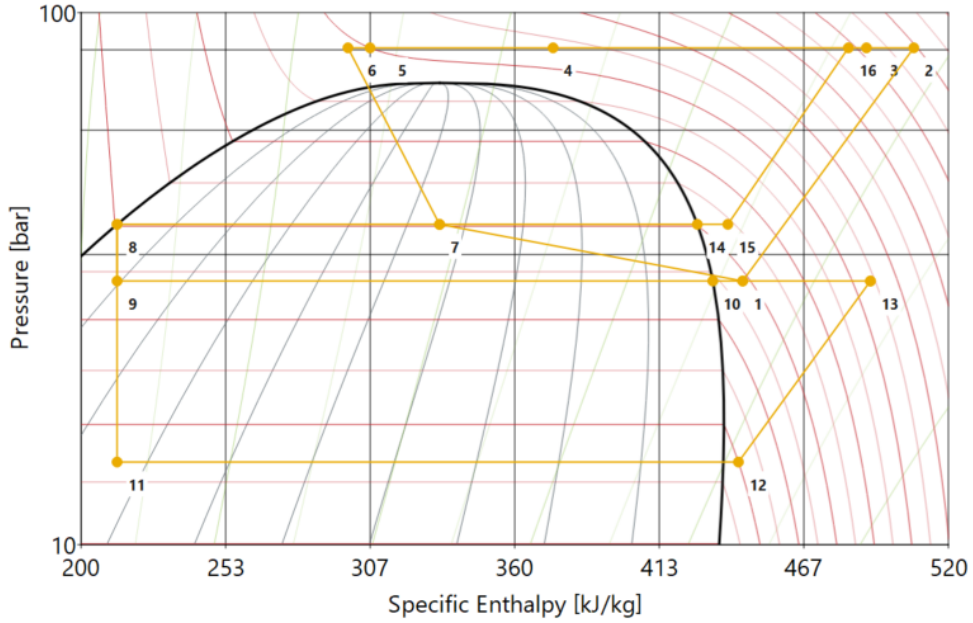

Figure 8.4: The log(p)-h diagram of the provision system when operating during the warm case at the best obtainable $COP_{c,\ prov}$, occurring at the lowest obtainable high side pressure (86 bar).

8.5 Cold thermal energy storage

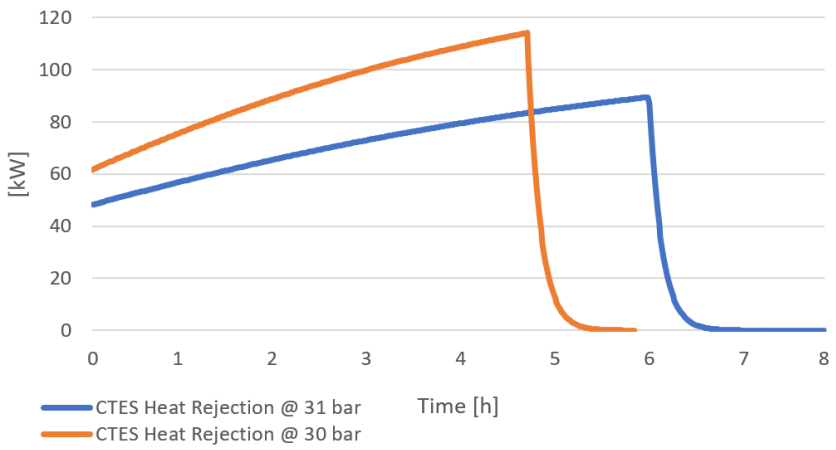

Figure 8.5: How the charging time of one CTES module is influenced by reducing the CO_2 pressure one bar.

As stated in the results, in Section 7.4.2, can the CTES charging time of be influenced by changing the CO_2 pressure. This can be utilized if the CTES have to be charged faster. Figure 8.5 shows the charging curves of one CTES module with 31 bar and 30 bar CO_2 pressure. By lowering the pressure 1 bar, the charging time is reduced by 1.3 hours. Furthermore, since the same amount of cold has to be stored, the peak load increases with 27 kW. As may be seen from the CTES charging strategy in Figure 7.10, does the CTES charging already almost increase the AC system overall peak load. Thus, would this CO_2 pressure reduction result in a greater capacity need from the AC system. However, since the CTES contains parallel modules, it enables the possibility to charge them individually. Consequently, can other charging strategies be investigated. This has to be done in parallel with AC system performance evaluation, and is therefore listed in further work.

9 Validation

Table 9.1, lists the results for the investigated ejector supported AC- and provision systems, and the simple expansion valve systems, during each case. As expected, does the COP improvement for the provision system increase with increasing high side pressure, since the ejector can convey more of the CO_2 from the suction flow of the MT compressor. However, for the AC system, the COP improvement is greatest during the medium case, followed by the cold case and finally by the warm case. This is due to the addressed issue above in Section 8.2. As the high side pressure increases, consequently the pressure lift will too. Therefore, refrigerant will have to by-pass the ejector through a valve. This process emulate poorer ejector efficiency. As a matter of fact, the system may obtain the same COP improvement with an ejector efficiency of 14%, which is the point where all the refrigerant from the high side would be expanded through the ejector.

Table 9.1: Performance comparison between the AC- and provision system and simple expansion valve systems.

	Unit	AC system			Provision system		
Case	-	Cold	Medium	Warm	Cold	Medium	Warm
High side pressure	bar	66	76	87	72	78	87
Gas cooler outlet temperature	°C	21	28	35	21	28	35
COP ejector supported	-	5.85	4.18	2.87	3.43	2.92	2.33
COP expansion valve	-	4.99	3.54	2.49	3.03	2.42	1.79
COP improvement	-	**17.23 %**	**18.08 %**	**14.86 %**	**13.20 %**	**20.66 %**	**30.17 %**

9.1 Validation of the AC system

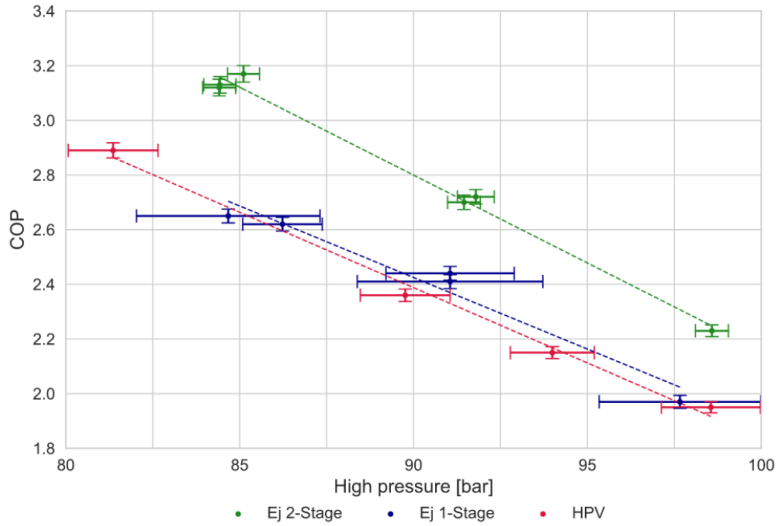

Figure 9.1: Experimental data. Shows how the COP changes with different high side pressures and gas cooler outlet temperature, as the system always operates at the optimum high side pressure [13].

Schaan et al. [13] performed experimental tests at the SuperSmart Rack at NTNU. The collected data is shown in Figure 9.1. As parts of the experiments, both an AC ejector supported two-staged evaporation system (Ej 2-stage) and a AC expansion valve system (HPV) was tested. As the rack always operates with optimum high side pressure for a given gas cooler outlet temperature, it can be seen from the trend

line in the figure, that for a high side pressure of 87 bar, and thus a gas cooler outlet temperature of approximately 35°C, the two-staged system nearly operates at a COP_c of 3, and the expansion valve system at a COP_c of approximately 2.55. Thus it seems like the simulated results in this work are trending to be a bit less than the experimental data. However, as may also be seen from the figure, are there some uncertainties related to the measured data. So, it hard to come to a conclusion, apart from that the simulated AC system operates about the same COP.

9.2 Validation of the provision system

Gullo et al. [41] investigated several supermarket refrigeration systems theoretically, to prove that CO_2 systems can outperform refrigeration systems utilizing synthetic fluids in warm climates. As a part of the work, an ejector supported parallel compression system was examined. The only difference in configuration from the provision system in this work, was the employment of liquid ejectors, enabling the first evaporator to be flooded. The first evaporator temperature was set to -4°C, i.e. the same as in this work, and the second evaporator was set to -35°C, 5°C less than in this work. The resulting COPs are shown in Figure 9.2, where the COP of the ejector supported parallel compression system is represented by abbreviation EJ. While the system operates transcritically, it always operates at the optimum high side pressure. From the figure, it can be seen that with an ambient temperature of 30°C, the COP is approximately 2.1. Which is a bit less than obtained in this work. However, considering the differences in configuration and operational specifications, the results are quite similar.

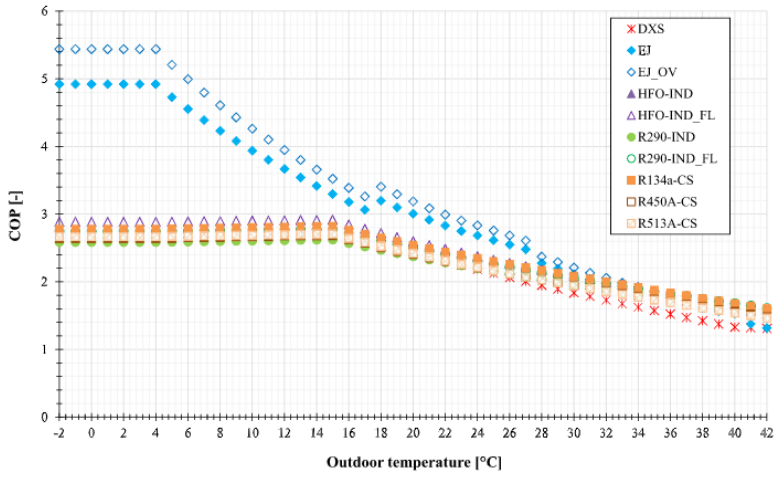

Figure 9.2: COPs of different supermarket refrigeration systems at different ambient temperatures. The abbreviation EJ represents an ejector supported parallel compression system [41].

10 Conclusion

In this thesis, CO_2 refrigeration systems and thermal energy storage for cruise ships have been examined. An ejector supported two-staged evaporation AC system and an ejector supported parallel compression provision system was designed, modeled and simulated in the dynamic simulation software Dymola, to analyse their performances. As well as the performance related to cooling, has the potential for heat recovery been examined too.

To obtain realistic results for cruise ship applications, three reference cases was defined with corresponding cooling loads for both systems. The cooling load of the provision system is assumed constant, whereas the cooling demand for the AC system is dynamic. The scope only contains summer conditions, hence, as the refrigeration systems utilizes sea water cooling, the reference cases have sea water temperatures of 30°C, 23°C and 16°C, and are referred to as the warm-, medium- and cold case, respectively.

Furthermore, cold thermal energy storage (CTES) was investigated. With a cooling demand collected from the coldest reference case of the AC system, a CTES double bundle system that can supply the demanded cold for a two hour long port was constructed. As well as simulations of charging and discharging in Dymola, the influence on the AC system performance was examined, as the AC system charges the CTES prior port call.

As the AC system supplies a dynamic cooling load, the cooling COP ($COP_{c,\ AC}$) fluctuates. At the best operating point, it has been found that the high side pressure fluctuations are very small, and that the system is able to operate with a $COP_{c,\ AC}$ around 2.86, 4.19 and 5.99 respectively for the warm-, medium- and cold case. Since the AC system utilizes two-staged evaporation, some of the refrigerant has to be routed around the ejector in transcritical operation, to be able to fix the evaporator pressures. Hence, the potential pressure lift generated by the ejector cannot be fully enhanced. Thus, the $COP_{c,\ AC}$ improvement, relative to an expansion valve system, is not as good as theoretically possible when employing an ejector. Next, at best operation point, the provision system is able to operate at a $COP_{c,\ prov}$ of 2.33, 2.98 and 3.54 respectively for the warm-, medium-, and cold case.

The AC system is the only system which are able to achieve an optimum high side pressure, but only during the warm case at 87 bar. During the two coldest cases, the relatively low gas cooler outlet temperatures results in no optimum high side pressure for both systems. Furthermore, due to the provision system model not being able to reduce the high side pressure below 86 bar, it is not able to reach its optimum high side pressure. However, 86 bar is very close, thus the concluded $COP_{c,\ prov}$, for the warm case, is approximately the best obtainable COP.

Further, the recovered heat from the AC system ranges from 400 kW at the lowest high side pressure during the cold case, to 5000 kW at the highest investigated pressure during the warm case. Furthermore, the recovered heat from the provision system ranges from 55 kW during the cold case, to 140 kW at the highest investigated high side pressure in the warm case. Both models is not equipped with temperature control of the heat recovery gas cooler, disabling the systems from enhancing all the recoverable heat.

Finally, the simulated AC- and provision model were validated with results collected from literature. From the validation it is clear that the models operates about the same performances as collected, thus it substantiates that the models operates as expected.

Lastly, CTES was examined. It has been found that the CTES needs to contain 21163 kg of water as phase change material, and a total volume of 38.0 m^3 to supply the demanded 1914 kWh of cold. The

system is arranged in parallel modules, which can be discharged simultaneously in 2 hours. The charging operation takes 6 hours, and are able to be conducted by the AC system without increasing the overall peak load. However, the $COP_{c,\ AC}$ is decreased in the range from 6.13% to 9.73% during charging.

11 Further work

In this section, proposal for further work is listed. The suggestions are both related to improvements as well as extensions of the conducted work.

- Further develop the models with better high side pressure control, so, performance with fixed heat transfer area can be evaluated.
- Implement heat recovery gas cooler outlet temperature control, so more of the potential recovered heat can be enhanced.
- A comprehensive thermal analysis of a cruise ship, to see to what extent recovered heat from the refrigeration systems is needed.
- As the cruise ships are associated with very different operational modes, other reference cases should be developed, to see how the refrigeration system performances changes and if cold thermal energy storage can be utilized in another way.
- Develop an ejector supported one stage evaporation model and compare the examined AC system to see which one is better.
- As the results are obtained through simulation, validation through experimental tests should be conducted to substantiate the conclusion.
- As cold thermal energy storage was examined for relatively cold conditions, and it is very relevant for hotter, it should be examined for warmer conditions to see the required dimensions.
- As the cold thermal energy storage contains parallel modules, the charging strategy can be investigated further, so the strategy which compromises the cooling COP of the AC system the least can be found.

References

[1] Cruise Industry Outlook. Cruise lines international association (clia), 2021.

[2] Evangelia Stefanidaki and Maria Lekakou. Cruise carrying capacity: A conceptual approach. *Research in Transportation Business & Management*, 13:43–52, 2014.

[3] Western norway research institute. https://www.vestforsk.no/en. Accessed: 2022-06-03.

[4] Ing A Hafner, CH Gabrielii, and K Widell. *Refrigeration units in marine vessels: Alternatives to HCFCs and high GWP HFCs*. Nordic Council of Ministers, 2019.

[5] Hfk-gasser. https://www.linde-gas.no/no/products_ren/refrigerants/hfc_gases/index.html. Accessed: 2021-12-15.

[6] M Schulz and D Kourkoulas. Regulation (eu) no 517/2014 of the european parliament and of the council of 16 april 2014 on fluorinated greenhouse gases and repealing regulation (ec) no 842/2006. *Off. J. Eur. Union*, 2014(517):L150, 2014.

[7] Man-Hoe Kim, Jostein Pettersen, and Clark W Bullard. Fundamental process and system design issues in co2 vapor compression systems. *Progress in energy and combustion science*, 30(2):119–174, 2004.

[8] M Pieve, G Boccardi, L Saraceno, R Trinchieri, and G Zummo. Co2 transcritical refrigeration cycles: potential for exploiting waste heat recovery with variable operating conditions. In *Journal of Physics: Conference Series*, volume 796, page 012021. IOP Publishing, 2017.

[9] F Murena, L Mocerino, F Quaranta, and D Toscano. Impact on air quality of cruise ship emissions in naples, italy. *Atmospheric Environment*, 187:70–83, 2018.

[10] The european union's proposal on alternative fuels and its impact on shore power adoption. https://powertechresearch.com/the-european-unions-proposal-on-alternative-fuels-and-its-impact-on-shore-power-adoption/. Accessed: 2022-05-07.

[11] Norwegian parliament adopts zero-emission regulations in world heritage fjords. https://whc.unesco.org/en/news/1824. Accessed: 2022-05-08.

[12] Planung & technik - kältetechnik – co2 als kältemittel. https://assets.danfoss.com/documents/91478/AD000086412355de-000101.pdf. Accessed: 2021-10-19.

[13] Larissa Schaan. Design and evaluation of co2 based integrated heating and cooling systems for zero emission cruise ships. Master's thesis, NTNU, 2020.

[14] Friedrich Kauf. Determination of the optimum high pressure for transcritical co2-refrigeration cycles. *International Journal of Thermal Sciences*, 38(4):325–330, 1999.

[15] Nicholas Joseph Czapla, Harshad Inamdar, Riley Barta, and Eckhard Groll. Theoretical analysis of the impact of an energy recovery expansion device in a co2 refrigeration system. 2016.

[16] Stefan Elbel and Neal Lawrence. Review of recent developments in advanced ejector technology. *International journal of refrigeration*, 62:1–18, 2016.

[17] P Nekså, A Hafner, A Bredesen, and TM Eikevik. Co2 as working fluid—technological development on the road to sustainable refrigeration. In *Proceedings of the 12th IIR Gustav Lorentzen Natural Working Fluids Conference, Edinburgh, UK*, pages 21–24, 2016.

[18] Piotr A Domanski, David A Didion, and JP Doyle. Evaluation of suction-line/liquid-line heat exchange in the refrigeration cycle. *International Journal of Refrigeration*, 17(7):487–493, 1994.

[19] Zhen-ying Zhang, Yi-tai Ma, Hong-li Wang, and Min-xia Li. Theoretical evaluation on effect of internal heat exchanger in ejector expansion transcritical co2 refrigeration cycle. *Applied Thermal Engineering*, 50(1):932–938, 2013.

[20] The danfoss multi ejector range for co refrigeration: design, applications and benefits. https://www.danfoss.com/en/service-and-support/case-stories/dcs/the-danfoss-multi-ejector-range-for-co2-refrigeration/. Accessed: 2021-11-17.

[21] Stefan Elbel. Historical and present developments of ejector refrigeration systems with emphasis on transcritical carbon dioxide air-conditioning applications. *International Journal of Refrigeration*, 34(7):1545–1561, 2011.

[22] Michal Haida, Jacek Smolka, Michal Palacz, Jakub Bodys, Andrzej J Nowak, Zbigniew Bulinski, Adam Fic, Krzysztof Banasiak, and Armin Hafner. Numerical investigation of an r744 liquid ejector for supermarket refrigeration systems. *Thermal Science*, 20(4):1259–1269, 2016.

[23] S Girotto. Improved transcritical co2 refrigeration systems for warm climates. In *Proceedings of the 7th IIR Ammonia and CO2 Refrigeration Technologies Conference, Ohrid, Macedonia*, pages 11–13, 2017.

[24] Daqing Li and Eckhard A Groll. Transcritical co2 refrigeration cycle with ejector-expansion device. *International Journal of refrigeration*, 28(5):766–773, 2005.

[25] Y Ozaki, H Takeuchi, and T Hirata. Regeneration of expansion energy by ejector in co2 cycle. In *Proceedings of the 6th IIR-Gustav Lorentzen Conference on Natural Working Fluids*, pages 10–15. Glasgow, UK, 2004.

[26] Jian-qiang Deng, Pei-xue Jiang, Tao Lu, and Wei Lu. Particular characteristics of transcritical co2 refrigeration cycle with an ejector. *Applied Thermal Engineering*, 27(2-3):381–388, 2007.

[27] Transcritical co_2 refrigeration with heat reclaim. https://www.danfoss.com/en-gb/service-and-support/case-stories/dcs/transcritical-co2-refrigeration-with-heat-reclaim/. Accessed: 2022-05-04.

[28] Georgios Maouris, Emilio Jose Sarabia Escriva, Salvador Acha, Nilay Shah, and Christos N Markides. Co2 refrigeration system heat recovery and thermal storage modelling for space heating provision in supermarkets: An integrated approach. *Applied Energy*, 264:114722, 2020.

[29] C Veerakumar and A Sreekumar. Phase change material based cold thermal energy storage: Materials, techniques and applications–a review. *international journal of refrigeration*, 67:271–289, 2016.

[30] Ioan Sarbu and Calin Sebarchievici. A comprehensive review of thermal energy storage. *Sustainability*, 10(1):191, 2018.

[31] Francesco Baldi, Fredrik Ahlgren, Francesco Melino, Cecilia Gabrielii, and Karin Andersson. Optimal load allocation of complex ship power plants. *Energy Conversion and Management*, 124:344–356, 2016.

[32] Clemens Boertz, RG Hekkenberg, and Richard van der Kolk. Improved prediction of the energy demand of fuel cell driven expedition cruise ships. In *Proceedings of the 12th Symposium on High-Performance Marine Vehicles, HIPER'20*. Technische Universität Hamburg-Harburg, 2020.

[33] Clemens Boertz. Energy demand of a fuel cell-driven cruise ship: Analysis and improved prediction method of the operational power variation under different loading and environmental conditions. 2020.

[34] Hoval Enventus. Rotary heat exchangers for heat recovery in ventilation systems, 2018.

[35] Fan coil systems (enigma). https://www.teknotherm.no/marine/hvac-systems/fan-coil-systems-enigma/. Accessed: 2022-03-22.

[36] Maria Alessandra Ancona, Francesco Baldi, Michele Bianchi, Lisa Branchini, Francesco Melino, Antonio Peretto, and J Rosati. Efficiency improvement on a cruise ship: Load allocation optimization. *Energy Conversion and Management*, 164:42–58, 2018.

[37] Weather park. https://weatherspark.com/. Accessed: 2022-04-04.

[38] Marcel R Escoffier. Food service operations in the cruise industry. *Hospitality Review*, 13(1):3, 1995.

[39] Giacomo Tosato, Silvia Minetto, Antonio Rossetti, Armin Hafner, Christian Schlemminger, and Sergio Girotto. Field data of co2 integrated refrigeration, heating and cooling systems for supermarkets. In *Proceedings of the 14th IIR-Gustav Lorentzen Conference on Natural Refrigerants*. IIR, 2020.

[40] Jahar Sarkar and Neeraj Agrawal. Performance optimization of transcritical co2 cycle with parallel compression economization. *International Journal of Thermal Sciences*, 49(5):838–843, 2010.

[41] Paride Gullo, Konstantinos M Tsamos, Armin Hafner, Krzysztof Banasiak, T Ge Yunting, and Savvas A Tassou. Crossing co2 equator with the aid of multi-ejector concept: A comprehensive energy and environmental comparative study. *Energy*, 164:236–263, 2018.

Appendix

The AC expansion valve system utilized for validation

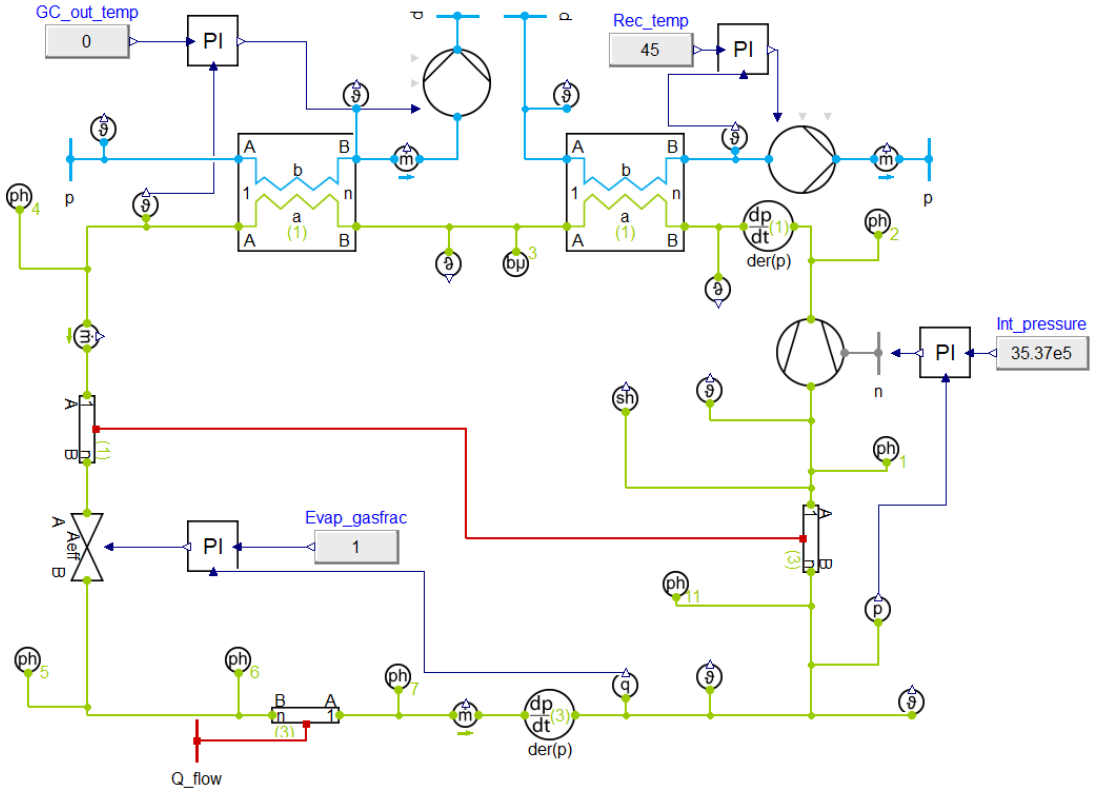

The provision expansion valve system utilized for validation

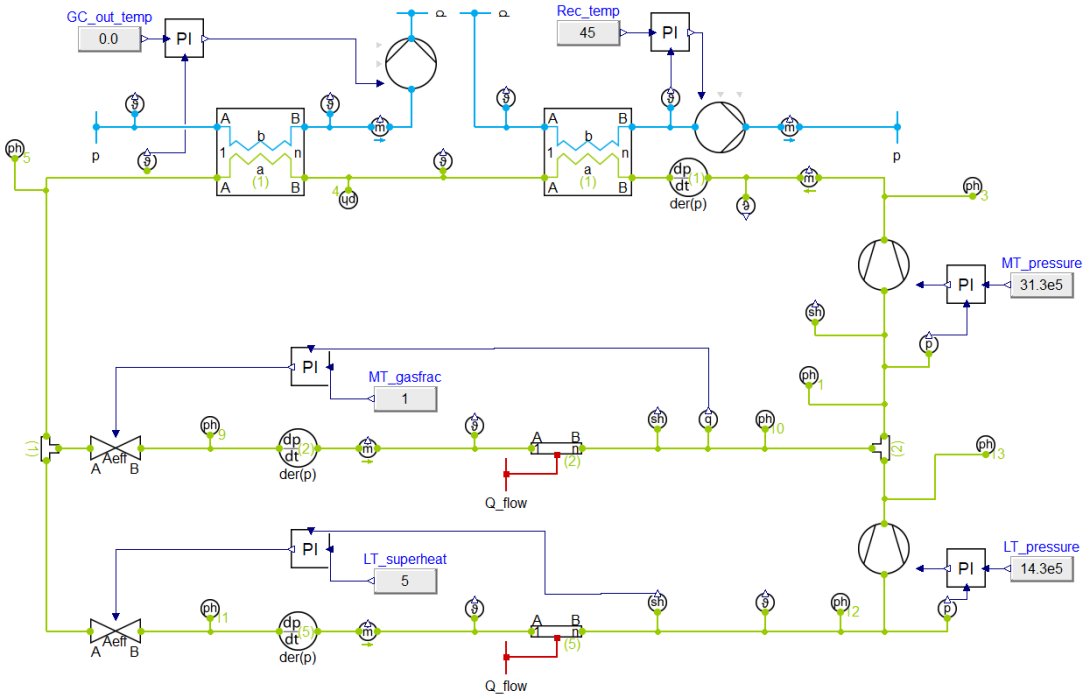

The AC system model equipped with CTES simulated in Dymola

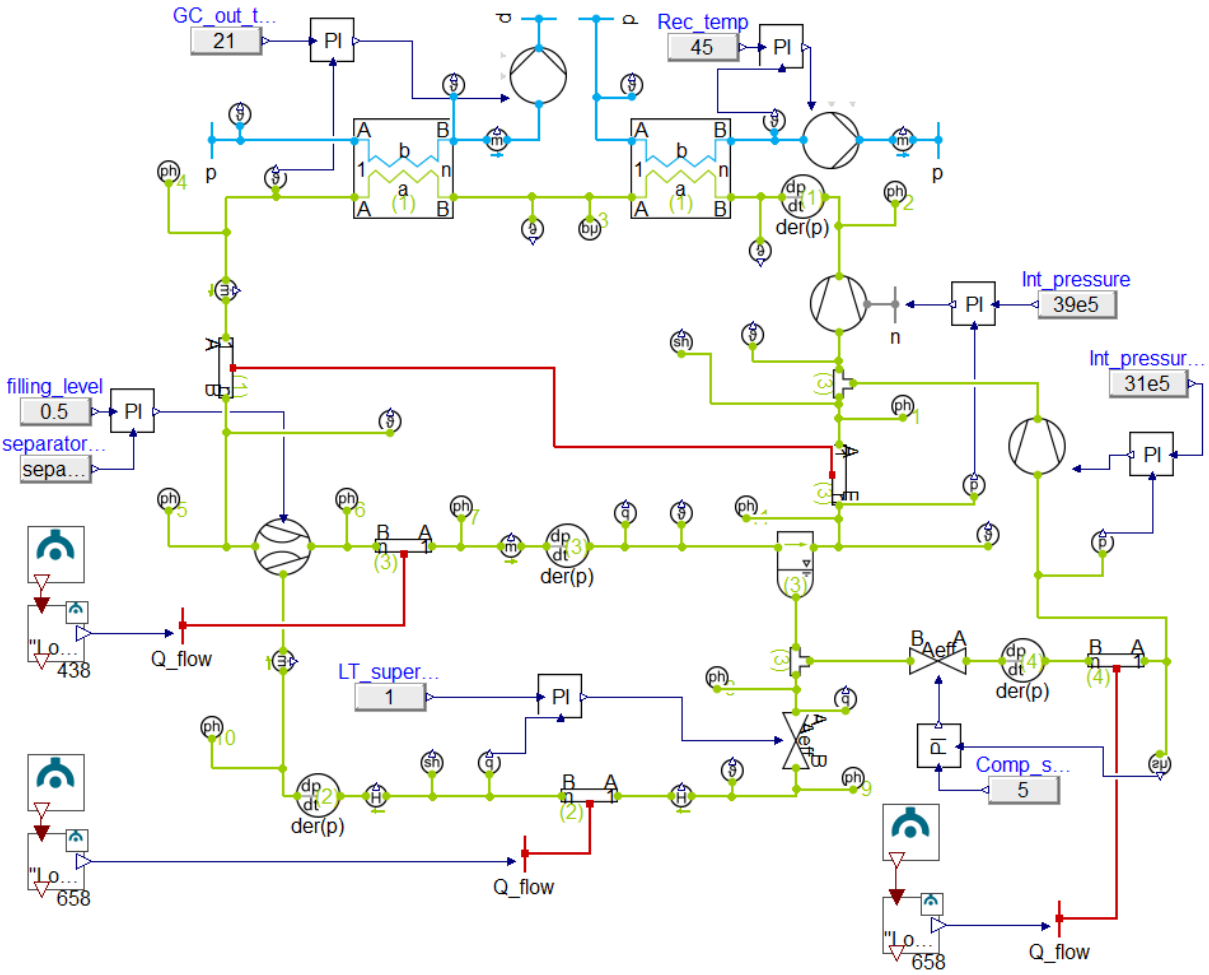

Scientific paper

Development of CO_2 refrigeration systems and thermal energy storage for cruise ships

Henrik ANDERSEN

Norwegian University of Science and Technology
Trondheim, 7030, Norway, henrande@stud.ntnu.no

ABSTRACT

As potent global warming refrigerants are becoming increasingly regulated, natural refrigerants has resurrected as working fluids. Cruise ships utilize refrigeration systems as AC chillers and to preserve provision. Through simulation the performance of two energy-efficient CO_2 refrigeration systems for a medium sized cruise ship, utilized for air conditioning and for provision cooling and freezing, are examined. Furthermore, how cold thermal energy storage (CTES) can be utilized to supply the cooling demand of a two hour port stay, have been investigated. Three reference cases with different boundary conditions are defined and referred to has warm-, medium, and cold case. Respectively for the cases, it has been found that the maximum cooling COP of AC system is about 2.89, 4.19 and 5.99. Furthermore, for the provision system, it is 2.33, 2.98 and 3.54, respectively. Lastly, the CTES must contain 21163kg of water as phase change material, and a total volume of 38.0m^3.

Keywords: Refrigeration, Carbon Dioxide, Ejector, COP, Energy Efficiency, CTES.

1. INTRODUCTION

There are great greenhouse emissions (GHG) related to the cruise industry. According to Western Norway research institute [1], 3% of the total GHG from Norway has its origin from the cruise industry, consuming about 170 million liters of fuel. However, burning fossil fuel is not the only source of GHG emissions. Today R134a, R404A and R407C are the dominating refrigerants on passenger ships [2], they have a global warming potential (GWP) of 1430 or greater [3]. Leakages of such synthetic refrigerants contributes significantly to the GHG emissions. Therefore, in 2014, EU introduced a new regulation on fluorinated greenhouse gases [4]. Here there is a ban for centralised refrigeration systems exceeding 40 kW capacity, relying on fluorinated greenhouse gases with a GWP of 150 or more. As an alternative refrigerant, CO_2 is a great option, as refrigeration systems utilizing CO_2 has proven to be environmentally friendly, personal safe and energy-efficient.

Another measure towards zero emissions, will require ships to connect to onshore power during port stays longer than two hours [5], to reduce the need for auxiliary engines. As this will not regulate port stays less than two hours. It is interesting to investigate if cold thermal energy storage (CTES) can be utilized to cover the cooling demand during these port stays.

The aim of this work is to develop energy-efficient CO2 refrigeration models in Dymola, and simulate to find the expected performances from such systems when applied to cruise ships. Furthermore, examine how CTES can be utilized to supply the cooling demand related to a two hour long port stay. Since only refrigeration systems are investigated, the scope only contains summer conditions.

2. REFERENCE CASE

To be able to conclude on the system applicability and performance, it should be applied on specific scenarios. Further, the scenarios should be representative of real applications. Furthermore, to be able to investigate how AC- and provision system performance changes with environmental conditions, three different cases containing three different cooling loads are defined in this section.

2.1. Air condition and cold thermal energy storage

To the author's knowledge, it exists very few studies on passenger ships AC cooling demand. Thus, the reference cases are based on two studies, Ancona et al. [6] and Boertz et al. [7].

Boertz et al. [7] calculated the energy demand of a 139 m long and 22 m wide fuel cell driven expedition cruise ship during constant sailing. The hottest investigated climate was with weather data collected from Singapore. The resulting cooling demand curve is shown as the red curve in Fig 1. This reference case is referred to as the warm reference case. In this case the AC system will have to operate with a sea water temperature of 30 °C as heat sink.

Furthermore, Boertz has calculated the cooling demand with weather data from Amsterdam during summer. However, these conditions are very similar to the conditions of cold reference case defined below. Although the cooling demand was calculated for Amsterdam climate, the profile is fairly like the Singapore case. Therefore, to get a case in between, the demand was linearly interpolated based on weather data collected from Barcelona during summer. The resulting cooling demand curve is shown in Fig 1, as the yellow curve. This reference case is referred to as the medium reference case. In this case the AC system will have to operate with a sea water temperature of 23 °C as heat sink.

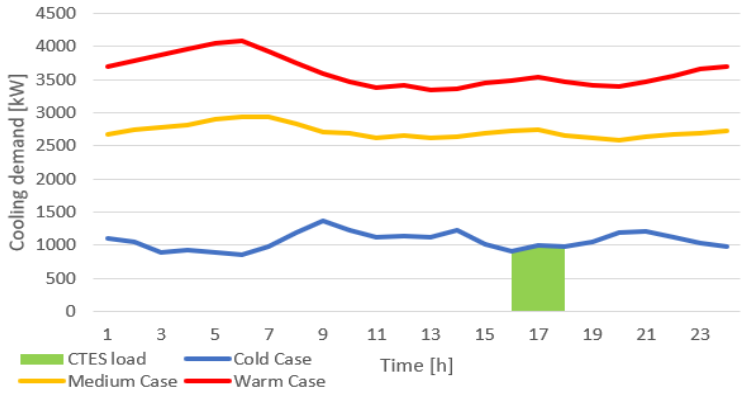

Figure 1: The cooling load for every AC reference case and the CTES load. Value for the warm- and medium case are collected from [7], values for the cold case and CTES are collected from [6]

Ancona et al. [6] conducted a study of a 177 m long and 28 m wide passenger ship sailing between Stockholm and Mariehavn in Sweden. As a part of the study, energy demand was gathered through measurement and calculation. The cooling demand of the ship during summer is shown as the cold case in Fig 1. The ship makes the same route every day. The ship leaves Stockholm around 06:00 PM, after reaching open sea, it stops for some hours prior reaching Mariehavn early in the morning. It leaves again one hour later and arrives back in Stockholm 04:00 PM. This reference case is referred to as the cold reference case. In this case the AC system will have to operate with a sea water temperature of 16 °C as heat sink.

Since cold reference case includes port stays, it is convenient to collect data for the CTES case from here. The ship has two port stays, one hour in the morning and two hours in the afternoon. From the cooling demand of the second port stay it can be found that the CTES will have to supply 1914 kWh of cold. Fig 1 shows the cooling demand that must be supplied by the CTES, represented by the green shaded area.

2.2. Provision cooling and freezing

It is assumed that the ship would need a food capacity equivalent to a medium sized supermarket. Additionally, it is assumed that the activity is low, and that the provision is already chilled/frozen when it is stored, i.e. loading and unloading does not influence the cooling and freezing demand. It is also assumed that the construction and placement of cabinets and rooms result in a constant heat leakage, i.e. the cooling and freezing demand is constant. The cooling and freezing demand are collected from Tosato et al. [8], where a medium sized supermarket was studied, hence 90 kW of cooling and 22 kW of freezing is demanded. The system will operate under the same environmental conditions as the AC system. As a result, are three

different cases with the same load, but different heat sink temperatures created. The key values for each case are listed in Table 1.

Table 1: Key values for the three different cases for the provision system. Cooling- and freezing load collected from [8]

Reference Case		Cold	Medium	Warm
Sea water temperature	°C	16	23	30
Cooling load	kW	90	90	90
Freezing load	kW	22	22	22

3. SYSTEM DESIGN AND SIMULATIONS

3.1. AC- and provision system

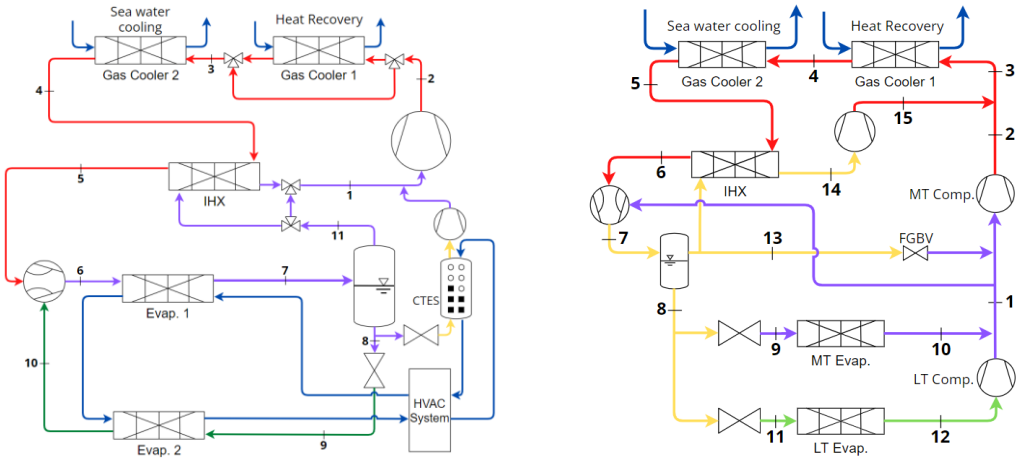

Figure 2: Simplified schematics of the AC system equipped with CTES (left) and the provision system (right)

The investigated AC system is an ejector supported two stage evaporation system and is shown in Fig 2. From the compressor the refrigerant enters the first of two gas coolers, dedicated to heat recovery. Depending on the heat recovery demand, the gas cooler may be fully or partially bypassed through a three-way-valve. The rest of the heat is rejected in the last gas cooler to sea water. The cooled down refrigerant enters an IHX. Here, it is subcooled by the refrigerant upstream from the compressor. For work recovery purposes the expansion device is an ejector. The expansion of the high-pressure fluid conveys the refrigerant from the secondary side (suction flow). The discharged flow then enters the first evaporator before it is discharged into the liquid receiver. From here, the liquid is throttled by and expansion valve, which corresponds to the ejector pressure lift. Further, the fluid enters the second evaporator before it is conveyed by the ejector. The refrigerant is fully evaporated in the second evaporator prior suction. The vapor from the liquid receiver enters the IHX where it is superheated before it is compressed by the compressor. A three-way-valve is installed to be able to control the superheat of the compressor suction flow. The system chills water from 12°C to 6°C before it is supplied to the HVAC system.

The designed provision system is shown in Fig 2, and is an ejector supported parallel compression system. From the MT compressor the refrigerant enters gas cooler 1 for heat recovery. Heat is recovered by cooling water. The rest of the heat rejection happens in gas cooler 2 which utilizes sea water. Further, the refrigerant passes through the IHX where it is cooled further before entering the ejector. The ejector conveys refrigerant from the suction line of the MT compressor. the mixed fluid is discharged into a liquid receiver. Since the system supplies cold to both cooling and freezing of provision, it has two evaporators which are fed with liquid from the receiver. The pressure in the LT evaporator is lower than in the MT evaporator, hence this refrigerant enters the LT compressor before it is mixed with the refrigerant from the MT evaporator. The vapor in the liquid receiver is drawn by the parallel compressor through the IHX before it is compressed to high side pressure. Due to the ejector, increasing gas cooler pressure shifts compressor work from the MT

compressor to the parallel compressor, therefore the MT compressor is not needed in warm climates, as long as the receiver pressure is sufficiently low enough. Table 2 summarize the most important conditions of the AC- and provision system.

Table 2: Key conditions and parameters for the AC and provision system.

System		AC	Provision
Temperature difference gas cooler outlet	°C	5	5
Receiver pressure	bar	39	40
MT-/first evaporator pressure	bar	39	31.3
LT-/second evaporator pressure	bar	35	14.3
Ejector efficiency	-	0.3	0.3
Heat recovery exit temperature	°C	45	45
Heat recovery gas cooler heat transfer area	m^2	24.7	1483.6

3.1.1. Control of high side pressure

To control the high side pressure of the simulated models, the second gas cooler heat transfer area is varied. The high side pressure is very dependent on gas cooler heat transfer area, thus it can be changed to influence the pressure. To better see the impact on recovered heat with increasing high side pressure, the areas of the first gas coolers was not changed but fixed to the values shown in Table 2. Hence, only the heat transfer area of the second gas cooler was varied.

3.2. Cold thermal energy storage

The CTES utilizes latent heat storage with water as phase change material (PCM). It has to be able to be charged during sailing and discharged in port. The charging will be done by the AC-system, and the discharging is done by circulating water connected to the HVAC system. As space on board a cruise ship is limited, the final system will contain several CTES systems in parallel. Since the PCM is stored in containers the designed systems will utilize double bundle containers.

Table 3: Key values CTES.

CTES	Unit	Size
Volume	m^3	6.9
Number of serial charging tubes	-	100
Number of parallel charging tubes	-	100
Number of parallel charging tube side flows	-	100
Number of serial discharging tubes	-	42
Number of parallel discharging tubes	-	42
Number of parallel discharging tube side flows	-	42
Total mass PCM	kg	4633

To investigate what impact CTES charging has on the AC system performance, the AC system is further developed. Fig 2 shows how the AC system configuration is equipped with CTES. When charging is initiated, liquid from the receiver is throttled to 31 bar before entering the LHS where it is superheated 5°C. Downstream the refrigerant is compressed to receiver pressure, before it is mixed with the refrigerant from the IHX. This figure only shows how one LHS is integrated. With multiple, they would have been connected in parallel. Fig 2 also illustrates how the CTES can be discharged. Water from the HVAC system is chilled in the LHS and returns. Table 3 summarize the key values of one investigated CTES module.

4. RESULTS AND DISCUSSIONS

4.1. AC system performance

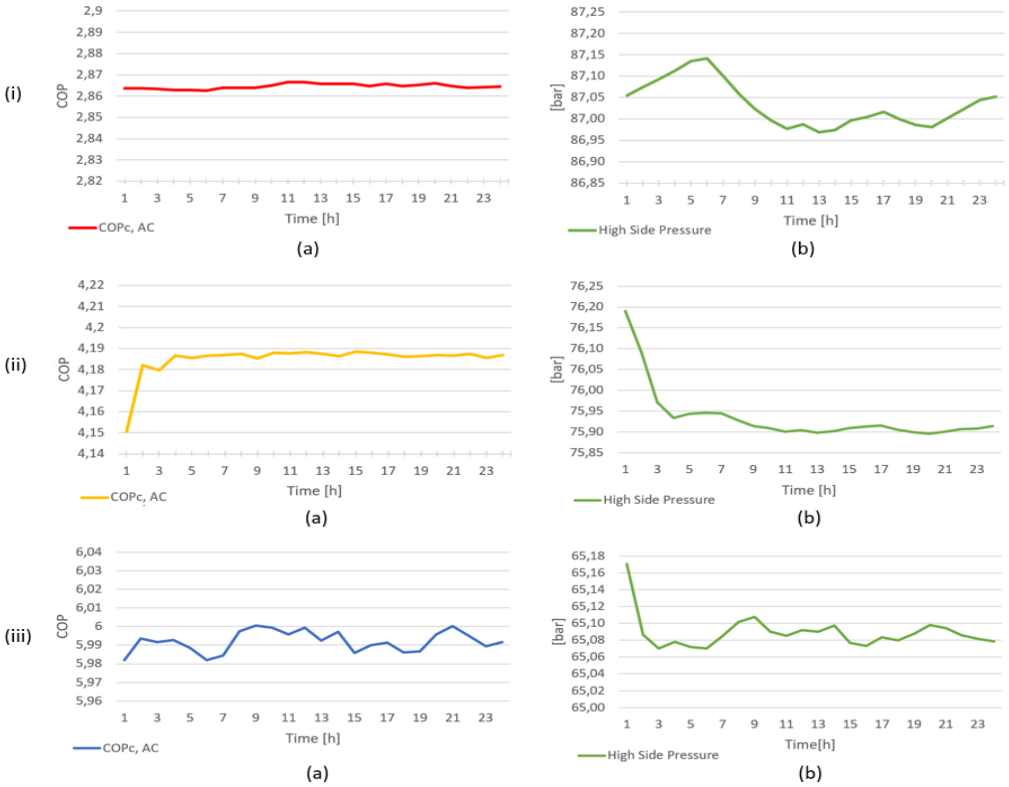

Figure 3: AC system dynamic performance for each case. (i), (ii) and (iii) represents to the warm, medium and cold case, respectively. (a) illustrates the $COP_{c, AC}$ and (b) the corresponding high side pressure.

The graphs in Fig 3 shows the dynamic performance of the modelled AC system. The $COP_{c, AC}$ curves represent the best obtainable performance from the simulated system during each case. During the warm case, the system operates with a $COP_{c, AC}$ in the range of 2.863-2.867. Further, in the medium case, it is able to operate in the range of 4.185-4.188. And finally, in the coldest case, the $COP_{c, AC}$ is in the range of 5.982-6.000. Note that during the first hours, the medium and cold case have not yet converged, thus values from here are unreliable.

As expected the high side pressures increases with increasing cooling load. Further, it was expected that the lowest $COP_{c, AC}$ would occur with the highest pressures, and vice versa. This trend can only be seen in the warm case. Unexpectedly, this is not the situation for the two other cases. As a matter of fact, in the coldest case, the highest $COP_{c, AC}$ occurs with the highest pressures. However, if the high side pressure is increased, the $COP_{c, AC}$ fluctuations behaves as expected, so, the behaviour is most likely due to instabilities in the control system and small state changes in other parts of the system.

Because of two-staged evaporation, both the low side pressure and the receiver pressure has to be fixed. So, by by-passing the ejector with a proportion of the refrigerant through a valve, the system is able to control the pressure lift generated by the ejector, thus the pressure levels in the heat exchangers. Because of this, it would have been interesting to compare the AC system with an ejector supported one-staged evaporator system. When only having one evaporator pressure, the receiver pressure may fluctuate, thus all of the pre-compression capacity of the ejector can be utilized. On the other hand, the employment of one-staged evaporation would increase the exergy destruction rate.

4.2. Provision system performance

From Table 4 the provision system performance can be seen. As for the AC system, the listed $COP_{c,prov}$ is the highest obtainable system performance for each case. As expected are the $COP_{c,prov}$ greatest for the coldest case and least for the warm case. This is of course due to the heat sink temperature being greatest for the warm case and least for the cold state. This is also reflected by the high side pressure. The difference in heat sink temperature is also influencing the allocation of work between the compressors. The LT compressor work is the same for all cases, but one can see that work is shifted from the MT compressor to the parallel compressor with increasing heat sink temperature. Due to the increase in gas cooler exit temperature and the increase in ejector entertainment ratio, more work has to be done by the parallel compressor and less is required by the MT compressor.

Table 4: Provision system performance and key numbers.

Reference case	Unit	Warm	Medium	Cold
$COP_{c,\ prov}$	-	2.334	2.997	3.538
High side pressure	bar	86	76	70
Gas cooler outlet temperature	°C	35	28	21
Parallel compressor work	kW	28.45	12.98	6.18
MT compressor work	kW	14.86	20.02	20.80
LT compressor work	kW	4.67	4.67	4.67
Entrainment ratio	-	0.31	0.20	0.13

4.3. Heat recovery and optimum high side pressure

In this section the possibility of heat recovery will be presented. Since the first gas cooler in both systems are dedicated to heat recovery, an increase in high side pressure will shift heat rejection from the second to the first gas cooler. At the same time can the optimum high side pressure for each system be investigated. Hence, it is presented together.

4.3.1. Heat recovery and optimum high side pressure for the AC system

Since the AC system is simulated with a dynamic cooling load, the $COP_{c,AC}$ fluctuate, as shown above. Therefore, the values in this section are collected from the point where the system is supplying maximum cooling load.

Fig 4 shows the heat recovery and optimum high side pressure for the AC system during the warm case. In (a), it can be seen that with regards to $COP_{c,\ AC}$, the optimum high side pressure is 87 bar. Further, the reduction in $COP_{c,\ AC}$ with increasing pressure is relatively small. As expected, does the $COP_{rec,AC}$ increase with increasing high side pressure before it reaches a maximum of approximately 3.2. In (b), the total recovered heat is shown. The investigated high side pressures allows the system to recover between 3000 kW and 5000 kW of heat. In (c), the $COP_{t,AC}$ is shown. It reaches a maximum at approximately 99 bar. From here, increasing high side pressure will result in decreasing $COP_{t,AC}$. In other words, if the pressure is increased more, the payback of cold and heat is less than the electricity required to drive the compressor.

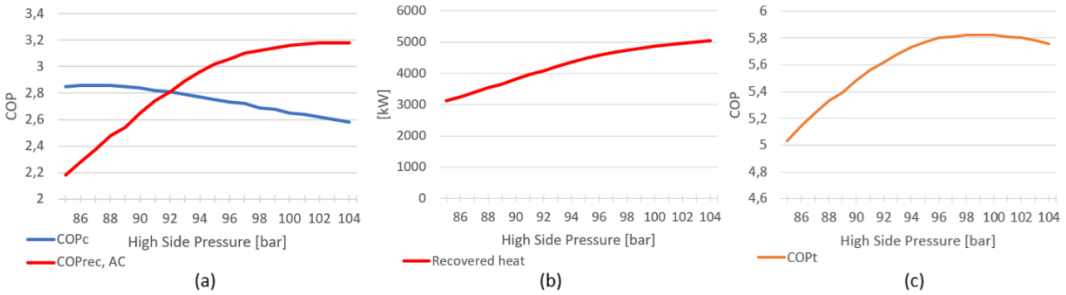

Figure 4: Heat recovery and optimum high side pressure for the AC system during the warm case. With increasing high side pressure: (a) the change in COP_c and $COP_{rec,\ AC}$; (b) the change in total amount of heat recovered; (c) the change in COP_t. Gas cooler outlet temperature = 35°C.

As for the warm case, the $COP_{c,AC}$ in the medium- and cold case decreases with increasing high side pressures. However, due to the relatively low gas cooler outlet temperature, they have not an optimum high side pressure with regards to $COP_{c,AC}$. Further, the smallest amount of heat recovered occurs at the lowest pressure in the cold case. At that point the system is able to recover 400 kW of heat.

4.3.2. Heat recovery and optimum high side pressure for the provision system

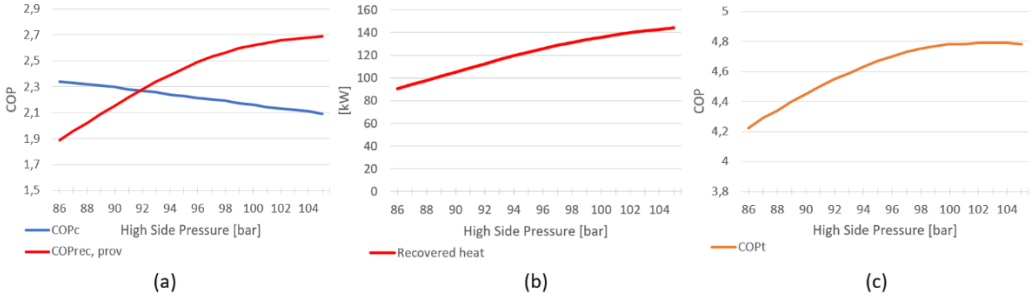

Figure 5: Heat recovery and optimum high side pressure for the provision system during the warm case. With increasing high side pressure: (a) the change in COP_c and $COP_{rec,\ prov}$; (b) the change in total amount of heat recovered; (c) the change in COP_t. Gas cooler outlet temperature = 35°C.

Fig 5 illustrates the results from investigating heat recovery and optimum high side pressure for the provision system during the warm case. The $COP_{c\ prov}$ is depicted in (a). In contrast to the AC system, the provision system is not able to reach a maximum, even with the relatively high gas cooler outlet temperature. This is because the model is not able to reduce the pressure below 86 bar. In parallel, the $COP_{rec,\ prov}$ strictly increases, it does not reach a maximum either but starts to flatten out at the highest pressures. The heat recovery gas cooler in the provision system is relatively small compared to the one in the AC system, therefore will the relatively small heat transfer area cause the curve to flatten out slower and later. Further is the to heat recovered depicted in (b). The system is able to recover between 90 kW and 140 kW of heat, depending on the high side pressure. Obviously can it recover more heat by increasing the pressure further, but as shown in (c) is the maximum COPt, prov located at approximately 103 bar.

Due to the same reason as for the AC system, the provision is not able to reach an optimum high side pressure with regards to $COP_{c,prov}$. Furthermore, the system recovers the least amount of heat at the lowest high side pressure in the cold case, with 55 kW.

4.4. Cold thermal energy storage

To meet the total cooling demand, several CTES modules will have to operate in parallel. From the simulated results the total system will have to include 21163 kg of water as PCM and a total volume of 38.0 m^3. This translates to 4.56 parallel modules of the one specified in Table 3.

Fig 6 shows a possible CTES charging strategy when all of the modules are charged at the same time. Apart from being able to be discharged during the two hour port stay, the system is able to be charged in six hours without increasing the peak load of the overall AC cooling load. During charging the $COP_{c,AC}$ is decreased in the range from 6.13% to 9.73%.

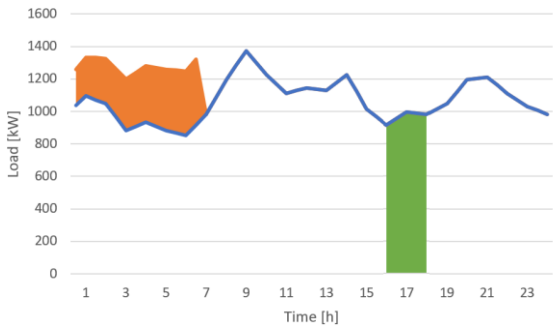

Figure 6: CTES charging strategy, CTES discharging and overall cooling load. Charging is shown as the orange shaded area and discharging as green

5. CONCLUSIONS

In this work, the performance of two energy-efficient CO_2 refrigeration systems for a medium sized cruise ship, utilized for air conditioning and for provision cooling and freezing, have been examined through simulation. To obtain realistic results for cruise ship applications, three reference cases with different boundary conditions was defined with corresponding cooling loads, and was referred to as the warm-, medium- and cold case. As the AC system supplies a dynamic cooling load, the cooling COP ($COP_{c,\ AC}$) fluctuates. At the best operating point, it has been found that the high side pressure fluctuations are very small, and that the system is able to operate with a $COP_{c,\ AC}$ around 2.86, 4.19 and 5.99 respectively for the warm-, medium- and cold case. Next, at best operation point, the provision system is able to operate at a $COP_{c,\ prov}$ of 2.33, 2.98 and 3.54 respectively for the warm-, medium-, and cold case. Within the three reference cases, the AC system can recover from 400 kW to 5000 kW of heat. The provision system can recover from 55 kW to 140 kW of heat.

CTES have also been examined. It has been found that the CTES must contain 21163kg of water as phase change material, and a total volume of 38.0m^3, to be able to supply the cooling demand of a two hour port stay.

REFERENCES

[1] Western norway research institute. https://www.vestforsk.no/en. Accessed: 2022-06-03.

[2] Ing A Hafner, CH Gabrielii, and K Widell. Refrigeration units in marine vessels: Alternatives to HCFCs and high GWP HFCs. Nordic Council of Ministers, 2019.

[3] Hfk-gasser. https://www.linde-gas.no/no/products ren/refrigerants/hfc gases/index.html. Accessed: 2021-12-15.

[4] M Schulz and D Kourkoulas. Regulation (eu) no 517/2014 of the european parliament and of the council of 16 april 2014 on fluorinated greenhouse gases and repealing regulation (ec) no 842/2006. Off. J. Eur. Union, 2014(517):L150, 2014.

[5] The european union's proposal on alternative fuels and its impact on shore power adoption. https://powertechresearch.com/ the-european-unions-proposal-on-alternative-fuels-and-its-impact-on-shore-power-adoption/. Accessed: 2022-05-07.

[6] Maria Alessandra Ancona, Francesco Baldi, Michele Bianchi, Lisa Branchini, Francesco Melino, Antonio Peretto, and J Rosati. Efficiency improvement on a cruise ship: Load allocation optimization. Energy Conversion and Management, 164:42–58, 2018.

[7] Clemens Boertz. Energy demand of a fuel cell-driven cruise ship: Analysis and improved prediction method of the operational power variation under different loading and environmental conditions. 2020

[8] Giacomo Tosato, Silvia Minetto, Antonio Rossetti, Armin Hafner, Christian Schlemminger, and Sergio Girotto. Field data of co2 integrated refrigeration, heating and cooling systems for supermarkets. In Proceedings of the 14th IIR-Gustav Lorentzen Conference on Natural Refrigerants. IIR, 2020.

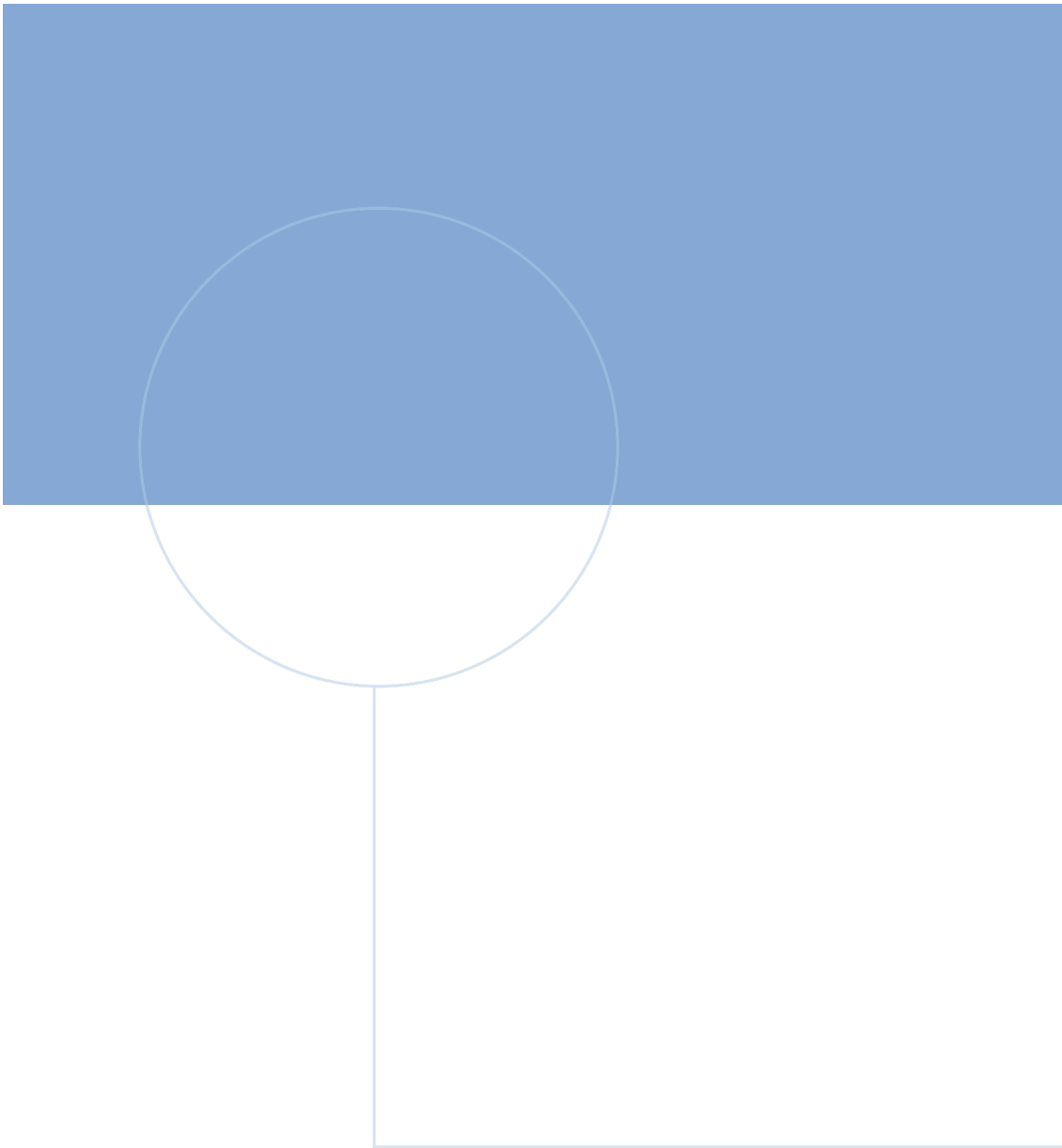

NTNU

Norwegian University of
Science and Technology